

**Transcriptomic and proteomic characterizations of
goldfish (*Carassius auratus*) radial glia reveal
complex regulation by the neuropeptide
secretoneurin**

Dillon Da Fonte

Thesis submitted to the
Faculty of Graduate and Postdoctoral Studies
University of Ottawa
in partial fulfillment of the requirements for the
Master of Science degree in biology

Department of Biology
Faculty of Science
University of Ottawa

Acknowledgements

Finishing this thesis has been both a challenging and rewarding experience. This accomplishment would not have been possible without the never-ending support of colleagues, friends, family. First, I would like to express my most sincere gratitude to my supervisor and mentor, Dr. Vance Trudeau. Thank you for the opportunities you have given me, this experience has truly solidified my passion for research. I appreciate our many conversations that were enjoyed over a beer – it was truly a memorable experience. I would also like to thank my M.Sc. advisory committee, Dr. Michael Jonz and Dr. Marc Ekker for your time and insightful comments. A special thank you to Dr. Chris Martynuik who taught me the bioinformatics needed to analyze both transcriptomic and proteomic data and for all your help during my time at the University of Florida. I would like to also acknowledge my funding support from University of Ottawa, NSERC, and the Michael Smith Foreign Study Award for supporting my research stay at the University of Florida.

To all current and past members of TeamENDO, thank you for the sense of community you all instilled in the lab. Both inside and outside the lab, I have made memories with all of you that I will cherish forever. I am indebted to Lei Xing for his unwavering guidance, professional advice, and his willingness to help and answer questions. To my ‘lab wife’ Maria, thank you for tolerating my constant urge to annoy/distract you and for always reminding me to be confident in my research. Thank you to Kim and Crystal for your assistance with zebrafish dissections. I would also like to acknowledge and thank Myy Mikwar for kindly providing me with samples from her ICV injection experiment. Also, to Maddie thank you for taking the time to translate my

abstract. Thank you to Bill Fletcher and Christine Archer from the aquatic facility for your animal care and maintenance.

Finally, to my parents, although you may not understand what is written in these pages, you were the driving force that allowed me to push myself to finish this endeavor. The sacrifices you have made for my life have not and will never go unnoticed. Thank you to my grandparents, both alive and deceased, for instilling in me perseverance and dedication. To my sisters, thank you for your unconditional love and for being the guiding forces in my life. To my community of friends, I am truly grateful to have you all who both love and believe in me and for the many nights of laughter that got me through this experience.

Abstract

In the teleost brain, radial glial cells (RGCs) are the main macroglia and are stem-like progenitors that express key steroidogenic enzymes, including the estrogen-synthesizing enzyme, aromatase B (*cyp19a1b*). As a result, RGCs are integral to neurogenesis and neurosteroidogenesis in the brain, however little is known about the permissive factors and signaling mechanisms that control these functions. The aim of this thesis is to investigate if the secretogranin-derived neuropeptide secretoneurin (SN) can exert regulatory control over goldfish (*Carassius auratus*) RGCs. Immunohistochemistry revealed a close neuroanatomical relationship between RGCs and soma of SNa-immunoreactive magnocellular and parvocellular neurons in the preoptic nucleus in both goldfish and zebrafish (*Danio rerio*) models. Both intracerebroventricular injections of SNa into the third brain ventricle and SNa exposures of cultured goldfish RGCs *in vitro* show that SNa can reduce *cyp19a1b* expression, thus implicating SNa in the control of neuroestrogen production. RNA-sequencing was used to characterize the *in vitro* transcriptomic responses elicited by 1000 nM SNa in RGCs. These data revealed that gene networks related to central nervous system function (neurogenesis, glial cell development, synaptic plasticity) and immune function (immune system activation, leukocyte function, macrophage response) were increased by SNa. A dose-response study using quantitative proteomics indicates a low 10 nM dose of SNa increased expression of proteins involved in cell growth, proliferation, and migration whereas higher doses down-regulated proteins involved in these processes, indicating SNa has dose-dependent regulatory effects. Together, through these altered gene and protein networks, this thesis proposes SNa exerts trophic and immunogenic effects in RGCs. These datasets identified

a total of 12,180 and 1,363 unique transcripts and proteins, respectively, and demonstrated that RGCs express a diverse receptor and signaling molecule profile. Therefore, RGCs can respond to and synthesize an array of hormones, peptides, cytokines, and growth factors, revealing a multiplicity of new functions critical to neuronal-glial interactions.

Résumé

Les cellules gliales radiaires sont les principaux microglies retrouvées dans le cerveau des poissons téléostéens. Ces cellules sont des nombreuses progénitrices qui ressemblent aux cellules souches et expriment des enzymes clés de la stéroïdogénèse tel que l'enzyme aromatasase B (*cyp19a1b*) responsable de la synthèse des oestrogènes. Par conséquent, les cellules gliales radiaires font une partie intégrale de la neurogenèse et de la neurostéroïdogénèse dans le cerveau. Par contre, les facteurs permissifs et les mécanismes de signalisation qui contrôle ces fonctions sont toutefois très peu connus. Le but de cette thèse est d'étudier la possibilité que la sécrétoneurine (SN), un neuropeptide dérivé de la sécrétogranine, peut exercer un contrôle réglementaire sur les cellules gliales radiaires chez le poisson rouge (*Carassius auratus*). Une relation neuroanatomique proche a été révélée par l'immunohistochimie entre les cellules gliales radiaires et le soma des neurones magnocellulaires et parvocellulaires, qui sont immunoréactives à la SNa. Ces neurones sont retrouvés dans le noyau préoptique chez les modèles du poisson rouge et du poisson zèbre (*Danio rerio*). La SNa est impliquée dans le contrôle de la production des neuro-oestrogènes puisqu'elle peut diminuer l'expression du gène *cyp19a1b* suite à des injections intra-cérébro-ventriculaire du SNa dans le troisième ventricule cérébrale, ainsi qu'après l'exposition des cellules gliales radiaires cultivées *in vitro* en présence du SNa. Les réponses transcriptomiques *in vitro* des cellules gliales radiaires exposées à 1000 nM SNa ont été caractérisées par le séquençage d'ARN. Les ensembles de données révèlent que la SNa augmente les réseaux de gènes liés aux fonctions du système nerveux centrale (neurogenèse, développement des cellules gliales, plasticité synaptique) et les fonctions immunitaires (activation du système immunitaire,

fonction leucocytaire, réponse macrophagique). Une étude protéomique quantitative de la relation dose-réponse indique qu'une faible dose de 10 nM SNa augmente l'expression de protéines impliqués dans la croissance cellulaire, la prolifération et la migration tandis que des doses plus élevées diminuent l'expression de ces protéines. Ceci indique que la SNa a des effets régulateurs qui sont dose-dépendants. Cette thèse propose que la SNa exerce des effets trophiques et immunogéniques sur les cellules gliales radiaires selon les réseaux de protéines et de gènes modifiés. Les ensembles de données ont identifié un total de 12 180 et 1 363 transcrits et de protéines uniques, respectivement, et ont démontré que les cellules gliales radiaires expriment un profil moléculaire diversifié de récepteurs et de signalisation. Par conséquent, les cellules gliales radiaires peuvent répondre et synthétiser une gamme d'hormones, de peptides, de cytokines et de facteurs de croissance. Ceci révèle une multiplicités de nouvelles fonctions essentielles pour les interactions neurones-glie.

Table of contents

Acknowledgments	II
Abstract	IV
Résumé	VI
Table of contents	VIII
List of figures	XI
List of tables	XIII
List of abbreviations	XIV
Thesis outline and rationale	XV
Chapter 1: General Introduction	1
1.1. The granin family	1
1.1.1. Secretogranin II	2
1.1.2. Distribution of secretogranin II and factors that control its synthesis and release	5
1.1.3. Secretoneurin	7
1.1.4. Distribution of secretoneurin	10
1.1.5. Neurogenic properties of secretogranin II and secretoneurin	11
1.1.6. Secretoneurin regulates inflammatory and immune responses	13
1.1.7. Secretoneurin receptor and signal transduction pathways	15
1.2. Radial glial cells	16
1.2.1. Steroidogenic capacity of radial glial cells	18
1.2.2. Radial glial cells and neurogenesis	21
1.2.3. Neuronal control of radial glial cell functions	22
Chapter 2: Interactions between secretoneurin-A and radial glial cells in the preoptic area – implications for control of neurosteroidogenesis	24
2.1. Introduction	24
2.2. Materials and methods	27
2.2.1. Experimental animals	27
2.2.2. Immunohistochemistry	27
2.2.3. Intracerebroventricular injection of secretoneurin-A	28
2.2.4. Cell culture and exposure	29
2.2.5. RNA extraction, cDNA synthesis, and qRT-PCR	30
2.2.6. Statistics	31
2.3. Results	33
2.3.1. Close anatomical relationship between secretoneurin-A-immunoreactive neurons and radial glia	33
2.3.2. Intracerebroventricular injection of secretoneurin-A affects the expression of <i>cyp19a1b</i>	36
2.3.3. Secretoneurin-A affects the expression of steroidogenic enzymes in radial glia cultures	38
2.4. Discussion	40

Chapter 3: <i>De novo</i> assembly of the transcriptome of goldfish radial glial cells and analysis of differentially expressed genes for the identification of gene network responsive to secretoneurin-A	45
3.1. Introduction	45
3.2. Material and methods	48
3.2.1. Experimental animals	48
3.2.2. Cell culture and exposure	48
3.3.3. RNA extraction and Illumina sequencing	49
3.3.4. <i>De novo</i> transcriptome assembly and annotation	50
3.3.5. Differential gene expression analysis	51
3.3.6. qRT-PCR validation of differentially expressed genes	51
3.3.7. Gene set enrichment analysis and sub-network enrichment analysis	53
3.3. Results	55
3.3.1. <i>De novo</i> transcriptome assembly and quality analysis	55
3.3.2. Annotation and gene ontology classification	55
3.3.3. Differential gene expression analysis	65
3.3.4. qRT-PCR validation of DGE analysis	67
3.3.5. Gene set enrichment analysis	69
3.3.6. Sub-network enrichment analysis	74
3.4. Discussion	78
Chapter 4: Secretoneurin-A regulated proteomic profiles and networks in goldfish radial glial cells <i>in vitro</i>	88
4.1. Introduction	88
4.2. Materials and methods	90
4.2.1. Experimental animals	90
4.2.2. Cell culture and exposure	90
4.2.3. Protein extraction, iTRAQ labeling, and LC-MS/MS	90
4.2.4. Gene ontology and pathway analysis	92
4.3. Results	94
4.3.1. Identification and gene ontology classification of radial glial cell proteins	94
4.3.2. Quantitative proteomic responses in primary cultures of radial glia to secretoneurin-A <i>in vitro</i>	98
4.3.3. Identifying cellular processes affected by secretoneurin-A by sub-network enrichment analysis	105
4.4. Discussion	111
Chapter 5: General discussion and future directions	117
5.1. Implications of secretoneurin-A regulation of aromatase B in the preoptic nucleus	117
5.2. Transcriptomic and proteomic responses suggest SNa exert trophic and immunogenic effects	119
5.3. Concluding remarks	120
5.4. Future Directions	121

Appendix 1: Zebrafish telencephalic stab lesion assay implicates aromatase B and secretogranin II systems in injury and repair	124
A1.1. Introduction	124
A1.2. Methods	126
A1.2.1. Animal care	126
A1.2.2. Telencephalic injury	126
A1.2.3. RNA extraction, cDNA synthesis, and qRT-PCR	126
A1.2.4. Statistics	127
A1.3. Results	128
A1.3.1. Stab lesions in the zebrafish telencephalon affects the mRNA levels of <i>scg2a</i> , <i>scg2b</i> , and <i>cyp19alb</i>	128
A1.4. Discussion	130
Appendix 2: Other research contributions	132
References	134

List of figures

Figure 1.1. Amino acid sequence alignment of SN between species _____	8
Figure 2.1. Immunofluorescence against SN (red) and GFAP (green) in the goldfish periventricular preoptic nucleus _____	34
Figure 2.3. Immunofluorescence against SN (red) and GFP (green) in the zebrafish <i>Tg(cyp19a1b-GFP)</i> transgenic line _____	35
Figure 2.4. Quantitative real-time PCR analysis showing the effect of ICV injection of SNa at 0.2 ng/g and 1 ng/g on relative <i>cyp19a1b</i> mRNA levels in female goldfish brain _____	37
Figure 2.5. Quantitative real-time PCR analysis showing the effects of various concentrations of SNa on the mRNA levels of <i>star</i> (A), <i>cyp17</i> (B), <i>cyp19a1b</i> (C), and <i>hsd17b4</i> (D) in primary RGC culture _____	39
Figure 3.1. Annotation summary of assembled RGC unigenes against UniProt database _____	57
Figure 3.2. GO classification of assembled RGC unigenes into molecular function, biological function, and cellular component categories _____	59
Figure 3.3. GO classification of assembled RGC unigenes by protein class _____	61
Figure 3.4. GO classification of assembled RGC unigenes by receptor and signaling molecule classes _____	62
Figure 3.5. Quantitative real-time PCR analysis for (A) <i>baiap2b</i> , (B) <i>fgf4</i> , (C) <i>grapa</i> , (D) <i>nab1a</i> and (E) <i>smad6b</i> mRNA in primary RGC culture exposed to 1000nM SNa _____	68
Figure 3.6. Cadherin adherens junction assembly was significantly enriched by GSEA in primary RGC culture after 1000nM SNa treatment _____	71
Figure 3.7. T cell activation signaling was significantly enriched by GSEA in primary RGC culture after 1000nM SNa treatment _____	72
Figure 3.8. Dopamine D1 receptor signaling pathway was significantly enriched by GSEA in primary RGC culture after 1000nM SNa treatment _____	73
Figure 3.9. Genes involved in neurogenesis were significantly enriched by SNEA in primary RGC culture after 1000nM SNa treatment _____	76

Figure 3.10. Genes involved in immune system activation were significantly enriched by SNEA in primary RGC culture after 1000nM SNa treatment _____	77
Figure 4.1. GO classification of identified RGC proteins into molecular function, biological function, and cellular component categories _____	95
Figure 4.2. GO classification of identified RGC proteins by protein class _____	96
Figure 4.3. Volcano plots for protein expression in RGCs treated with various concentrations of SNa _____	99
Figure 4.4. Venn diagram showing the number of commonly expressed and dose-dependent differentially regulated proteins following SNa exposure in RGCs _____	101
Figure 4.5. Proteins involved in cellular processes (blood vessel development, actin organization, cytoskeleton organization and biogenesis, cell proliferation, growth, and migration) that were significantly enriched by SNEA in primary RGC culture after 10nM SNa treatment _____	107
Figure 4.6. Proteins involved in cellular processes (actin organization, cell proliferation, and growth) that were significantly enriched by SNEA in primary RGC culture after 100nM SNa treatment _____	108
Figure 4.7. Proteins involved in cellular processes of (A) neurite outgrowth and nerve fiber regeneration and (B) tight and gap junction assembly that were significantly enriched by SNEA in primary RGC culture after 1000nM SNa treatment _____	109
Figure 4.8. Proteins involved in Alzheimer, Parkinson, and neurodegenerative diseases that were significantly enriched by SNEA in primary RGC culture after 1000nM SNa treatment _____	110
Figure 5.1. Summary of the <i>in vitro</i> effects of SNa on goldfish radial glial cells as determined by transcriptomics and proteomics _____	123
Figure A1.1. Quantitative real-time PCR analysis showing the effects of telencephalic injury on the relative amounts of <i>scg2a</i> (A), <i>scg2b</i> (B), and <i>cyp19a1b</i> (C) mRNA in female zebrafish 2 and 4 days post injury _____	129

List of tables

Table 2.1. Primers (5' → 3') used for qRT-PCR in goldfish _____	31
Table 3.1. Primers (5' → 3') used for qRT-PCR for differential gene analysis validation _____	53
Table 3.2. Top 25 assigned pathway ontologies for assembled RGC unigenes based on the number of genes identified in each pathway _____	64
Table 3.3. List of differentially expressed genes compared to control in primary RGC culture after 24 h 1000nM SNa treatment _____	66
Table 3.4. GSEA of responses in primary RGC culture mediated by 1000nM SN _____	70
Table 3.5. Cell processes identified by SNEA that were regulated by 1000nM SNa in primary RGC culture _____	74
Table 4.1. Top 25 assigned pathway ontologies of identified RGC proteins based on number of protein identified in each pathway _____	97
Table 4.2. Expression patterns of the differentially regulated proteins in RGCs treated with various concentrations of SNa _____	100
Table 4.3. The 20 most significantly differentially expressed proteins identified by iTRAQ in RGCs treated with various concentrations of SNa _____	102
Table A1.1. Primers (5' → 3') used for qRT-PCR in zebrafish _____	127

List of abbreviations

5-HT	Serotonin
BLBP	Brain lipid binding protein
cAMP	Cyclic adenosine monophosphate
Cg	Chromogranin
CSF	Cerebrospinal fluid
DA	Dopamine
DAPI	4,6-diamino-2-phenylindole
DEG	Differentially expressed gene
dpi	Days post-injury
ER	Estrogen receptor
FBS	Fetal bovine serum
Fgf	Fibroblast growth factor
GABA	γ -aminobutyric acid
GFAP	Glial fibrillary acidic protein
GFP	Green florescent protein
GO	Geno ontology
GSEA	Gene set enrichment analysis
ICV	Intracerebroventricular
iTRAQ	Isobaric tag for relative and absolute quantification
JAM	Junctional adhesion molecules
PC	Prohormone convertase
PBS	Phosphate buffered saline
PFA	Paraformaldehyde
PKA	Protein kinase A
PKC	Protein kinase C
qRT-PCR	Quantitative reverse transcription polymerase chain reaction
RT	Room temperature
RTN4	Reticulon 4
RGC	Radial glial cell
Sg	Secretogranin
Sox2	Sex determining region Y box 2
SN	Secretoneurin
SNEA	Sub-network enrichment analysis
StAR	Steroidogenic acute regulatory protein
TGF β	Transforming growth factor β
TGN	Trans-Golgi network
ZO-1	Tight junction protein 1

Thesis outline and rationale

The role of the secretogranin II-derived neuropeptide secretoneurin A (SNa) to control radial glial cells (RGCs) is the major focus of this research. SN has many attributed biological functions, particularly in the central nervous system (CNS), however nothing is known about its influences on glia. In fish, RGCs are the major macroglia but their functions are not well described. Emerging data suggest they have typical astrocyte-like functions such as transmitter uptake/release and regulation of ionic and water homeostasis in the brain. Teleost RGCs structurally organize the CNS, produce neuroestrogens, and are progenitor cells aiding in neurogenesis (Forlano et al., 2001; Pellegrini et al., 2007; Lyons et al., 2014; Xing et al., 2014). Since RGCs have a multitude of functions they should be under tight regulation to maintain proper brain homeostasis. Only recently have studies started to address how neuronal-RGC interactions through neurotransmitters exert control over RGC function, although regulatory effects of neuropeptides are largely unknown (Pérez et al., 2013; Xing et al., 2015b). Therefore, this gap in knowledge led to the generation of the following hypotheses: SNa is a key regulator of RGC function in (a) neurosteroidogenesis, specifically neuroestrogen production and (b) in neurogenesis.

The neuroanatomical relationship between SNa-positive neurons and RGCs is described in Chapter 2. In goldfish, numerous SNa-positive magnocellular neuron cell bodies were located adjacent to networks of RGC fibers immunoreactive for glial fibrillary acidic protein (GFAP). These observations were extended to zebrafish. In the transgenic line Tg(*cyp19a1b*-GFP) green fluorescent protein expression is under the control of the promoter for the estrogen-synthesizing enzyme, aromatase B (*cyp19a1b*),

which is exclusively found in RGCs. SNa-positive neuronal-RGC interactions were also clearly evident in this model system (Chapter 2). To study the effects of SNa on *cyp19a1b* mRNA expression both *in vivo* and *in vitro*, intracerebroventricular injections of SNa into the goldfish third brain ventricle, targeting the preoptic nucleus, was performed in conjunction with *in vitro* SNa exposures of cultured goldfish RGCs. Results from these studies suggest SNa specifically reduces *cyp19a1b* mRNA levels, implicating SNa in the regulation of neuroestrogen production in these cells (Chapter 2).

Both transcriptomics and proteomics were used to characterize RGCs while profiling the molecular responses to SNa treatment. Both Chapters 3 and 4 reveal RGCs express an array of neurotransmitter, hormone, and neuropeptide receptors and signaling pathways, suggesting a multiplicity of new functions critical to neuronal-RGC communication. In addition, the identification of immune system pathways, proinflammatory signals and receptors indicate RGCs may also be involved in regulating neuroinflammation processes in the fish brain (Chapters 3 and 4). The transcriptomic responses to 1000 nM SNa elicited changes in gene networks associated with processes of the CNS (e.g. neurogenesis, synaptic plasticity, axon guidance) and immune system (e.g. immune system activation, phagocyte activity, leukocyte function, macrophage response) (Chapter 3). Quantitative proteomics were used to understand SNa regulation of RGCs at the molecular level across low, medium and high doses in the nanomolar range (Chapter 4). Lower doses of SNa were stimulatory while higher doses of SNa were inhibitory, generating dose-dependent effects. Proteins regulated by SNa were involved in many cell processes including blood vessel development, actin organization, cytoskeleton organization and biogenesis, neurite outgrowth, nerve fiber regeneration,

cell growth, migration, and proliferation. Lastly, Chapter 5 outlines the key findings of this thesis while discussing the physiological significance of SNa in CNS and future directions for research. This research has expanded on the functions of SNa in CNS while providing a molecular representation of a cell type often used in the fields of neurogenesis and neuroendocrinology.

Chapter 1: General introduction

1.1. The granin family

The granins are a diverse group of proteins distributed in secretory granules of neurons and endocrine cells distinguished by their acidic and heat-stable properties (Huttner et al., 1991). Some of these proteins are involved in the biogenesis of dense-core secretory granules and regulate the release of their co-localizing hormones and neuropeptides through the secretory pathway (Blázquez and Shennan, 2000; Bartolomucci et al., 2011). The mechanisms in which granins exert their granulogenic properties occur at the trans-Golgi network (TGN). Granins are synthesized in the rough endoplasmic reticulum then through vesicular transport are targeted to the TGN. Conditions such as low pH and presence of calcium in the TGN cause granins to aggregate while interacting with sorting receptors to form secretory granules along with other granule proteins such as prohormones and processing enzymes. Within these secretory granules granins are processed into bioactive peptides and released upon stimulation and fusion of the secretory granule with the cell membrane (Bartolomucci et al., 2011).

The granin family can be classified into two groups, the chromogranins (Cg) and the secretogranins (Sg) based on the presence of a disulfide-bonded loop at the N-terminus of Cg but not in Sg proteins (Helle, 2004; Zhao et al., 2009b). The Cg proteins are divided into the chromogranins A (CgA) and chromogranins B (CgB); and the Sg proteins consists of seven members: secretogranin II (SgII), secretogranin III (SgIII), secretogranin IV (SgIV), secretogranin V (SgV), secretogranin VI (SgVI), secretogranin

VII (Sg VII), and proSAAS (Zhao et al., 2009b). Many shared biochemical properties make the granin proteins a related family. Granins are hydrophilic heat stable proteins that have a high proportion of acidic amino acids, the capacity to bind calcium, and the ability to form aggregates at low pH levels (Ozawa and Takata, 1995). Granins are precursor proteins for biologically active peptides through the proteolytic processing by prohormone convertases (PCs) PC1/PC3 and PC2 at multiple dibasic cleavage sites (Huttner et al., 1991; Helle, 2004). Several granin-derived peptides have been identified across various species and exert diverse biological activities in endocrine, neuroendocrine, cardiovascular, inflammatory, and neuronal systems (Bartolomucci et al., 2011). The most well characterized peptides produced from granins are vasostatin I, vasostatin II, pacreastatin, bovine CgB₁₋₄₁, and secretoneurin (Taupenot et al., 2003; Zhao et al., 2009b). Despite their shared biochemical properties, sequence and phylogenetic analyses have revealed no clear evolutionary relationship except for the Cgs (CgA and CgB) (Zhao et al., 2009b). Both CgA and CgB proteins exhibit considerable homology between different vertebrate species having a high degree of DNA and amino acids similarity (Sato et al., 2000; Zhao et al., 2009b). In contrast, SgII is poorly conserved compared to CgA and CgB, however a peptide known as secretoneurin (SN) in the middle domain of SgII shows high sequence similarity among vertebrates (Zhao et al., 2009b; Trudeau et al., 2012).

1.1.1. Secretogranin II

Secretogranin II is one of the most well studied Sg proteins and was first identified in the bovine anterior pituitary (Rosa and Zanini, 1983) and rat PC12 cell lines

(Lee & Huttner, 1983). Secretogranin II is an approximately 600 amino acid long, acidic, tyrosin-sulfated preproprotein processed into small peptides by PCs at several dibasic cleavage sites in secretory granules of vertebrate endocrine and neuronal cells (Fischer-Colbrie et al., 1995). Like other granins, SgII is involved in the biogenesis of secretory granules as upon its depletion both the number and size of dense-core secretory granules decreased in PC12 cells (Courel et al., 2010). Because of its granulogenic properties, SgII is thought to participate in the sorting and packaging of hormones and neuropeptides in secretory granules (Miyazaki et al., 2011).

The SgII gene (*scg2*) located on human chromosome 2 comprises two exons and encodes a 2476 bp transcript (Bartolomucci et al., 2011). Mammalian SgII is well conserved through evolution being 79-87% identical between species. In contrast, the SgII sequences of some non-mammalian vertebrates have a low degree of conservation compared to mammalian SgII sequences (Montero-Hadjadje et al., 2008). Comparing goldfish SgII with human SgII shows an overall 28% identity and 48% similarity in amino acids sequences (Blázquez et al., 1998). However, only a discrete domain in the middle of the SgII precursor, called secretoneurin (SN) is relatively well conserved across the vertebrate taxa (Trudeau et al., 2012). The goldfish SN (SgII₂₁₄₋₂₄₈) amino acid sequence shares 59% identity to human SN and more than 75% similarity with other vertebrate SN sequences (Blázquez et al., 1998). This conservation of the SN peptide indicates important physiological functions that may be similar in the different vertebrate classes. Besides SN, only two other peptides have been identified in mammalian SgII, which are EM66 and manserin (Fisher-Colbrie et al. 1995; Yajima et al. 2004). Flanking SN at the C-terminus, is the 66 amino acid peptide EM66 which is well conserved in

human and tetrapods, but is not at all conserved in fish (Anouar et al., 1998; Zhao et al., 2009b). This peptide has been implicated in the control of food intake and the fasting-induced stress response in the jerboa (Boutahricht et al., 2005). Manserin, the most recently discovered peptide processed from SgII, was first investigated in the rat anterior lobe of the pituitary and hypothalamus, suggesting that manserin might have a role in the neuroendocrine system (Yajima et al., 2004), but no specific biological activity has yet been reported.

Secretogranin II, also known as CgC, was the first Cg to be cloned and sequenced in fish. Two different SgII transcripts of approximately 2975 bp and 2650 bp were detected in the goldfish pituitary (Blázquez et al. 1998). Later phylogenetic analysis revealed two SgII paralogs in other teleost species generated by a gene duplication event and have been named SgIIa and SgIIb (Zhao et al., 2009b). The existence of two SgII genes is likely due to the whole genome duplication event that occurred in the teleost emergence (Zhao et al., 2010). The expression of both SgIIa and SgIIb have been found in some species such as zebrafish whereas others only one gen has been identified to date. For example, the only known goldfish SgII is SgIIa while the known pufferfish and grass carp SgIIs are of the SgIIb type. However, a partial cDNA sequence for goldfish SgIIb has been isolated but not yet reported (Unpublished data, Trudeau lab). Further investigations are required to determine if another SgII gene exists or if a differential deletion occurred in these species (Zhao et al., 2009b). In addition, the “a” and “b” nomenclature applies to the peptides derived from their corresponding SgII subtype precursors.

1.1.2. Distribution of secretogranin II and factors that control its synthesis and release

Secretogranin II has a widespread distribution in both the endocrine and nervous systems (Fischer-Colbrie et al. 1995). In the adult rat brain, SgII protein was found to be expressed in the olfactory bulb, hypothalamus, dentate gyrus and inferior colliculus, hippocampus, and cerebellum (Miyazaki et al., 2011). Bergmann glia and other astrocytes *in vivo* express SgII in rodent brain (Cozzi et al., 1989; Miyazaki et al., 2011). Furthermore, *in vitro* studies support that cultured rat astrocytes synthesize and release SgII through storing SgII in dense-core secretory granules in a regulated secretory pathway. Although SgII produced in culture does not undergo any proteolysis it does not exclude that it could be processed extracellularly in the brain to other bioactive peptides (Fischer-Colbrie et al., 1993; Calegari et al., 1999).

Several studies reveal that SgII is stored together with hormones in pituitary cells. In the human pituitary, SgII immunoreactivity is found in gonadotrophs, thyrotrophs, and corticotrophs (Vallet et al., 1997). In the bovine anterior pituitary, SgII co-localizes with thyroid-stimulating hormone and luteinizing hormone (Bassetti et al., 1990). Some heterogeneity in the pattern of distribution of prolactin and SgII in rat mammotrophs has been observed with the majority of cells co-localize prolactin with SgII in secretory granules (Ozawa et al., 1994). Using several different tissues, *scg2a* transcripts were detected in the goldfish interrenal, ovary, cerebellum, and telencephalon with noticeably higher transcript levels in the brain and pituitary than in peripheral tissues (Zhao et al., 2006a). Peripherally, SgII immunoreactivity has been documented in the following human tissues: adrenal medulla, thyroid, gonads, pancreas, stomach and intestine (Fisher-

Colbrie et al. 1995). This wide distribution of SgII indicates several potential biological activities however possible roles remain to be elucidated for most tissues (Zhao et al., 2009b).

A variety of factors has been identified to regulate the synthesis and release of SgII. Microarray analysis of female goldfish telencephalon following fadrozole-induced estrogen decline showed an up-regulation of *scg2a* mRNA levels (Zhang et al., 2014). Furthermore, a combination of *in vivo* and *in vitro* studies in female rat pituitary reveal that estradiol has a direct effect to decrease *scg2* mRNA (Anouar et al., 1991; Anouar and Duval, 1992). Together this provides support for the estrogen-responsive properties of the *scg2a* gene. In rat pituitary cells, gonadotropin-releasing hormone stimulates SgII secretion from gonadotrophs (Conn et al., 1992). Similarly, *in vivo* injection of a GnRH agonist increases *scg2a* transcript levels in female goldfish anterior pituitary (Samia et al., 2004). During the seasonal reproductive cycle of the female goldfish, *scg2a* mRNA levels vary, with levels being highest in winter and lowest in spring (Samia et al., 2004). Increasing endogenous brain and pituitary γ -aminobutyric acid (GABA) levels by the GABA transaminase inhibitor increases *scg2a* gene expression in goldfish pituitary (Blázquez et al. 1998). Indeed, this is how Blázquez et al. (1998) were able to isolate the *scg2a* cDNA for the first time using a differential display strategy. The neuropeptide pituitary adenylate cyclase-activating polypeptide has a rapid and long lasting effect to increase *scg2a* mRNA abundance in bovine chromaffin cells (Turquier et al., 2001). In bovine chromaffin cells, histamine exerts a stimulatory effect on *scg2a* mRNA levels (Bauer et al., 1993). Chronic exposure to vasopressin causes the increase of biosynthesis of SgII in male rat brain (Mahata et al., 1992). Under osmotic stimulation, SgII

expression is observed in a subpopulation of vasopressinergic magnocellular neurons in rat supraoptic and paraventricular nuclei (Ang et al., 1997). These hypothalamic nuclei also exhibit an increase in *scg2* transcript levels during lactation in rats (Mahata et al., 1993). Overall, SgII production and secretion is under the control of a diverse number of regulators including hormones, neuropeptides, and neurotransmitters.

1.1.3. Secretoneurin

Endoproteolytic processing of the middle domain of SgII produces the bioactive peptide secretoneurin (SN). Secretoneurin is moderately conserved in evolution and found across vertebrate taxa from sea lamprey to humans, ranging in size from 31 to 43 amino acids. In all tetrapods SN is 33 amino acids in length while in goldfish and zebrafish SNa is 34 amino acids long (Trudeau et al., 2012). Mammalian SN is highly conserved in evolution in species such as human, pig, hamster, and rat (Kähler and Fischer-Colbrie, 2002). In marked contrast, goldfish SN shares low degree of identity to mammalian SN, nevertheless domains in the N- terminus (TNE) and in the middle (QYTP and LATLEQSVFQEL) of teleost SNa are identical with those of mammals (Trudeau et al., 2012). Unlike SNa, only two segments in the middle of teleost SNb (EQYTPQSLA and FE(Q)ELG) are moderately conserved in comparison to mammalian SN (Trudeau et al., 2012). Therefore, these conserved domains might confer SN its biological activity. Comparing zebrafish SNa and SNb reveals only 40% of amino acids in the middle core are conserved. Although the biological functions of SNb have not been elucidated they are predicted to be different from SNa (Zhao et al., 2010). Comparisons of SN amino acid sequences between select vertebrates are shown in Figure 1.1.

(31aa) Zebrafish-SNb	<u>AT</u> EDLDEQYTPQSLANMRSIFEELGKLSAA-----
(34aa) Zebrafish-SNa	TNENAAEQYTPQKLATLQSVFEELSGIASSKTNT-----
(34aa) Goldfish-SNa	TNENAAEQYTPQKLATLQSVFEELSGIAASNANS-----
(33aa) Frog	TNEIVEGQYTPQSLATLQSVFQELGKLGQANN-----
(42aa) Shark	TNEIVEEQYTPQSLATLESFRELGKYAGPYKEQGRLEEEHF
(33aa) Human	TNEIVEEQYTPQSLATLESVFQELGKLTGPNNQ-----
(33aa) Chicken	TNEIVEEQYTPQSLATLESVFQELGKMAGPSNH-----
	: . * : * * * * * . * * . : * * * * . .

Figure 1.1. Amino acid sequence alignment for chicken (*Gallus gallus*) SN, human (*Homo sapiens*) SN, shark (*Squalus acanthius*) SNa, frog (*Rana rdibunda*) SN, goldfish (*Carrasius auratus*) SNa and zebrafish (*Danio rerio*) SNa and SNb using MUSCLE program. The number in brackets indicates the length of the peptide and YTPQ-X-LA-X₇-EL signature is underlined. This figure was adapted from Trudeau et al., 2012.

The SgII precursor is processed to yield free SN peptide by a group of endoproteolytic enzymes called prohormone convertases (PCs) at dibasic cleavage sites. Some of these dibasic cleavage sites are conserved between mammals and fish allowing for species variation in SgII processing (Blázquez and Shennan, 2000). While at least 7 PCs having been identified, only PC1 and PC2 have been shown to cleave SgII to generate both SN containing intermediate fragments and free SN peptide. Both PC1 and PC2 are colocalized with SN in neurosecretory granules in the bovine posterior pituitary (Egger et al., 1994). However, only PC1 is capable of generating SN in neurons suggesting that processing of SgII is tissue specific in neurons expressing different subsets of PCs (Hoflehner et al., 1995). In another study, PC12 cells transfected with either PC1 or PC2 reveal both enzymes process SgII into SN although the ability to generate free SN peptide was more pronounced with PC2 than with PC1 (Laslop et al., 1998). Moreover, in the absence of PC2, SN levels in mice brain remain unchanged, implying the importance of PC1 in yielding SN peptide (Laslop and Becker, 2002). Although evidence supports the role of both PC1 and PC2 in generating SN from SgII the relative involvement of either PC seems to depend on tissue and experimental system.

The degree of precursor processing to SN varies greatly depending on tissue, reaching 89-97% in the brain, 49% in the adrenal medulla, and only 26% in the anterior pituitary of the rat (Kirchmair et al., 1993).

Due to its wide distribution of expression, SN exerts a diverse array of biological functions, including regulating nervous, endocrine, immune, and vascular systems (Fisher-Colbrie et al., 1995; Zhao et al., 2009b). Secretoneurin has been shown to regulate several neurotransmitter systems, for instance SN increases dopamine release from rat striatum both *in vitro* (Saria et al., 1993) and *in vivo* (Agneter et al., 1995). Expanding on this study to the substantia nigra and neostriatum, SN infusion can increase levels of glutamate, dynorphin B, dopamine, and GABA extracellularly (You et al., 1996). In the endocrine system, SN has neuroendocrine control on the vertebrate pituitary by stimulating the synthesis and release of luteinizing hormone (Zhao et al., 2006b, 2009a, 2011). Through activating vascular endothelium chemotaxis, proliferation, angiogenesis, and vascularization, SN is thought to have a significant role in tissue repair (Helle, 2010). The neurogenic properties of SN and its role in regulating inflammatory and immune responses will be discussed below. Other than its roles in physiological processes, SN is also implicated in many pathophysiological conditions of the central nervous system. In several reports, SN has been correlated with many neurological diseases such as Alzheimer disease, Parkinson disease and epilepsy (Wiedermann, 2000; Shyu et al., 2008).

1.1.4. Distribution of secretoneurin

Secretoneurin is abundant in a wide variety of nervous and endocrine tissues. A high density of immunoreactive fibers and terminals were found in several areas of the rat brain such as the lateral septum, the medial parts of the amygdala, some medial thalamic nuclei, the hypothalamus, dentate gyrus, habenula, nucleus interpeduncularis, locus coeruleus, nucleus tractus solitarii, the substantiae gelatinosae of the caudal trigeminal nucleus and of the spinal cord (Marksteiner et al., 1993; Schwarzer et al., 1997). In the brain, dense SN immunoreactivity is found in the median eminence of the rat and infundibular area of the goldfish suggesting a conserved hypophysiotropic role (Trudeau et al., 2012). In goldfish, SN-immunoreactive cell bodies were found in both the telencephalon and hypothalamus while fibers were specifically localized in the dorsal and ventral telencephalon, the periventricular preoptic nucleus, pituitary gland, and ventrocaudal aspects of the nucleus of the lateral recess and nucleus of the posterior recess (Canosa et al., 2011). The most obvious SN immunoreactivity was found in the magnocellular and parvocellular cells of the goldfish preoptic nucleus that project their fibers to the neurohypophysis of the pituitary (Canosa et al., 2011). Strikingly in the preoptic nucleus, SN-immunoreactivity is colocalized with isotocin, the fish homolog of mammalian oxytocin. This expression pattern and colocalization with isotocin or oxytocin is evolutionarily conserved between the rat and goldfish preoptic area (Marksteiner et al., 1993; Canosa et al., 2011).

The pattern of SN immunoreactivity in the anterior pituitary varies across species (Trudeau et al., 2012). Depending on the mammalian species, SN-immunoreactivity can be found to colocalize with luteinizing hormone, follicle stimulating hormone, growth

hormone, prolactin, thyroid-stimulating hormone and adrenocorticotrophic hormone (Fisher-Colbrie et al., 1995; Crawford and McNeilly, 2002; Trudeau et al., 2012). However in the goldfish pituitary, SN-immunoreactivity is restricted to lactotrophs and not gonadotrophs of the rostral pars distalis (Zhao et al., 2009a). As most cells in the pituitary express SgII, the differential expression of SN can be attributed to cell type specific SgII precursor processing.

The cerebrospinal fluid (CSF) is another major source of free SN peptide, where levels of 260 fmol/ml in ventricular CSF and 1500 fmol/ml in lumbar CSF can be found in human. These concentrations are relatively high compared to levels of other neuropeptides or CgA and CgB, which range from 20-200 fmol/ml in the same fluids (Kirchmair et al., 1994a). Secretoneurin is also distributed in various peripheral nerves and tissues. In human endocrine tissues, SN immunoreactivity is found in the adrenal medulla, thyroid, pancreas, GI tract, and the prostate (Schmid et al., 1995). Additional peripheral tissue localizations of SN include human dental bulb, carotid body, and retina (Wiedermann, 2000). In the peripheral nervous system, SN expression has been demonstrated in ganglion cells, primary afferent (C-fiber) neurons and autonomic nerves (Kirchmair et al., 1994b; Schmid et al., 1995). This pervasive expression of SN indicates a wide array of biological functions for this peptide.

1.1.5. Neurogenic properties of secretogranin II and secretoneurin

Secretogranin II is a positive regulator of neuronal differentiation and maturation. Neuronal differentiation induced by nerve growth factor in PC12 cells (Laslop and Tschernitz, 1992; Scammell et al., 1995) or human neuroblastoma cells treated with

phorbol esters (Weiler et al., 1990) is often accompanied by an increased biosynthesis of SgII. Furthermore, other neurotrophic factors such as basic fibroblast growth factor and epidermal growth factor can increase SgII expression in human neuroblastoma cells (Weiss et al., 2001). These data shows that the up-regulation of SgII is a characteristic of phenotypic differentiation after neurotrophic growth factor treatment. The ability of a neural stem cell to differentiate and acquire a neuronal phenotype is regulated intrinsically by transcription factors such as RE-1 silencing transcription factor (REST). As a master negative regulator of neuronal differentiation, REST controls neurogenesis by repressing neuronal gene expression. Secretogranin II is a major REST-regulated secreted factor that promotes the differentiation and maturation of hippocampal progenitors *in vitro* (Kim et al., 2015). Loss-of-function of *scg2* repressed differentiation while exogenous SgII partially rescued this phenotype; therefore REST mediates non-cell-autonomous neuronal differentiation and maturation via SgII acting in a paracrine manner (Kim et al., 2015).

After endoproteolytic processing of SgII, the resultant SN neuropeptide has trophic properties. In cultured immature mouse cerebellar granule cells *in vitro* SN promotes neurite outgrowth, a measure of differentiation, in a concentration-dependent manner. Exposure to pertussis toxin inhibited SN-induced outgrowth, suggesting SN causes neurite outgrowth by acting through a G-protein-coupled mechanism. This suggests that SN acts as a trophic substance involved in the differentiation of cerebellar granule cells (Gasser et al., 2003).

The functions of SN share parallels to those of glial cell-derived neurotrophic factor (GDNF), in respect to growth (Jögi et al., 2004; Kirchmair et al., 2004a; Srinivasan

et al., 2005) and repair (Gasser et al., 2003; Lu et al., 2003; Kirchmair et al., 2004b) of injured neural tissue. In murine models of stroke SN promotes neuroprotection and neuronal plasticity (Shyu et al., 2008). During cerebral ischemia, SN expression increases in both rodents and humans. SN mediates its neuroprotective effects *in vitro* in primary cortical cell (PCC) culture by reducing lactate dehydrogenase activity and increasing neuronal survival under oxygen/glucose deprivation. Both *in vivo* and *in vitro*, SN treatment significantly attenuates apoptotic enzyme caspase-3 activity and upregulates expression of antiapoptotic proteins Bcl-2 and Bcl-xL through the Jak2/Stat3 pathway. This suggests SN promotes neuroprotection through an antiapoptotic effect. Intravenous administration of SN in rats following cerebral ischemia resulted in less cerebral infarction, improved motor performance, and increased brain metabolic activity. Furthermore, SN not only promotes neuroprotection, but can also enhance neurogenesis. Secretoneurin increased the mobilization of endogenous stem cells to ischemic areas of the brain and promoted these engrafted stem cells to differentiate into neural cells (Shyu et al., 2008).

1.1.6. Secretoneurin regulates inflammatory and immune responses

Neurogenic inflammation is the process resulting from the release of pro-inflammatory neuropeptides from sensory neurons in the periphery (Wiedermann, 2000). Upon injury leukocytes and mesenchymal cells migrate and accumulate in the injured tissue, secrete cytokines and chemokines, proliferate, and aid in tissue remodeling. Neuropeptides released from sensory nerves in part elicit these cellular responses to neurogenic inflammation (Wiedermann, 2000). In sensory C-fibers, SN is colocalized

and released with other neuropeptides suggesting SN is involved in neurogenic inflammation (Marksteiner et al., 1993). In response to injury, both *in vivo* and *in vitro*, SN can stimulate the migration of human monocytes also acting synergistically with other sensory neuropeptides such as substance P or somatostatin (Reinisch et al., 1993). Similar to other chemoattractants, SN triggers migration of monocytes through a G-protein coupled protein kinase C activation and intracellular Ca^{2+} release signaling pathway (Schratzberger et al., 1996b). Furthermore, SN facilitates the transmigration of monocytes across the endothelial layer, this transendothelial migration is often the initial step in inflammatory processes (Kahler et al., 1999). Secretoneurin is also an effective chemoattractant for human eosinophils comparable in its potency to interleukin-8 and requiring the activation of phosphodiesterases (Dunzendorfer et al., 1998b). Other than monocytes and eosinophils, SN can induce chemotaxis of neutrophils but not at physiologically relevant concentrations between 1 nM and 1000 nM (Reinisch et al., 1993). However, pretreatment of neutrophils with SN reveals possible priming actions such as increase in random locomotion and inhibition of chemoattractant-stimulated migration (Schratzberger et al., 1996a). Secretoneurin exerts a combination of chemotactic and antiproliferative effects on endothelial cells, suggesting that SN acts as a regulatory peptide of vascular cell functions (Kähler et al., 1997). Further establishing the functions of SN as a sensory neuropeptide, SN can trigger the selective migration of human fibroblasts but does not stimulate their proliferation (Kähler et al. 1996).

1.1.7. Secretoneurin receptor and signal transduction pathways

Binding sites were identified on a human monocyte cell line (Mono Mac 6) with a K_d value of 7.3 nM. Interestingly, during competition studies the 15 C-terminal amino acids of SN were able to displace SN while other shorter SN peptide fragments were unsuccessful (Schneitler et al., 1998). An additional study demonstrated SN interacts with a specific cell surface binding site on human monocytes with a similar K_d value of 14.5 nM and other chemoattractants could not compete for SN binding sites (Kong et al., 1998). Although these studies suggest functional monocyte cell surface receptors for SN, the SN receptor has yet to be identified but is believed to be a G-protein coupled receptor. Several studies indicate SN effects are sensitive to pertussis toxin lending support to the hypothesis that SN receptor is a pertussis toxin-sensitive G-protein (Schratzberger et al., 1996b; Kong et al., 1998; Gasser et al., 2003). In mouse LβT2 gonadotropin cells, SN increases cyclic AMP (cAMP) and activates both protein kinase A (PKA) and protein kinase C (PKC) causing the subsequent activation of extracellular signal-regulated kinase (ERK) signaling pathways (Zhao et al., 2011). Secretoneurin also mediates its effects on mouse endothelial progenitor cells in the inflammatory system through ERK-dependent pathways (Kirchmair et al., 2004a). In both human monocytes (Schratzberger et al., 1996b) and goldfish gonadotrophs (Zhao et al., 2011) SN activates PKC and induces a rise in intracellular Ca²⁺ levels.

There is also evidence to support SN acting through a non-G-protein coupled receptor growth factor-like signaling cascade (Zhao et al., 2010). For instance, SN exerts neuroprotective effects in models of stroke through the activation of antiapoptotic proteins via the Jak/Stat3 signal transduction pathway (Shyu et al., 2008). SN can also

induce vasculogenesis through activation of the Akt signaling pathway (Kirchmair et al., 2004a). Due to the activation of several different transduction pathways, there may be several SN receptor types, or a single receptor converging on several signaling pathways (Zhao et al., 2010). Although investigations have identified SN binding sites and potential signal transduction pathways, remaining work is needed to isolate, clone and express the putative SN receptor.

1.2. Radial glial cells

Radial glial cells (RGCs) are a glial cell type differentiated from neuroepithelial cells in the developing CNS of all vertebrates. During development RGCs symmetrically divide generating more RGCs that expand along the developing lateral ventricles (Schmechel and Rakic, 1979). As development progresses, RGCs predominately undergo asymmetric cell division where one daughter cell remains an RGC while the other becomes an intermediate progenitor or a neuron. Ultimately at the end development, the RGC population diminishes by undergoing neurogenesis and/or gliogenesis to produce neurons, astrocytes, and oligodendrocytes (Radakovits et al., 2009). Morphologically, RGCs are characterized by their bipolar shape with a periventricular cell body and an elongated radial fiber terminating with endfeet on the walls of blood vessels or at the pial surface (Barry et al., 2014). Because of this radial morphology, they function to structurally organize the CNS serving as a scaffold for neuronal migration and axonogenesis (Rakic, 1971; Silver et al., 1982).

In mammals, RGCs are mainly a transient cell type during development with only two populations remaining in adulthood – the anterior part of the subventricular zone of

the lateral ventricle and subgranular zone of the dentate gyrus. These two areas are the only constitutive neurogenic regions of the adult mammalian brain, which helps to explain the limited capacity for neurogenesis in mammals (Brunne et al., 2010; Ming and Song, 2011). In contrast, the teleostean brain has remarkable proliferative and regenerative capacities due to numerous brain neurogenic zones (Alunni and Bally-Cuif, 2016). The zebrafish brain for example has 16 different loci of proliferation and neurogenesis that give rise to new neurons explaining why teleost fish exhibit the most pronounced and widespread adult neurogenesis of any vertebrate studied thus far (Zupanc, 2006; Kaslin et al., 2008). Interestingly, teleost fish and other non-mammalian vertebrates have the persistent abundance of RGCs throughout adulthood, which may largely contribute to their extensive neurogenic capabilities (Strobl-Mazzulla et al., 2010). In support of the RGC subpopulation contributing to neurogenesis, studies have reported that newborn neuroblast cells arising from adult RGCs can differentiate into neurons in zebrafish (Kroehne et al., 2011; Diotel et al., 2013).

In the brain of teleost fish, RGCs are the predominant type of macroglial cells (Kálmán, 1998). Since fish lack typical stellate astrocytes like those found in the mammalian CNS, RGCs may serve multiple functions in fish to compensate for not having differentiated astrocytes typical of the mammalian brain (Lyons et al., 2014). One of the main functions of mammalian astrocytes is to regulate ionic and water homeostasis in the CNS. The main water channel of the vertebrate brain is aquaporin-4 expressed by astrocytes in a highly polarized manner. Aquaporin-4 is found in astrocyte perivascular endfeet (blood-brain barrier) and subpial and subependymal processes (CNS-CSF interfaces) (Papadopoulos and Verkman, 2013). This distribution of aquaporin-4 in

astrocytes suggests that aquaporin-4 controls water flow into and out of the brain (Tait et al., 2008). Zebrafish RGCs may retain this ability to regulate water homeostasis as they express aquaporin-4 protein not in a polarized fashion but distributed along the entire radial extent of the cell (Grupp et al., 2010). Astrocytes also function to buffer potassium (K^+) ions released extracellularly as a result of neuronal activity (Simard and Nedergaard, 2004). Astrocytes facilitate K^+ clearance through inwardly rectifying K^+ channel Kir4.1 and other astrocyte K^+ transporters (Papadopoulos and Verkman, 2013). Although no extensive studies have investigated the role of fish RGCs in buffering extracellular K^+ but given RGCs are the predominate fish macroglia, RGCs may have K^+ buffering capacity in order to effectively optimize the extracellular space for synaptic transmission. Both mammalian astrocytes and zebrafish RGCs share the ability of glutamate clearance via glutamate transporter GLT1 (McKeown et al., 2012). Acting as the major excitatory neurotransmitter in the brain, extracellular glutamate levels must be prevented from reaching excitotoxic levels (Theodosis et al., 2004). Since fish RGCs exhibit extensive interactions with neurons and share functions with mammalian astrocytes in regulating the interstitial space through ion, water and neurotransmitter homeostasis, fish RGCs are thought to be active participants in the tri-partite synapse.

1.2.1 Steroidogenic capacity of radial glial cells

The vertebrate brain is a steroidogenic organ capable of producing neurosteroids *de novo* or from peripheral precursors and is a target of steroid hormone action given the distribution of various steroid hormone receptors in the brain (Diotel et al., 2011a). In the steroidogenic pathway, aromatase is the only enzyme capable of converting androgens

into estrogens. The adult fish brain exhibits high aromatase activity compared to other vertebrates due to the expression of one of two aromatase genes, being about 100-1000 more active than in mammals (Callard et al., 1981; Pasmanik and Callard, 1988). In the teleost lineage, a genome duplication created two forms of the ancestral *cyp19a1* gene – *cyp19a1a* (aromatase A) expressed mainly in the gonads and *cyp19a1b* (aromatase B) expressed in the brain (Tchoudakova and Callard, 1998). Remarkably, *cyp19a1b* is expressed solely by RGCs in developing and adult fish, giving RGCs an estrogen-synthesizing role in the fish brain (Forlano et al., 2001). The localization of aromatase B in fish RGCs is distinct, given that aromatase in the brain of adult mammals, birds, and amphibians is mainly localized in neurons and reactive astrocytes (Sanghera et al., 1991; Balthazart and Ball, 1998; Peterson et al., 2005). Mechanical injury, excitotoxicity, and inflammation can induce aromatase expression in mammalian and avian astrocytes and RGCs (Garcia-Segura et al., 1999; Saldanha et al., 2013). Furthermore, one study documented aromatase expression in rat RGCs during CNS development (Martinez-Galan et al., 2004) Given the transient presence of RGCs in mammalian CNS development, fish models are optimal to study potential neurosteroidogenic roles of RGCs (Xing et al., 2014).

Steroid hormones are synthesized from cholesterol by a series of enzymes, including cytochrome P450 side chain cleavage (StAR; CYP11a1), 3-beta-hydroxysteroid dehydrogenase (3 β -HSD; HSD3B1), cytochrome P450 17-alpha-hydroxylase (CYP17a1), 17-beta-hydroxysteroid dehydrogenase (17 β -HSD; HSD17B1), 5 α reductase, and cytochrome P450 aromatase (CYP19a1) (Mellon et al., 2001). In all vertebrate classes, most of these enzymes are expressed in the brain allowing for *de novo*

steroidogenesis of neurosteroids (Do Rego et al., 2009; Diotel et al., 2011b). Strikingly, in the zebrafish brain, CYP11a1, CYP17a1, and 3 β -HSD share similar expression patterns with aromatase B predominantly found in the telencephalon, the preoptic area, the hypothalamus, and the cerebellum (Diotel et al., 2011b). Moreover, StAR, 3 β -HSD, and CYP17a1 were successfully cloned from cultured goldfish RGCs indicating RGCs have the potential of *de novo* estrogen synthesis from cholesterol and the production of steroid intermediates such as 17 α -hydroxypregnenolone and 17 α -hydroxyprogesterone (Xing et al., 2014).

The reasons for the cell-specific expression of aromatase B in RGCs of teleost fish are poorly understood. Studies in the Japanese eel, a basal teleost, reveal they have a single *cyp19a1* gene expressed only in RGCs. This provides evolutionary insight that indicates the expression pattern of *cyp19a1b* in teleost fish did not evolve after the genome duplication but rather reflect properties of the ancestral *cyp19a1* gene (Jeng et al., 2012). In the adult teleost fish, RGCs expressing aromatase B are neuronal progenitors that allow for considerable brain growth suggesting there is a role of aromatase and estradiol in neurogenesis (Pellegrini et al., 2007). Interestingly in mammals, aromatase can be expressed in reactive astrocytes after lesions or in RGCs adjacent to the lesion in birds, giving support to neuroprotective effects of estrogens (Garcia-Segura et al., 1999; Saldanha et al., 2013). Neuroestrogens have been well investigated in mammalian models for their neuroprotective and antiapoptotic properties in neurogenesis and brain repair (Garcia-Segura, 2008; Saldanha et al., 2009; Scott et al., 2012). However in teleost fish brain, the effects of estrogen on cell proliferation and neurogenesis remain inconclusive. In male zebrafish brain, blockade of nuclear estrogen receptors or inhibition of aromatase

caused an increase in proliferative cell nuclear antigen (PCNA)-positive cells in specific proliferative zones while 17- β estradiol treatment decreased the proliferative activity of several brain regions (Diotel et al., 2013). Likewise, another study administering 17- β estradiol in adult female zebrafish observed brain region-specific decreases in the number of proliferative cells (Makantasi and Dermon, 2014). Although these two studies contrast findings using mammalian models, Xing et al. found that in female goldfish, neurotoxin-induced transcripts related to dopamine neuron regeneration, RGC activation, and neurotrophic factor production and these responses were all aromatase dependent, implicating estrogens in neuroprotective mechanisms after neurotoxin insult (Xing et al., 2016b). Future work is needed to elucidate the action of estradiol in the highly plastic teleost brain focusing on various factors such as dose, duration of treatment, species, brain region, age and sex.

1.2.2. Radial glial cells and neurogenesis

One of the fundamental features in the CNS of teleost fish that sets them apart from mammals is their enormous capacity for post-embryonic neurogenesis. Within the adult teleostean brain several proliferative zones contain a heterogeneous population of progenitors where RGCs represent a subpopulation capable of proliferation and differentiation into other cell types (Rothenaigner et al., 2011). These proliferation zones generate new neurons that migrate over long distances using radial glial fibers (Zupanc and Clint, 2003; Pellegrini et al., 2007). Within the zebrafish brain about 50% of all adult-born cells express the neuron-specific protein Hu, indicating the new cells produced by the proliferative capacity of the zebrafish brain do differentiate into neurons (Zupanc

et al., 2005; Hinsch and Zupanc, 2007). Interestingly, new neurons are most abundant in the dorsal telencephalon, a brain region proposed to be homologous to the mammalian hippocampus, representing one of the only two neurogenic regions in the mammalian brain (Salas et al., 2003)

The distinctive ability for elevated levels of adult neurogenesis also presents the teleostean brain with the ability of compensatory neurogenesis or regeneration following brain injuries (Kaslin et al., 2008). The first major response to post-injury is the increases in apoptotic cells to ensure rapid removal of damaged cells (Zupanc et al., 1998). This is followed by an acute inflammatory response where the density of microglia and leukocytes increases (Kroehne et al., 2011). Following injury, RGCs react to inflammatory signals by increasing their fiber density and proliferation (Clint and Zupanc, 2001; Kroehne et al., 2011; Kyritsis et al., 2012). Finally, reactive proliferation by RGCs increases levels of neurogenesis and produces mature neurons. Therefore, in this way, RGCs provide a major cell population that actively responds to brain insult, increase proliferation, and give rise to neuroblasts that migrate to the site of injury and differentiation into neurons (Kroehne et al., 2011).

1.2.3. Neuronal control of radial glial cell functions

As outlined above, two main roles of RGCs in the fish brain are in neurosteroidogenesis and neurogenesis. Consequently this cell type must be under tight control to regulate production of neurosteroids and the proliferation and differentiation of this progenitor cell population. Given the intimate relationship between neurons and glia in the brain, neurons may exert synaptic control over RGCs through the release of

neurotransmitters, neuropeptides, or hormones. Very little is known about the function of neuronal-RGC interactions, however recent studies suggest RGCs are under the control of two key neurotransmitters. Dopamine (DA), specifically through *in vivo* D1 receptor activation, regulates glial fibrillary acidic protein (GFAP) expression in female goldfish hypothalamus (Popesku et al., 2010). Other studies using cultures of goldfish RGCs demonstrated that D1 receptor activation increases *cy19a1b* mRNA levels while regulating protein networks associated with progenitor cell functions, providing further support for DA regulation of RGCs (Xing et al., 2015b, 2016a). Furthermore, RGCs are under the control of serotonin (5-HT), as 5-HT neurons share a close distribution with RGCs in the zebrafish paraventricular organ and *in vivo* inhibition of 5-HT synthesis decreases RGC proliferation (Pérez et al., 2013). Although the role of neurotransmitters on the control of the RGC physiology are beginning to be understood, less information exists on the effects of neuropeptides on the regulation of this cell type.

Chapter 2: Interactions between secretoneurin-A and radial glial cells in the preoptic area – implications for control of neurosteroidogenesis

2.1. Introduction

The radial glial cell (RGC) is a bipolar-shaped cell type in the central nervous system (CNS) of all vertebrates (Schmechel and Rakic, 1979). Attributed to their radial morphology, RGCs structurally organize the CNS serving as a scaffold for neuronal migration and axonogenesis (Rakic, 1971; Silver et al., 1982). As stem-like cells RGCs are capable of further development to give rise to neurons or other glial cells (Radakovits et al., 2009). At the end of mammalian CNS development, RGC populations diminish, differentiating into other cell types. However, in teleost fish RGCs remain abundant throughout adulthood contributing to high levels of neurogenesis and high regenerative abilities (Pellegrini et al., 2007; Strobl-Mazzulla et al., 2010). Another exceptional feature of fish RGCs is their ability of neuroestrogen production because they are the exclusive cell type in the teleost brain to produce the estrogen synthesizing enzyme, aromatase B (*cyp19a1b*) (Forlano et al., 2001; Tong et al., 2009). Aromatase B expressing RGCs are found throughout the teleost brain, however the periventricular layer of the preoptic area that lines the third ventricle has the highest aromatase B-immunoreactivity (Goto-Kazeto et al., 2004; Menuet et al., 2005; Diotel et al., 2010a). Recently, other steroidogenic enzymes have been cloned from cultured goldfish RGCs, suggesting this cell type is also capable of producing other steroid intermediates (Xing et al., 2014). As RGCs play a key role in both neurosteroidogenesis and neurogenesis in the

brain, it is important to discover the permissive factors and signaling mechanisms that control these functions.

Previous investigations have shown that RGCs are under the control of several neurotransmitters, such as dopamine (Popescu et al., 2010; Xing et al., 2015b, 2016a) and serotonin (Pérez et al., 2013), demonstrating the importance of neuronal-RGC interactions in the regulation of this cell type. Nonetheless, little research exists on the effects of neuropeptides on the control of RGC physiology. Interestingly, the preoptic nucleus contains dense populations of neurons expressing a neuropeptide called secretoneurin (SN) (Canosa et al., 2011) and through neuronal-glia communication may regulate the large RGC population in the preoptic nucleus. SN is produced by endoproteolytic processing of its precursor protein secretogranin II (SgII) and is found in dense-core secretory granules in a wide variety of cell types of the endocrine and nervous systems (Kirchmair et al., 1993; Fisher-Colbrie et al., 1995). SgII belongs to the chromogranin family that is characterized by its location in secretory granules, acidity, and heat-stability (Huttner et al., 1991). In teleost fish there are two SgII genes, SgIIa and SgIIb, which produce their respective SNa and SNb peptides caused by the whole genome duplication process that occurred around the teleost emergence (Zhao et al., 2010). The precursor protein SgII is poorly conserved in fish with exception of the central SN domain which is conserved from fish to mammals (Zhao et al. 2009). Several biological functions have been reported for SN including regulating nervous, endocrine, immune, vascular systems (Fisher-Colbrie et al., 1995; Zhao et al., 2009b). Some of these include, stimulating dopamine release (Saria et al., 1993; Agneter et al., 1995) and luteinizing hormone release (Zhao et al., 2006b, 2009a, 2011), chemotaxis of various

cells of the immune system (Reinisch et al., 1993; Dunzendorfer et al., 1998b, 2001), promoting neuroprotection and neuroplasticity (Shyu et al., 2008), and stimulating neurite outgrowth in cerebellar granule cells (Gasser et al., 2003).

In goldfish SNa-immunoreactivity was found in many parts of the forebrain, however the most obvious SNa-immunoreactivity was found in the magnocellular and parvocellular neurons of the preoptic area co-localizing with isotocin, the fish homolog of mammalian oxytocin (Canosa et al., 2011). The preoptic area contains the most aromatase B expressing RGCs in the fish brain (Diotel et al., 2010a), however the relationship between RGCs and SNa-positive neurons in this area have yet to be elucidated. Therefore, the objectives of this study are to investigate the neuroanatomical relationship between SNa-positive neurons and RGCs in both goldfish and zebrafish species and to determine if this neuronal-RGC interaction through SNa can regulate the neurosteroidogenic capacity of RGCs.

2.2. Materials and methods

2.2.1. Experimental animals

All procedures used were approved by the University of Ottawa Protocol Review Committee and followed standard Canadian Council on Animal Care guidelines on the use of animals in research. Common adult female goldfish (*Carassius auratus*) were purchased from a commercial supplier (Mt. Parnell Fisheries Inc., Mercersburg, PA, USA) and allowed to acclimate for at least 3 weeks prior to experimentation. Goldfish were maintained at 18 °C under a stimulated natural photoperiod and fed standard flaked goldfish food. This study aimed to confirm that *cyp19a1b*-positive RGCs were in close proximity to SNa-positive neurons in the preoptic area were in close proximity. No antibody against goldfish aromatase B exists therefore the transgenic *cyp19a1b*-GFP zebrafish (*Danio rerio*) line was used, generously donated by O. Kah and B.C. Chung (Tong et al., 2009). These animals were held in the closed re-circulated facility at the University of Ottawa and maintained at 28.5 °C and on a 14-10 h light-dark cycle. Sexually mature female goldfish (18–35 g) and 6-8 month old sexually mature female zebrafish were anesthetized using 3-aminobenzoic acid ethylester (MS222) for all handling and dissection procedures.

2.2.2. Immunohistochemistry

Brains were carefully dissected on ice and fixed overnight in 4 % paraformaldehyde (PFA) in phosphate buffered-saline (PBS; pH 7.4) at 4 °C. Fixed brains were then washed twice in PBS and placed in 30 % sucrose overnight. Brains were embedded in optimum cutting temperature (O.C.T.) compound (Tissue-Tek), frozen using liquid nitrogen and stored at -80 °C. Embedded tissue was sectioned using a

cryostat (Leica CM3050S) with a 14 µm thickness. Cryosections were transferred onto Superfrost Plus slides (Fisher) and stored at -20 °C until further use.

Frozen sections were allowed to thaw for 1 h at RT followed by a 45 min incubation in blocking buffer (0.3 % Triton PBS containing 1 % milk powder) at RT. For zebrafish brain sections antigen retrieval in sodium citrate buffer (0.1 M; pH 7.1) for 1.5 h at 63 °C was performed before blocking for non-specific binding. Sections were incubated overnight at 4 °C in PBS containing 1 % milk powder with either of the following antibodies: anti-porcine GFAP (mouse, 1:700, Millipore, MAB360) (Forlano et al., 2001), anti-GFP (mouse, 1:500, Rockland Antibodies, 600-301-215), and previously validated anti-goldfish SN (rabbit, 1:500) (Zhao et al., 2009a). The anti-goldfish SN antibody was generated against the most conserved domain of vertebrate SN and has been tested extensively for specificity (Zhao et al., 2009a; Canosa et al., 2011; Pouso et al., 2015). On the following day, sections were washed twice in PBS and incubated with donkey anti-rabbit Alexa fluor 594 (1:100, Invitrogen, A-21207) and donkey anti-mouse Alex fluor 488 (1:500, Invitrogen, R37114) diluted in blocking buffer for 1 h at RT. Finally, slides were washed twice in PBS and mounted with anti-fading Vectashield medium with 4,6-diamino-2-phenylindole (DAPI) (Vector Laboratories). Images were taken with either Zeiss Axiophot microscope or FV1000 Laser Scanning Olympus confocal microscope.

2.2.3. Intracerebroventricular injection of secretoneurin-A

Samples of hypothalamus and telencephalon were taken from a previous experiment by Mikwar et al., 2016. Briefly, goldfish were injected into the third brain ventricle with 0.2 and 1.0 ng/g goldfish SNa synthesized as previously reported (Zhao et

al., 2006b). A flap was cut into the skull and 2 μ l of test solution (either saline or SNa) was injected into the third brain ventricle using a 5 μ l Hamilton micro syringe (Model 75N, 5 μ l, SYR s6S/2/3) and stereotaxic apparatus under a dissecting microscope following the +1.0, M, D 1.2 coordinates from the goldfish forebrain stereotaxic atlas (Peter and Gill, 1975). The skull flap was then held in place using tissue adhesive (VetBond, 3M) and fish were returned to their tanks, and sacrificed following anesthesia and spinal transection, and the telencephalon and hypothalamus carefully dissected 2 or 5 h later.

2.2.4. Cell culture and exposure

The possible direct effects of SNa on RGC was tested using previously established and validated cell culture methods (Xing et al., 2015b). In short, the hypothalamus and telencephalon were dissected from female goldfish and rinsed twice with Hanks Balanced Salt Solution (HBSS; 400 mg KCl, 600 mg KH_2PO_4 , 350 mg NaHCO_3 , 8 g NaCl, 48 mg Na_2HPO_4 , and 1 g D-Glucose in 1 L ddH₂O) with Antibiotic-Antimycotic solution (Gibco) and minced into small explants. Radial glial cells were dissociated with trypsin (0.25 %; Gibco) and cultured in Leibovitz's L-15 medium (Gibco) with 15 % Fetal Bovine Serum (FBS; Gibco) and Antibiotic-Antimycotic. Cell culture medium was changed 4–7 days after isolation and then once a week thereafter. Radial glial cells were subcultured by trypsinization (0.125 %) for 3 passages then used for experimentation. Stock solutions of synthetic goldfish SNa peptide were made in water and stored at -20 °C until use. Aliquots were thawed on ice then diluted to desired concentrations in serum-free media. Cells were exposed for 24 h to various concentrations of goldfish SNa.

2.2.5. RNA extraction, cDNA synthesis, and qRT-PCR

Total RNA was extracted using RNeasy Micro Kit (Qiagen) including an on-column DNase treatment to remove genomic DNA. After extraction, the concentration and purification ratio of absorbance of 260/280 nm and 260/230 nm was assessed using a NanoDrop ND-1000 spectrophotometer (Thermo Scientific). Total cDNA was prepared using Maxima cDNA synthesis kit (Thermo Scientific) from 1 µg for hypothalamic samples, 2 µg for telencephalic samples, and 1 µg for RGC samples. Primers were designed using Primer3 (Untergasser et al., 2012) and synthesized by Integrated DNA Technologies (Table 2.1). Primer sets were tested for specificity by running the qRT-PCR product on a 1 % agarose containing SYBR Safe DNA gel stain (Invitrogen) to ensure a single product was produced from each reaction. Each product was gel extracted using NucleoSpin Gel and PCR Clean-up kit (Macherey-Nagel) and sequenced to confirm primer specificity by StemCore Laboratories at the Ottawa Hospital Research Institute. qRT-PCR analyses were conducted using the Maxima SYBR green qPCR Master Mix (Thermo Scientific) and CFX96 Real-Time PCR Detection System (Bio-Rad) to amplify the genes of interest. The thermal cycling parameters were: a single cycle Taq activation step at 95 °C for 3 min, followed by 40 cycles of 95 °C denaturation step for 10 s and primer annealing at 56-63 °C for 30 s. After 40 cycles, a melt curve was performed from a range of 65-95 °C with increments of 0.5 °C to ensure a single amplified product. Relative mRNA abundance was calculated using the relative standard curve method based on C_q values and normalized using NORMA-GENE algorithm (Heckmann et al., 2011) for *in vitro* data while *in vivo* data was normalized against the expression of the

18S reference gene. Normalized data were used to calculate fold-change against the average of control.

Table 2.1. Primers (5'→3') used for qRT-PCR

Gene	Primer Sequence (Forward)	Primer Sequence (Reverse)
<i>cyp19a1b</i>	TGCTGACATAAGGGCAATGA	GGAAGTAAAATGGGTTGTGGA
<i>star</i>	AGAGTGCCAATGGTGATAAGGT	GGTCCACTCCCCCATTTGTT
<i>hsd17b4</i>	TCAGTTCTCGCTCTTCA TCGT	GTTCCAGTCTCCGCTCAA TC
<i>cyp17</i>	AGAGTGCCAATGGTGATAAGGT	GGTCCACTCCCCCATTTGTT
<i>18s</i>	AAACGGCTACCACATCCAAG	CACCAGATTTGCCCTCCA

2.2.6. Statistics

All statistical analyses were conducted using IBM SPSS Statistics Version 22. Before analysis, data was tested for normality (Shapiro-Wilk's test) and homogeneity of variance (Levene's test). Data that were not normally distributed were transformed to meet parametric assumptions. For normally distributed data, comparison between groups were performed using one-way analysis of variance (ANOVA) followed by a Tukey post-hoc or Dunnett's post-hoc test if the data did not pass Levene's test of homogeneity of variance. For data that were non-normally distributed a Kruskal-Wallis non-parametric test was used to determine if data varied across treatments. If differences were detected, a

non-parametric Mann-Whitney *U*-test was performed to determine which treatments were different from each other. Normally distributed data are expressed as mean + SEM while non-normally distributed data are presented as median values with interquartile range (25-75 %) and minimum-maximum range. A P value less than 0.05 was considered to be statistically significant.

2.3. Results

2.3.1. Close anatomical relationship between secretoneurin-A-immunoreactive neurons and radial glia

Immunohistochemical analysis show for the first time the close anatomical proximity between SNa-positive cell bodies and GFAP-positive RGC fibers in the goldfish preoptic nucleus (Fig. 2.1D,H). Heavily labeled SNa-immunoreactive cell bodies (Fig. 2.1A,E) of the magnocellular and parvocellular neurons were observed in the periventricular preoptic nucleus. Note the strong staining in the cytoplasm but not the nucleus of these cell. These SNa-immunoreactive somas are embedded and often make direct contact with GFAP-positive RGCs in the periventricular layers of the preoptic nucleus with RGC fibers projecting ventrolaterally through the parenchyma (Fig. 2.1B,F). In order to investigate this similar anatomical relationship but with aromatase B-positive RGCs, *cyp19a1b*-GFP transgenic zebrafish were used as both validated SNa and aromatase B antibodies were produced in the same host. Intensely SNa-labeled cell bodies, again with strongly labeled cytoplasm and voided nucleus (Fig. 2.2A) were lining the ventricular surface of the zebrafish preoptic nucleus and share a close proximity with *cyp19a1b*-positive RGC fibers (Fig. 2.2D). RGCs are found between the ventricular surface and the SNa-immunoreactive cell bodies with their fibers coursing ventrolaterally (Fig. 2.2B).

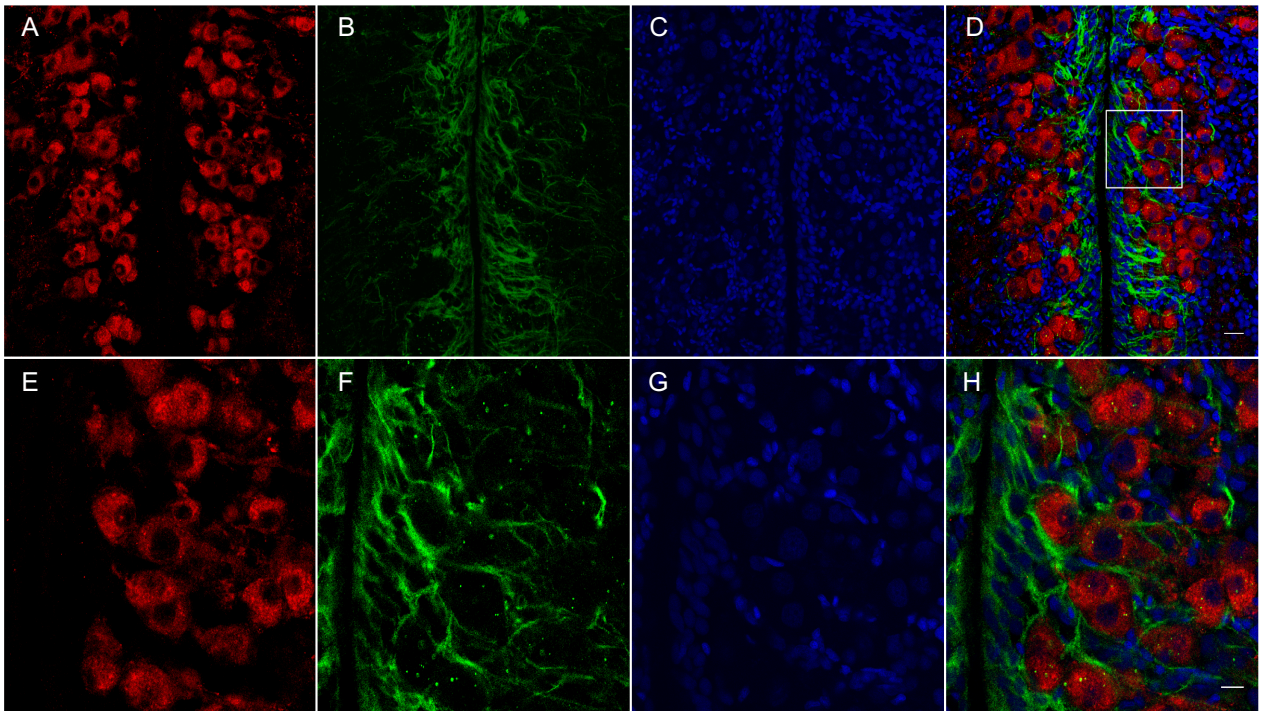


Figure 2.1. Immunofluorescence against SN (red) and GFAP (green) in the goldfish periventricular preoptic nucleus. In this transverse brain section both magnocellular and parvocellular cell bodies are SN-ir (Fig. 2.1A,E) and are surrounded by widely distributed GFAP-ir RGC fibers (Fig. 2.1B,F). The nuclear stain DAPI (blue) is also shown (Fig. 2.1C,G). Scale bar in panel D = 20 μm and in panel H = 10 μm .

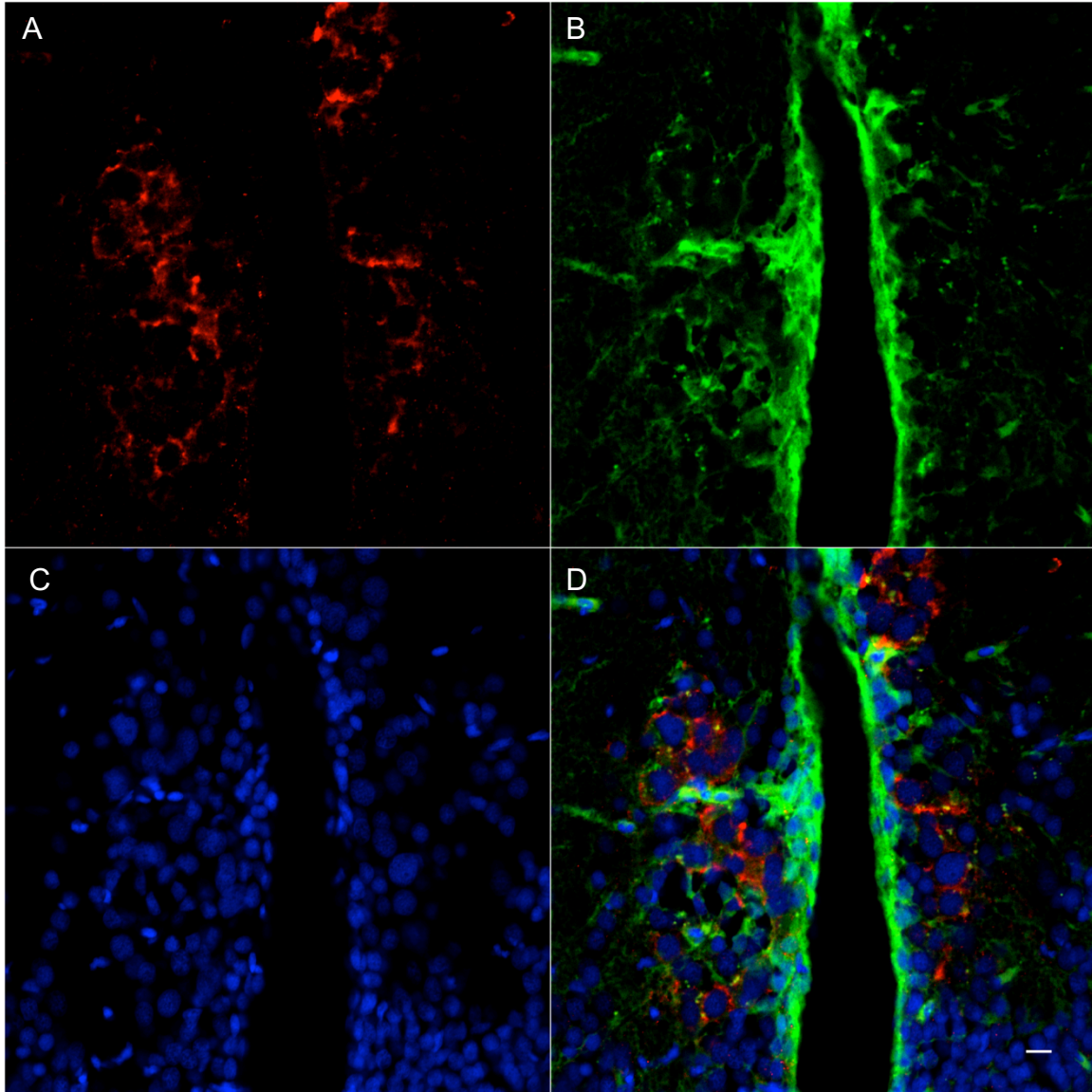


Figure 2.2. Immunofluorescence against SN (red) and GFP (green) in the zebrafish *Tg(cyp19alb-GFP)* transgenic line. In this transverse brain section of the preoptic nucleus magnocellular cell bodies are SN-ir (Fig. 2.3A) and are surrounded by widely distributed GFP-ir RGC fibers (Fig. 2.3B). The nuclear stain DAPI (blue) is also shown (Fig. 2.3C). Scale bar = 45 μ m.

2.3.2. Intracerebroventricular injection of secretoneurin-A affects the expression of *cyp19a1b*

Female goldfish were injected with SNa into the third brain ventricle, targeting the preoptic nucleus, to determine the *in vivo* effects of SNa on neuroestrogen production via *cyp19a1b*. Tissue-specific effects were observed two hours post-injection. At two hours post-injection both doses did not affect *cyp19a1b* mRNA levels ($P > 0.05$) in the hypothalamus (Fig. 2.3A). In contrast, the low dose of SNa (0.2 ng/g) elicited a 147 % increase ($P < 0.05$) in *cyp19a1b* mRNA abundance in the telencephalon (Fig. 2.3B). At five hours post-injection, both 0.2 and 1.0 ng/g SNa decreased *cyp19a1b* mRNA levels by 86 % ($P < 0.05$) and 61 % ($P > 0.05$), respectively in the hypothalamus (Fig. 2.3C), and by 88 % ($P < 0.05$) in the telencephalon (Fig. 2.3D).

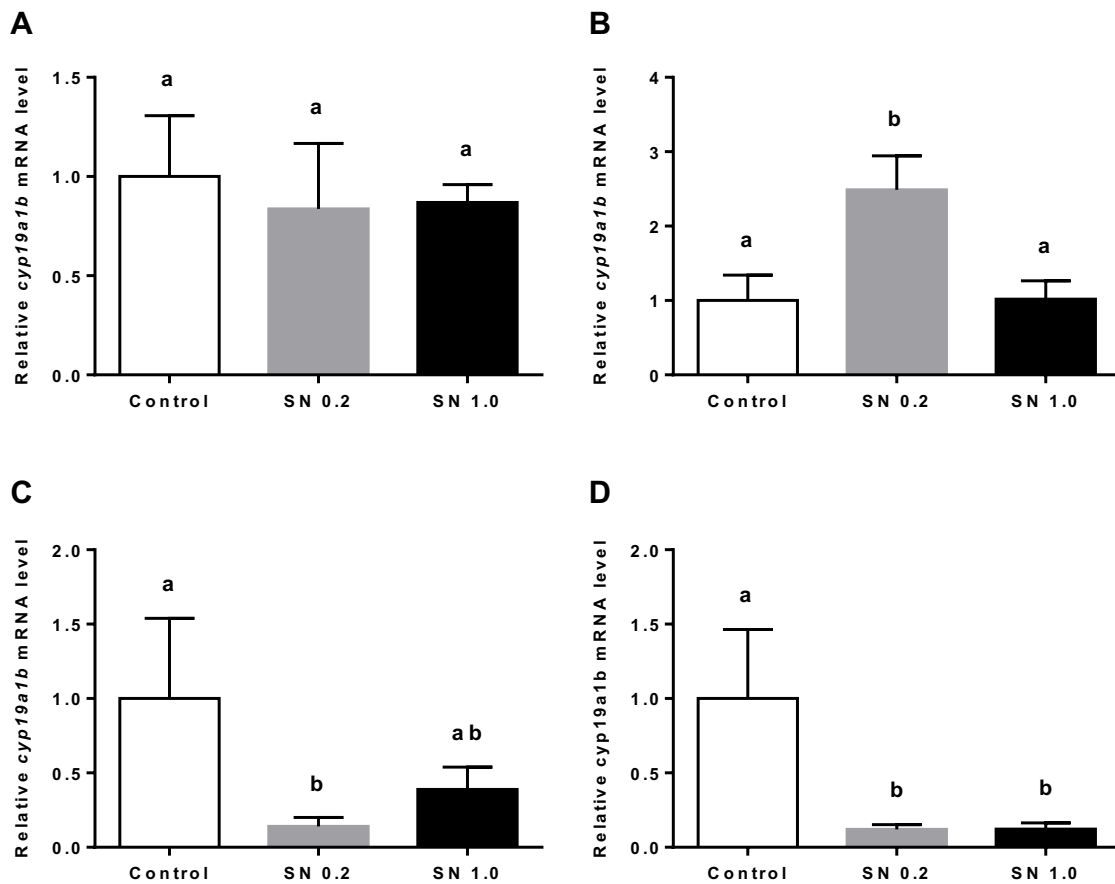


Figure 2.3. Quantitative real-time PCR analysis showing the effect of ICV injection on SNa at 0.2 ng/g and 1 ng/g on relative *cyp19a1b* mRNA levels in female goldfish brain. Hypothalamic and telencephalic *cyp19a1b* mRNA levels two hours (A and B respectively) and five hours (C and D respectively) following SNa injection. Data were normalized and defined as fold change relative to control. Bars represent the mean + SEM (n = 8-12). Groups marked by different letters are significantly different (P < 0.05).

2.3.3. Secretoneurin-A affects the expression of steroidogenic enzymes in radial glia cultures

To study the possible direct effects of SNa on steroidogenesis, primary cultures of female goldfish RGCs were exposed to various doses of SNa. There were no significant differences ($P > 0.05$) in the abundance of *star* mRNA (Fig. 2.4A) and *cyp17* mRNA (Fig. 2.4B) across all doses of SNa. Although not significant, 500 nM SNa notably decreased the level of *cyp17* mRNA by 31 % ($P > 0.05$) (Fig. 2.4B). For all doses of SNa, the relative *cyp19a1b* mRNA level were lower relative to the controls (Fig 2.4C). At 10, 50, and 100 nM, *cyp19a1b* mRNA were 26 %, 23 %, and 26 % lower than those of the control, respectively, but this did not reach statistical significance ($P > 0.05$). In contrast, 500 nM SNa significantly decreased by 51 % ($P < 0.05$) (Fig. 2.4C). At the 1000 nM dose *cyp19a1b* mRNA were 12 % lower than those of the control but this did not reach statistical significance. The most prominent effect of SNa was on the level of *hsd17b4* mRNA. Relative to control, *hsd17b4* was decreased by 36 % ($P < 0.05$), 37 % ($P < 0.05$), 51 % ($P < 0.05$), and 40 % ($P < 0.05$) by 50 nM, 100 nM, 500 nM, and 1000 nM SNa, respectively (Fig. 2.4D).

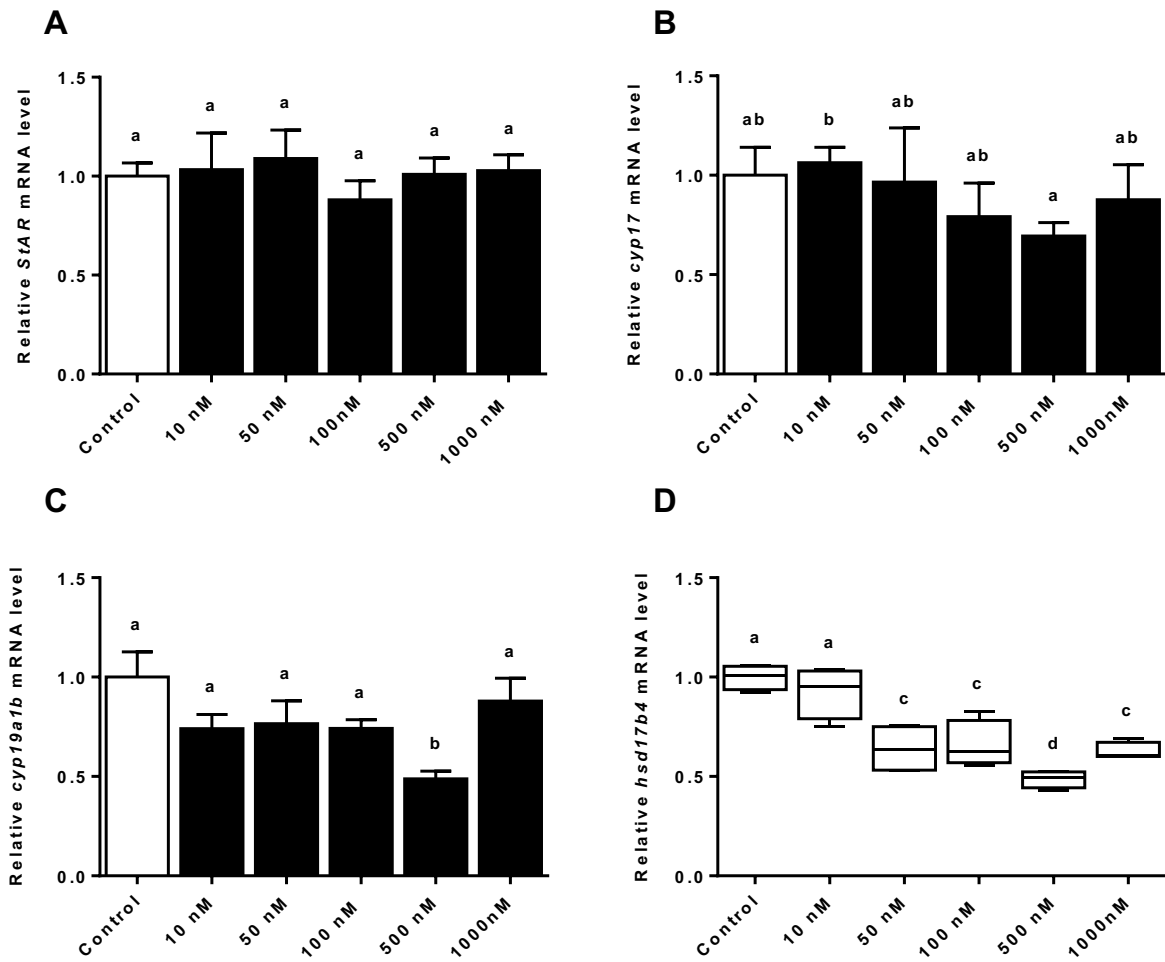


Figure 2.4. Quantitative real-time PCR analysis showing the effects of various concentrations of SNa on the mRNA levels of steroidogenic enzymes in primary RGC culture. The mRNA levels of *star* (A), *cyp17* (B), *cyp19a1b* (C), and *hsd17b4* (D) were analyzed after 24 h exposure to different doses of SNa. Data were normalized and defined as fold change relative to control. Mean values + SEM (n = 4) are presented in panels A, B, and C. Box-whisker plots of median values (n = 4) with interquartile range (25-75%) for the *hsd17b4* are presented in panel D where whiskers represent minimum-maximum range. Groups marked by different letters are significantly different (P < 0.05).

2.4. Discussion

We found that SNa-positive neuron cell bodies are in close proximity with both GFAP- and aromatase-B-positive RGCs in the preoptic nucleus of goldfish and zebrafish, respectively. Together, through ICV injections into the goldfish third brain ventricle, targeting the preoptic nucleus, and by *in vitro* SNa exposures of cultured goldfish RGCs, we show that SNa can regulate *cyp19a1b* expression, implicating SNa in the regulation of neuroestrogen production in these cells. These neuroanatomical observations of distinct SNa expression in the magnocellular and parvocellular cells are in support of previous studies in the rat (Marksteiner et al., 1993) and goldfish preoptic area, which have shown SN co-localized with isotocin, the fish homolog of mammalian oxytocin (Canosa et al., 2011). This is the first study to document this expression pattern in zebrafish, further substantiating SNa expression in the preoptic area to be conserved. This area in the teleost brain regulates a variety of physiological processes including behaviour, reproduction, and osmotic regulation (Peter, 1977).

Magnocellular and parvocellular neurons reside in the preoptic nucleus where in fish and amphibians exhibit a high level of plasticity reflecting a “physiological regeneration” of the nucleus (Garlov, 2005). These neurosecretory neurons after periods of increased activity, such as during spawning in fish or seasonal changes in frogs, undergo neuronal degeneration and are replaced by newly born neurons (Polenov et al., 1979; Polenov and Chetverukhin, 1993; Garlov, 2005). This is indicative of the increased ability of adult neurogenesis in non-mammalian vertebrates (Kaslin et al., 2008). Observations in frog brain show proliferating cells some with bipolar morphology in the preoptic ventricular zone which presumably are precursor cells for new neurosecretory

cells (Chetverukhin and Polenov, 1993). Given the identification of aromatase B-positive RGCs that are progenitor cells for newborn neurons in the preoptic nucleus of zebrafish, future research should address the involvement of RGCs in the neuronal regeneration of magnocellular and parvocellular neurons.

Mammalian magnocellular neurons are well known for their ability of dendritic synthesis and secretion of both neurosecretory peptides vasopressin and oxytocin in the supraoptic and paraventricular nuclei (Ludwig, 1998). Magnocellular neurons contain neurosecretory granules that undergo exocytosis from both the dendrites and cell bodies causing high extracellular concentrations of vasopressin and oxytocin in hypothalamic nuclei (Pow and Morris, 1989). Using immunoelectron microscopy it was demonstrated that SN and oxytocin are co-stored in large dense core vesicles in the rat paraventricular nucleus (Mahata et al., 1993). Along with oxytocin and vasopressin, SgII (*scg2*) mRNA are co-stimulated after lactation, adrenalectomy, and osmotic challenge (Mahata et al., 1992, 1993; Ang et al., 1997). Similarly, both lactation (de Kock et al., 2003; Rossoni et al., 2008) and osmotic stimulation (Landgraf and Ludwig, 1991) up-regulates dendritic secretion in rat magnocellular neurons. Therefore, while dendritic secretion has not been investigated in the fish preoptic nucleus, SN may also be released through similar mechanisms in the cell body and/or dendrites. The lack of observed dendritic processes in the present study could be attributed to the rapid release of SN, as with other peptides axonal transport blocker, colchicine, may have to be used to have complete visualization (Back and Gorenstein, 1989). Nonetheless, other reports in goldfish have documented magnocellular neurons with dendritic processes (Hayward, 1974), with isotocinergic neurons containing a medial projecting dendritic fiber extending towards the third

ventricle (Reaves Jr. and Hayward, 1980). After dendritic release neuropeptides can have autocrine effects to regulate signaling in neurons from which they are released or paracrine effects on adjacent neurons and glia (Ludwig et al., 2015). Besides direct contact, SNa can emit non-synaptic signals to RGCs as the CSF is a major source of free SN peptide (260 fmol/ml) (Kirchmair et al., 1994a) since RGCs both line and make direct contact with the ventricle in fish (Grupp et al., 2010). Because of this interaction between SNa and RGCs we aimed to understand the regulatory role of SNa on RGCs function in neurosteroidogenesis.

Injection of SNa into the third brain ventricle stimulated *cyp19a1b* mRNA levels in the telencephalon at 2 h post injection, however after 5 h post injection SNa had suppressive effects on *cyp19a1b* expression in both hypothalamic and telencephalic tissues. Using a previous established and validated culture of female goldfish RGCs (Xing et al., 2015b), *in vitro* SNa exposure had inhibitory effects on *cyp19a1b* mRNA levels and no effects on other steroidogenic enzymes such as steroidogenic acute regulatory protein (*star*) and 17 α -hydroxylase (*cyp17*), demonstrating a degree of specificity of action. In the steroidogenic pathway, StAR is involved in determining the availability of the cholesterol substrate (Anuka et al., 2013) while *cyp17* converts progesterone into 17-hydroxyprogesterone, a key intermediate in androgen and estrogen production (Leenders et al., 1996). The inhibitory effects of SNa on *cyp19a1b* expression *in vitro* were lesser than the clear suppression observed *in vivo* and there are several possible explanations for this differential degree of *cyp19a1b* inhibition. It is clear that there are dose-dependent effects of SNa, and as a result it is difficult to directly compare effective SNa concentrations *in vivo* and *in vitro*. Moreover, SNa acted rapidly *in vivo*,

and the incubation time *in vitro* was much longer, so there may be time-dependent effects requiring further transcriptomic analysis to fully elucidate the potential dynamic regulation of neurosteroidogenesis by SNa. *In vivo* there is also the distinct possibility that SNa is acting both directly on RGCs and indirectly on other neurons. This latter possibility is eliminated in the *in vitro* system. For instance, SN *in vivo* affects the release of dopamine (Agneter et al., 1995), glutamate and GABA (You et al., 1996) from the rat brain. Therefore, if SNa is affecting any of these neurotransmitter systems in the goldfish brain there is the possibility for complex responses *in vivo*. Our previous work characterized the stimulatory effects of dopamine D1R activation on *cyp19a1b* (Xing et al., 2015b). Moreover, our RNA-Seq data indicates that RGCs express multiple dopamine, glutamate, and GABA receptor subtypes (see chapter 3). The ability of SNa to control neuroestrogen production by regulating *cyp19a1b* expression may have implications on feedback signaling mechanisms controlling SN synthesis and release. As shown in the rat hypothalamus, 17 β -estradiol simulates neuropeptide release from both dendrites and cell bodies of the magnocellular neurons. Furthermore, SgII, the precursor to SN, is under the control of estrogens in both the female goldfish telencephalon (Zhang et al., 2014) and rat pituitary (Anouar et al., 1991; Anouar and Duval, 1992). Neuroestrogens in mammals, have neuroprotective and antiapoptotic properties in neurogenesis (Garcia-Segura, 2008; Saldanha et al., 2009; Scott et al., 2012), however in teleost fish brain the effects of estrogen on neurogenesis remain inconclusive.

As shown *in vitro*, SN can also decrease the expression of the *hsd17b4* gene encoding the D-bifunctional protein 17 β -hydroxysteroid dehydrogenase type IV (Leenders et al., 1996). This enzyme is involved in inactivating hormones as it oxidizes

estradiol through oxidation (Adamski et al., 1992). This enzyme is also involved in β -oxidation of fatty acids generating acetyl-CoA and short-chain acetyl CoA for intracellular energy and metabolic homeostasis (Möller et al., 2001). Knockdown of the *hsd17b4* gene in zebrafish embryos causes multiple defects, and most notable here is abnormal neuronal development (Kim et al., 2014). Although the role of HSD17B4 in RGCs requires further investigation, effects of SNa to decrease *hsd17b4* suggests SNa can alter pathways in steroid oxidation and fatty acid β -oxidation.

Together our data demonstrates an intimate anatomical relationship between SNa-positive neuron cell bodies and RGCs in the preoptic nucleus of both goldfish and zebrafish implying RGCs can be under control of the neuropeptide, SNa. Although other interactions in the forebrain were not observed in this study, additional areas of possible interaction include the dorsal and ventral telencephalon, ventrocaudal aspect of the nucleus of the lateral recess, and nucleus of the posterior recess where SNa-immunoreactivity (Canosa et al., 2011) and RGCs (Diotel et al., 2010a) have been documented separately. Though not studied in fish, neuronal-glia interactions have been well studied in the hypothalamus of mammals where surrounding glia modulate neuronal activity and synaptic remodeling of magnocellular neurons (Langle et al., 2002). Therefore, this research begins to elucidate how RGC function, specifically in neuroestrogen production, can be under control of neighbouring neurons by neuropeptides.

Chapter 3: *De novo* assembly of the transcriptome of goldfish radial glial cells and analysis of differentially expressed genes for the identification of gene networks responsive to secretoneurin-A

3.1. Introduction

Radial glial cells (RGCs) are a progenitor subtype in the developing central nervous system (CNS) of all vertebrates (Götz and Huttner, 2005) and have a bipolar morphology with a thin radial fiber serving as a scaffold for neuronal migration (Rakic, 1972). RGCs are self-renewing through proliferative symmetrical divisions and multipotent undergoing differentiative cell divisions producing neurons or other glial cells (Florio and Huttner, 2014). In mammals, RGCs are mostly a transient cell type differentiating into neurons and glia at the end of development and only persist in two areas of the adult brain, the anterior part of the subventricular zone of the lateral ventricle and subgranular zone of the dentate gyrus, where they serve as progenitor cells. These two areas are the only main constitutive neurogenic regions of the adult mammalian brain, which explains the limited capacity for adult neurogenesis in mammals (Brunner et al., 2010; Ming and Song, 2011). In contrast, RGCs are abundant throughout teleost development into adulthood in numerous brain neurogenic zones (Grandel and Brand, 2013), which may be why teleost fish exhibit the most pronounced and widespread adult neurogenesis of any vertebrate studied thus far (Zupanc, 2006; Kaslin et al., 2008).

Along with being a progenitor subpopulation, RGCs are also the only macroglia in fish, as they lack typical stellate astrocytes (Grupp et al., 2010). Other than studies that

have established their function in producing neurosteroids including neuroestrogens through the expression of steroidogenic enzymes (Forlano et al., 2001; Pellegrini et al., 2005; Tong et al., 2009), little is known on other RGC functions and regulatory factors that control this cell type to maintain proper brain homeostasis (Than-Trong and Bally-Cuif, 2015). Given their direct contact with cerebrospinal fluid and with adjacent neurons, RGCs may be under the regulatory action of numerous signaling molecules, such as hormones, neurotransmitters, neuropeptides, and cytokines. Previous reports in fish have identified dopaminergic (Xing et al., 2015a; b, 2016a) and serotonergic regulation (Pérez et al., 2013) of RGC physiology. Expanding on these neuronal-RGC interactions, Chapter 2 highlighted the interactions between SNa-positive neuron cell bodies and RGCs, specifically in the preoptic nucleus, indicating SN may be a modulator of RGC function. SN is an evolutionary conserved neuropeptide generated by endoproteolytic processing of its precursor protein SgII and is found in dense-core secretory granules in a wide variety of cell types of the endocrine, nervous, and immune systems (Kirchmair et al., 1993; Fisher-Colbrie et al., 1995; Zhao et al., 2010). Although SN exerts many biological effects two major functions that may relate to regulating RGC function include aiding in the growth and repair of neuronal tissue by promoting neuroprotection and plasticity (Shyu et al., 2008), acting as a trophic factor stimulating neurite outgrowth (Gasser et al., 2003), and participates in the immune response by chemotaxis of several types of immune cells (Reinisch et al., 1993; Dunzendorfer et al., 1998b, 2001).

While transcriptomics have been used previously to reveal the diversity of human radial glia (Johnson et al., 2015; Thomsen et al., 2015), fish RGCs remain uncharacterized at the transcriptomic level limiting our knowledge of their molecular

functions. Therefore, the objective of this study was to generate, to our knowledge, the first reference RGC transcriptome of any fish species while revealing new functions critical to neuronal-RGC communication through SNa.

3.2. Material and methods

3.2.1. Experimental animals

All procedures used were approved by the University of Ottawa Protocol Review Committee and followed standard Canadian Council on Animal Care guidelines on the use of animals in research. Common adult female goldfish (*Carassius auratus*) were purchased from a commercial supplier (Mt. Parnell Fisheries Inc., Mercersburg, PA, USA) and allowed to acclimate for at least 3 weeks prior to experimentation. Animals were maintained at 18°C under a natural stimulated photoperiod and fed standard flaked goldfish food. Sexually mature female goldfish (18–35 g) were anesthetized using 3-aminobenzoic acid ethylester (MS222) for all handling and dissection procedures.

3.2.2. Cell culture and exposure

Cell culture methods used in the present study have been previously established and validated (Xing et al., 2015b) In short, the hypothalamus and telencephalon were dissection from female goldfish and rinsed twice with Hanks Balanced Salt Solution (HBSS; 400 mg KCl, 600 mg KH₂PO₄, 350 mg NaHCO₂, 8 g NaCl, 48 mg Na₂HPO₄, and 1 g D-Glucose in 1 L ddH₂O) with Antibiotic-Antimycotic solution (Gibco) and minced into small explants. Radial glial cells were dissociated with trypsin (0.25 %; Gibco) and cultured in Leibovitz's L-15 medium (Gibco) with 15% Fetal Bovine Serum (FBS; Gibco) and Antibiotic-Antimycotic. Cell culture medium was changed 4–7 days after isolation and then once a week thereafter. Radial glial cells were subcultured by trypsinization (0.125 %) for 3 passages then used for experimentation. Goldfish SNa (TNENAEQYTPQKLATLQSVFEELSGIAASNANS) was synthesized previously by Dr. A. Basak (Zhao et al., 2006b). Stock solutions of purified goldfish SNa peptide were

made in water and stored at -20° until use. Aliquots were thawed on ice then diluted to desired concentrations in serum-free media. Cells were exposed to 1000 nM SNa for 24 h.

3.3.3. RNA extraction and Illumina sequencing

Total RNA was extracted using RNeasy Micro Kit (Qiagen) including an on-column DNase treatment to remove genomic DNA. The concentration of total RNA was determined using the Qubit RNA Assay Kit (Life Technologies). In order to evaluate the quality of the total RNA, RNA integrity value (RIN) was assessed using Agilent RNA 600 Nano Reagents and RNA Nano Chips in Agilent 2100 Bioanalyzer (Agilent Technologies).

Sequencing on 10 independent RGC cultures was performed by MR DNA next generation sequencing service provider (www.mrdnalab.com) using Illumina HiSeq (Illumina) following manufacturer's guidelines for paired end sequencing (151 bp). Using oligo(dT) magnetic beads, RNA with poly(A) tails were purified and fragmented into shorter sequences that were used as templates for cDNA synthesis. A total of 10 cDNA libraries were constructed using random-hexamer primers from 1 µg of total RNA from each sample using TruSeq RNA LT Sample Preparation Kits (Illumina). Following the library preparation, the final concentration of library was measured using the Qubit dsDNA HS Assay Kit (Life Technologies) and the average library size was determined using the Agilent 2100 Bioanalyzer (Agilent Technologies). A total of 5 pM library was clustered using cBot (Illumina) and sequenced paired end for 300 cycles using the HiSeq 2500 system (Illumina).

3.3.4. *De novo* transcriptome assembly and annotation

Both *de novo* assembly and annotation was performed under contract by Genotypic Technologies (<http://www.genotypic.co.in>). The Illumina paired end raw reads were quality checked using FastQC (<http://www.bioinformatics.babraham.ac.uk/projects/fastqc/>). Illumina raw reads were processed by GT proprietary tool for adapters and low quality bases trimming towards 3'-end. The high quality reads were further considered for further downstream analysis. Biological replicates were pooled together to generate a reference transcriptome using Trinity (Grabherr et al., 2013) using all default parameters with a k-mer of 25. Trinity combines three independent software modules: Inchworm, Chrysalis, and Butterfly applied sequentially to process large volumes of RNA-seq reads. Trinity partitions the sequence data into many individual *de Bruijn* graphs, each representing the transcriptional complexity at a given gene or locus, and then processes each graph independently to extract full-length splicing isoforms and to tease apart transcripts derived from paralogous genes. Once assembled, the sequences were clustered based on similarity between sequences with CD-Hit v4.5.4 (Niu et al., 2010) using the following parameters: 95 % coverage and 90 % identity, -r 1, and others were kept default. Clustering reduces overall size of the database without removing any sequence information by only removing redundant or highly similar sequence and the longest sequences for each cluster was used as the representative sequence. The clustered transcripts with ≥ 300 bp in length were considered for the analysis. Transcripts were annotated using the Basic Local Alignment Search Tool (BLAST+2.2.29) (E-value $<1.0e-4$) using Chordata protein sequences from the Uniprot database (Altschul et al., 1990). The remaining unannotated transcripts were further annotated using Pfam

database. After annotation, gene ontology terms were assigned using protein annotation through evolutionary relationships (PANTHER) in order to classify all unigenes identified in RGC cultures (Mi et al., 2015). Gene ontology categories for biological processes, molecular functions, cellular components, protein classes, and pathways were used to identify the distribution of unigenes within each gene ontology category in RGC cultures.

3.3.5 Differential gene expression analysis

The differential gene expression (DGE) levels between control (n = 3) and 1000nM SNa exposure (n = 3) in RGCs were calculated using the DESeq method (Anders et al., 2010). Briefly, after the variance is calculated for each unigene, DGE is calculated assuming a negative binomial distribution for the expression level and uses a Fisher's exact test to calculate P-value to test for significance between groups for each unigene. Once the DGE is calculated, results are separated as up-regulated and down-regulated based on a $|\log_2| > 0.5$ cut off. A false discovery rate (FDR) at 5 % was used for multiple hypothesis testing.

3.3.6 qRT-PCR validation of differentially expressed genes

qRT-PCR was conducted using the SYBR green detection system to determine relative gene expression and to validate the DGE analysis. Primers were designed using Primer3 (Untergasser et al., 2012) and synthesized by Integrated DNA Technologies (Table 3.1). Primer sets were tested for specificity by running the qRT-PCR product on a 1 % agarose containing SYBR Safe DNA gel stain (Invitrogen) to ensure a single product was produced from each reaction. Each product was extracted from the gel using NucleoSpin Gel and PCR Clean-up kit (Macherey-Nagel) and sequenced to confirm

primer specificity by StemCore Laboratories at the Ottawa Hospital Research Institute. Before qRT-PCR total cDNA was prepared from 1 µg of total RNA using Maxima First Strand cDNA Synthesis Kit for qRT-PCR (Thermo Scientific). qRT-PCR analyses were conducted using the Maxima SYBR green qPCR Master Mix (Thermo Scientific) and CFX96 Real-Time PCR Detection System (Bio-Rad) to amplify the genes of interest. The thermal cycling parameters were: a single cycle Taq activation step at 95 °C for 3 min, followed by 40 cycles of 95 °C denaturation step for 10 s and primer annealing at 56-63 °C for 30 s. After 40 cycles, a melt curve was performed from a range of 65-95 °C with increments of 0.5 °C to ensure a single amplified product. Data were analyzed using CFX Manager Software package (Bio-Rad). The efficiency of each assay was $100 \pm 10 \%$ and the R^2 of each standard curve was > 0.98 . Relative mRNA abundance was calculated using the relative standard curve method based on C_q values and normalized using NORMA-GENE algorithm (Heckmann et al., 2011). Fold-change was calculated against the average of the control using normalized data. Fold-change for each group were presented as mean + SEM from 4 biological replicates ($n = 4$) assayed in duplicate. Data were checked for normality with Shapiro-Wilk's W test. Student's t -test was used to test the differences in gene expression level.

Table 3.1. Primers (5'→3') used for qRT-PCR

Gene	Primer Sequence (Forward)	Primer Sequence (Reverse)
<i>smad6b</i>	CGGCGAATAAAATCCACAGA	CTGAACGGAACCAGGAACA
<i>grapa</i>	GGCTCACCCCTTTCCTCTCTT	CCCTTCCTGTTCACCAACTC
<i>fgf4</i>	GGGCTACGCATTCCATTCT	TAGGTGTTTTGGGGGTCTTG
<i>nab1a</i>	CGAACACAGCCTATCTCCATC	TAGTCGCTCTACGCACTCCA
<i>baiap2b</i>	TCCGTCCATTTCTCTCCAAC	GACCTTCTCCAACACCCTACCT

3.3.7. Gene set enrichment analysis and sub-network enrichment analysis

Gene set enrichment sub-network enrichment analyses were conducted using Pathway Studio 9.0 (Ariadne). Goldfish genes were annotated with their human homologs (NCBI) using Entrez Gene IDs that were obtained from the ID mapping service in Pathway Studio to the M.D. Anderson GeneLink (University of Texas, Huston, TX). If a human homolog could not be identified, the gene was not included in the pathway analysis. A total of 28,597 unigenes were mapped in Pathway Studio and for duplicated unigenes, the unigene that showed the lowest P-value was used for analyses. For gene set enrichment analysis (GSEA), genes were permuted 1000 times using the Kolmogorov-Smirnov classic approach as an enrichment algorithm. The gene set categories examined for enrichment included curated Ariadne cell processes, cell signaling and receptor signaling pathways. Sub-network enrichment analysis (SNEA) for proteins and chemicals regulating cell processes was performed to identify gene networks

regulated in RGCs following SNa exposure. SNEA utilizes known relationships (i.e., based on expression, binding, and common pathways) between genes to build networks focused around gene hubs. For both GSEA and SNEA the enrichment P-value was set at $P < 0.05$ and a minimum of 5 entities were required for inclusion as a significantly regulated process or pathway. These analyses have been utilized previously to build gene and protein networks in teleost fish (Martyniuk and Denslow, 2012; Martyniuk et al., 2012), including a preliminary proteomic profile of female goldfish RGCs (Xing et al., 2016a) .

3.3. Results

3.3.1. *De novo* transcriptome assembly and quality analysis

Before *de novo* transcriptome assembly the Illumina MiSeq paired end raw reads were processed to remove adapter fragments and low quality bases generating 161,704,300 clean reads from 163,641,713 raw reads. High-quality reads were subsequently assembled *de novo* using the Trinity program because goldfish do not have a reference genome. This program uses three sequential software modules: Inchworm, Chrysalis, and Butterfly for efficient and robust *de novo* reconstruction of transcriptome. Trinity assembler, with a *k*-mer size of 25 generated 170,967 unigenes with a total unigene sequence length of 150,361,946 bp. Lengths of the unigenes ranged from 301 to 20,585 bp with a mean size of 879.5 and an N50 of 1318 bp. The N50 is the contig length such that of equal to or longer that constitutes half of the entire assembly. Among the unigenes 85,984 (47.7 %) were 300–499 bp in length, 45,405 (27.4 %) were 500–999 bp, 39,523 (24.8 %) were 1,000–9,999 bp, and 55 (0.03 %) unigenes were >10,000 bp in length.

3.3.2. Annotation and gene ontology classification

Annotation of the RGC transcriptome was performed by aligning transcripts \geq 300 bp in length using BLASTX (Altschul et al., 1990) to all *Chordata* protein sequences from UniProt database (using a cut off at E-value $< 1.0e-4$). The unannotated transcripts were further annotated using Pfam database. A total of 67,486 unigenes were annotated (38.05 % from UniProt and 1.42 % from Pfam) while the remaining 96,145 unigenes (56.24 % of all unigenes) could not be annotated having no significant homology with

any database entries. This can be attributed to the lack of genomic characterization of goldfish, thus potentially compromising the identification of novel transcripts with important functions. Overall, 59 % of the transcripts were mapped with >80 % identity and 74 % of the matched sequence exhibited strong homology with an E-value <1e-50 with respect to the E-value distribution pattern (Fig. 3.1A,B). The BLASTX top-hit species matched against the UniProt database showed that most hits were against other fish with the top three species being *Danio rerio* (91.6 %), *Oncorhynchus mykiss* (1.72 %), and *Astyanax mexicanus* (1.31 %) (Fig. 3.1C).

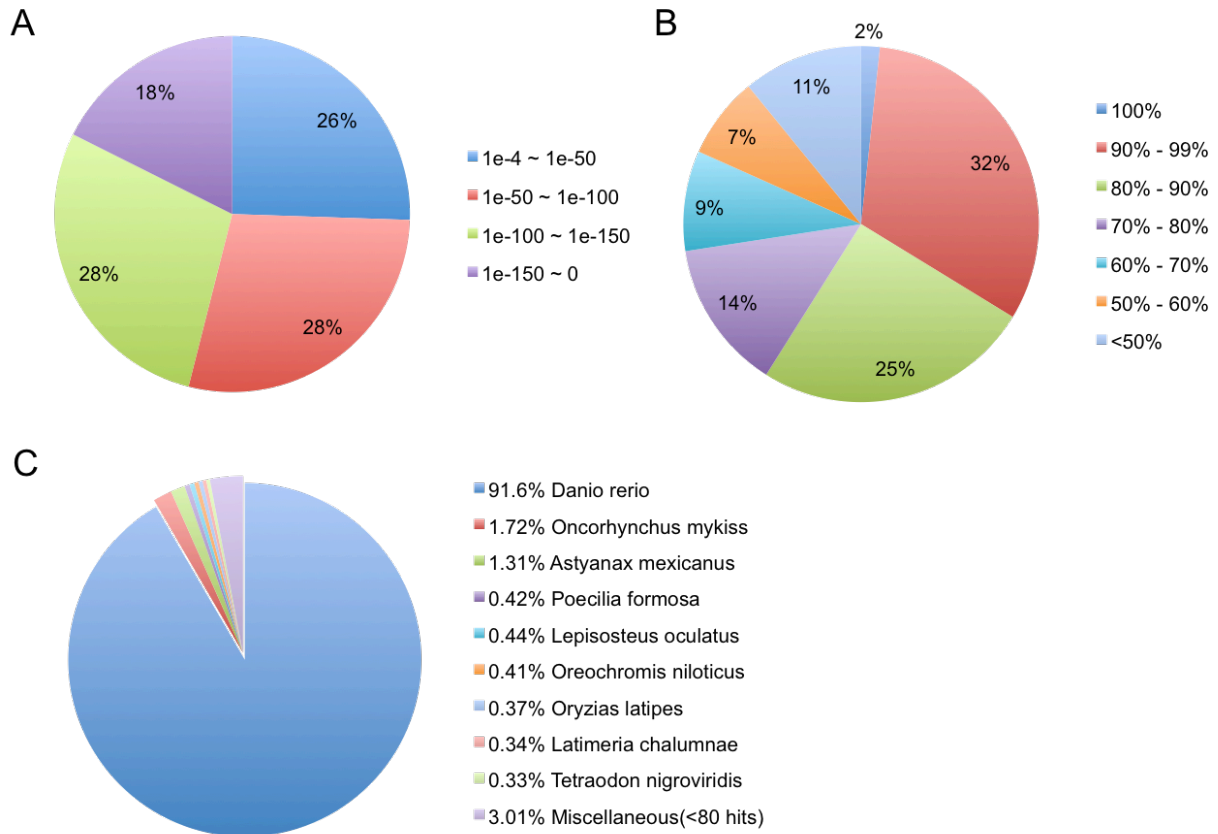


Figure 3.1. Annotation summary of assembled *Carassius auratus* RGC unigenes against UniProt database. (A) E-value distribution of BLASTX hits for each unigene with an E-value cut off of $1e-4$. (B) Similarity distribution of BLATX hits for each unigene. (C) Distribution of the top BLASTX species hits in the UniProt database.

The 12,180 non-redundant unigenes were assigned gene ontology (GO) terms for functional characterization of the annotated unigenes. The GO annotated unigenes were classified in three main ontologies: cellular component, biological function, and molecular function (Fig. 3.2). The most unigenes were ascribed to the biological function category (20,261 unigenes), followed by molecular function (11,412), and cell compartment (5,513) categories. Within the cellular compartment category, the RGC transcriptome was enriched in the cell part (2,240 unigenes; 40.4 %), organelle (1,393; 25.1 %), and membrane (705; 12.7 %). In addition, a few unigenes were assigned to GO categories such as cell junction (43 unigenes; 0.8 %) and synapse (27; 0.2 %). In the biological function category, metabolic process (5,587 unigenes; 27.6 %), cellular process (4,255; 21.0 %), and biological regulation (2,308; 11.4 %) were predominant, suggesting these genes are involved in metabolism and cell growth. Other notable biological function allocations include immune system process (708 unigenes; 3.5%) and biological adhesion (422; 2.10 %). Regarding molecular function, a high proportion of unigenes were assigned to catalytic activity (3,711, 32.5 %), binding (3,681; 32.3 %), and nucleic acid binding transcription factor activity (929; 8.1 %).

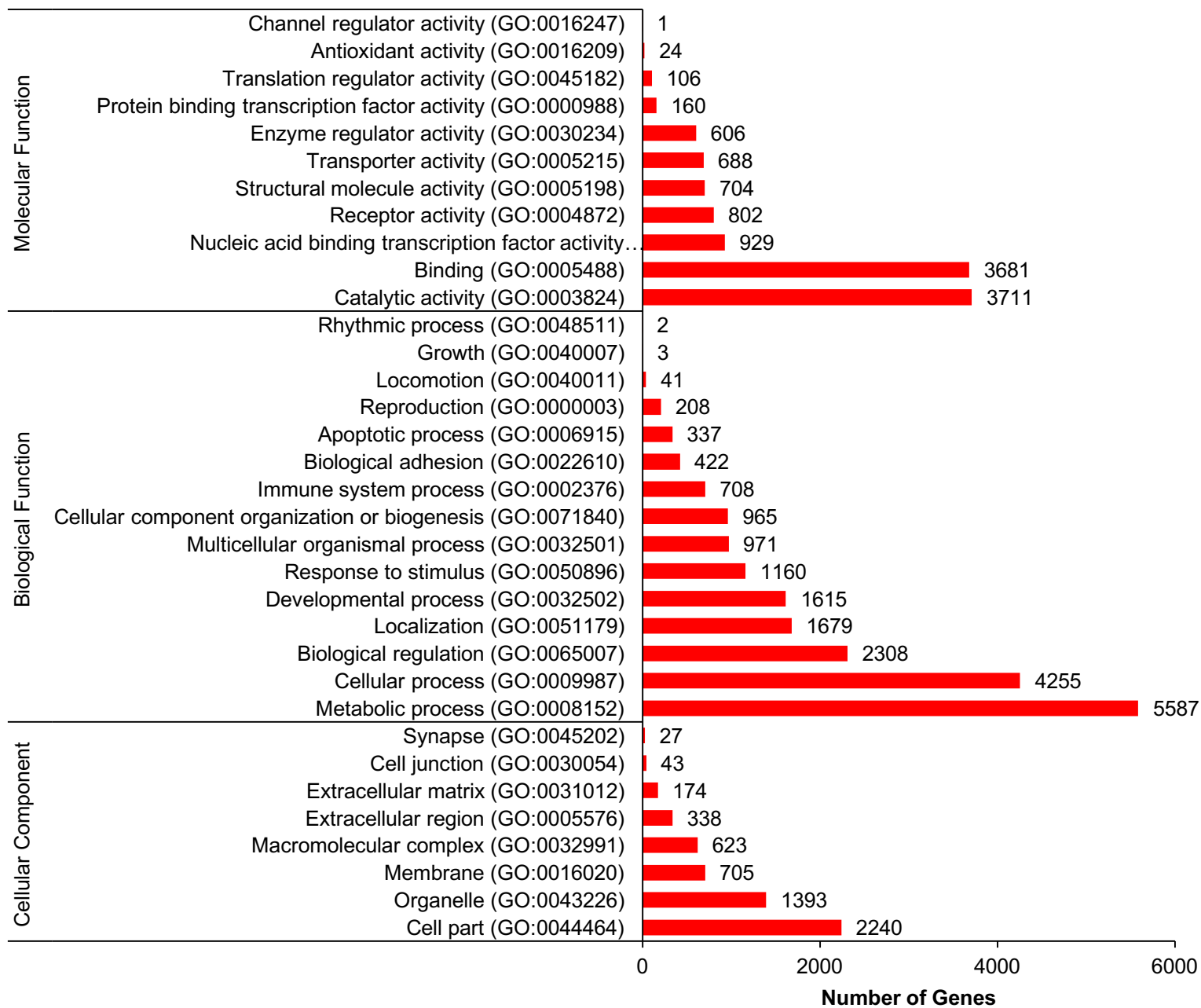


Figure 3.2. GO classification of assembled *Carassius auratus* RGC unigenes into molecular function, biological function, and cellular component categories. The number of unigenes ascribed to each classification is provided along with GO accession number

The transcriptome was categorized by protein class ontologies to elucidate the potential proteins expressed by RGCs (Fig. 3.3). Most assembled unigenes represented were classified as nucleic acid binding proteins (1,666 unigenes; 13.9 %), hydrolases (992; 8.3 %), and transcription factors (990; 8.3 %). Within protein classes, the receptor and signaling molecule ontologies were further categorized (Fig. 3.4). The RGC transcriptome expresses an array of receptor classes such as GPCRs (172 unigenes; 38.9 %), cytokine receptors (129; 29.2 %), ligand-gated ion channels (61; 13.8 %); nuclear hormone receptors (54; 12.2 %); and protein kinase receptors (26; 5.9 %). Within the signaling molecule category, unigenes were cataloged into membrane-bound signaling molecules (120 unigenes; 35.7 %), growth factors (80; 23.8 %), cytokines (72; 21.4 %), and peptide hormones (64 unigenes; 19.0 %). These GO analyses reveal a diverse receptor and signaling molecule profile, suggesting that RGCs can respond to and synthesize an array of hormones, peptides, cytokines, and growth factors.

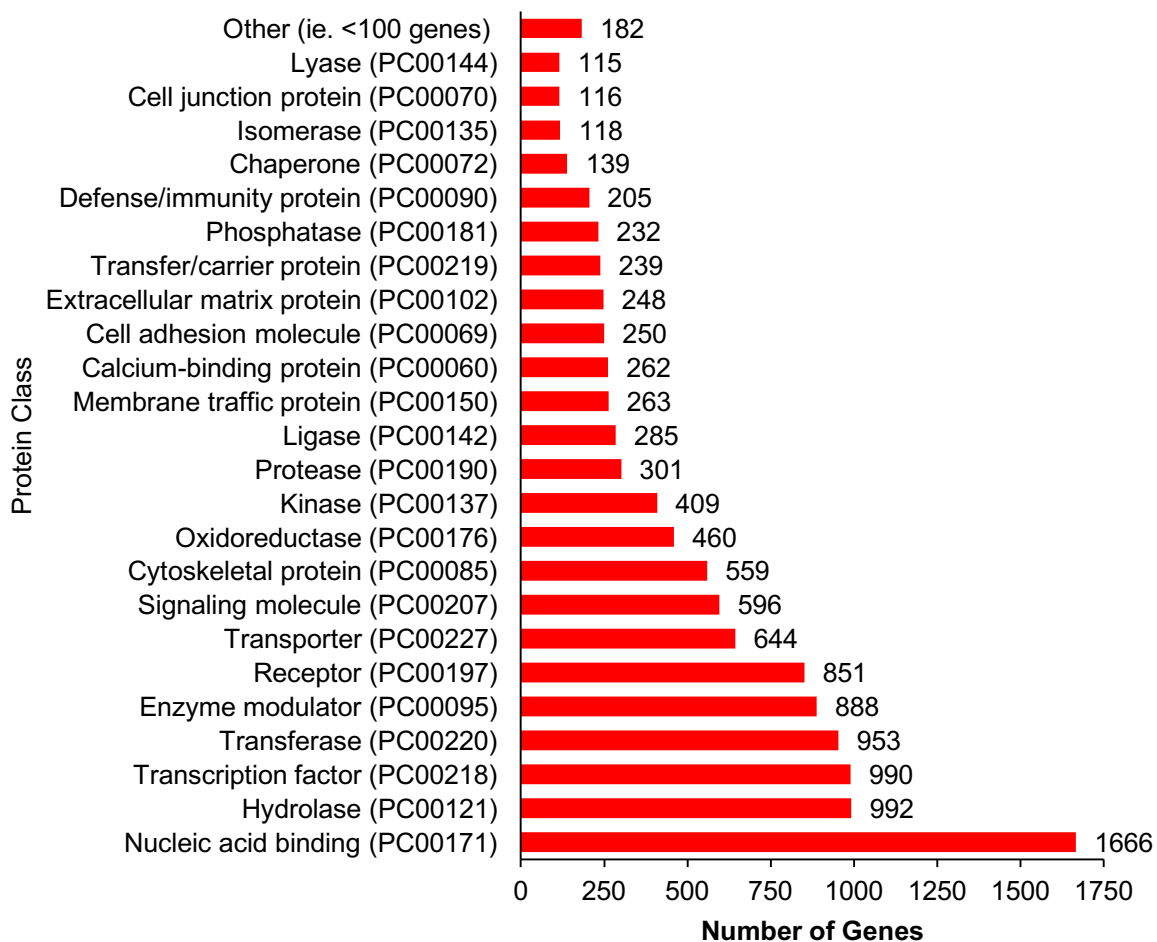


Figure 3.3. GO classification of assembled *Carassius auratus* RGC unigenes by protein class. The number of unigenes ascribed to each classification is provided along with protein class accession number.

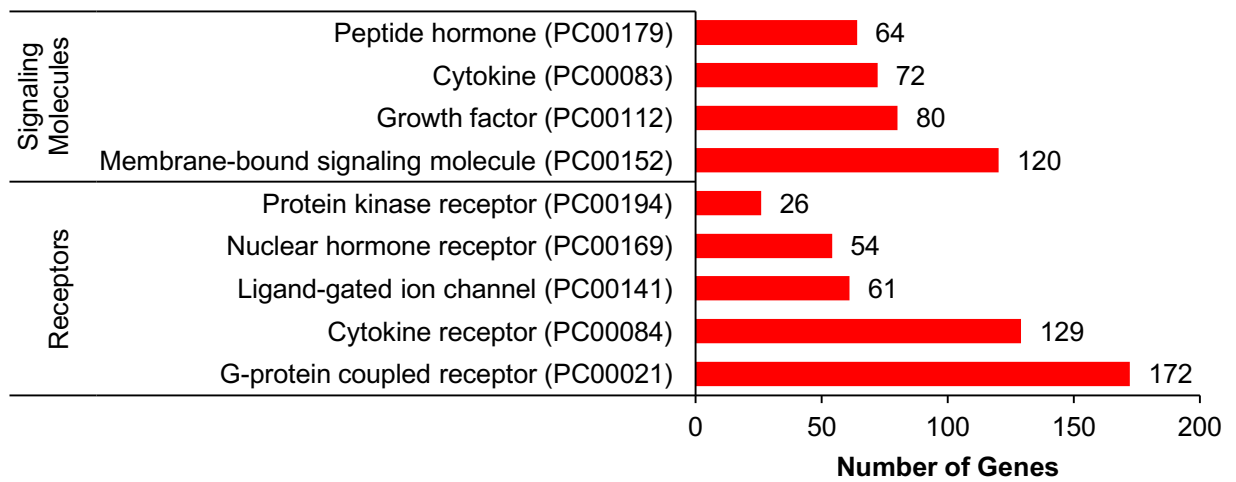


Figure 3.4. GO classification of assembled *Carassius auratus* RGC unigenes by receptor and signaling molecule classes. The number of unigenes ascribed to each classification is provided along with protein class accession number.

Overall, a total of 4,435 annotated unigenes were assigned to 160 unique pathway ontologies. Unigenes were the most enriched in the Wnt signaling pathway (191 unigenes; 4.3 %), gonadotropin-releasing hormone receptor pathway (180; 4.1 %), chemokine and cytokine signaling pathways (150; 3.4 %), and integrin signaling pathway (137; 3.1 %) (Table 3.2). Among all pathway ontologies many were neurotransmitter receptor related such as serotonin (P04374, P04373, P04376, P04375), dopamine (P05912), acetylcholine (P00043, P00042), GABA (P05731), glutamate (P00037, P00040, P00041), adrenaline (P04378, P04377, P00002, P04379), and histamine (P04385, P04386). Numerous unigenes were assigned hormone related pathways, including gonadotropin-releasing hormone receptor signaling (P06664), oxytocin receptor signaling (P04391), thyrotropin-releasing hormone receptor signaling (P04394), corticotropin-releasing factor receptor signaling (P04380), opioid proopiomelanocortin pathway (P05917), vasopressin synthesis (P04395), cholesterol biosynthesis (P00014), and androgen/estrogen/progesterone biosynthesis (P027237). In addition, several immune system pathways were identified, for example chemokine and cytokine signaling (P00031), epidermal growth factor signaling (P00018), fibroblast growth factor signaling (P00021), transforming growth factor β (P00052), interleukin signaling (P00036), both T and B cell activation (P00053, P00010), toll receptor signaling (P00054), and interferon γ signaling (P00035).

Table 3.2. Top 25 assigned pathway ontologies for assembled *Carassius auratus* RGC unigenes based on the number of genes identified in each pathway.

Pathway Name	Pathway Accession	# of genes identified
Wnt signaling pathway	P00057	191
Gonadotropin releasing hormone receptor pathway	P06664	180
Inflammation mediated by chemokine and cytokine signaling pathway	P00031	150
Integrin signaling pathway	P00034	137
CCKR signaling map	P06959	136
Angiogenesis	P00005	135
Huntington disease	P00029	115
EGF receptor signaling pathway	P00018	115
PDGF signaling pathway	P00047	113
FGF signaling pathway	P00021	112
Alzheimer disease-presenilin pathway	P00004	95
Parkinson disease	P00049	91
Heterotrimeric G-protein signaling pathway-Gi alpha and Gs alpha mediated pathway	P00026	87
Cadherin signaling pathway	P00012	87
TGF-beta signaling pathway	P00052	86
Cytoskeletal regulation by Rho GTPase	P00016	80
Apoptosis signaling pathway	P00006	80
Ras Pathway	P04393	73
Endothelin signaling pathway	P00019	68
Heterotrimeric G-protein signaling pathway-Gq alpha and Go alpha mediated pathway	P00027	64
Nicotinic acetylcholine receptor signaling pathway	P00044	62
Interleukin signaling pathway	P00036	61
p53 pathway	P00059	60
T cell activation	P00053	57
Ubiquitin proteasome pathway	P00060	55

3.3.3. Differential gene expression analysis

To assess transcriptomic changes in RGCs after a 24 h 1000nM SNa exposure, DGE analysis was performed by using DESeq and the unigene expression data. With a fold change cut off $|\log_2| > 0.5$ the DGE analysis revealed 1,776 differentially expressed genes (DEGs) after SNa treatment at $P < 0.05$ and 123 DEGs at $P < 0.001$. A total of 42 DEGs, 31 up-regulated and 11 down-regulated, passed a false discovery rate (FDR) < 0.05 correction for multiple hypothesis testing. All of the 31 up-regulated DEGs were not annotated, thus likely representing novel transcripts with no detected similarities to other species. Of the 11 down-regulated DEGs, 8 were annotated to homologous *Danio rerio* genes (Table 3.3). Unigenes that were differentially down-regulated (FDR < 0.05) included: mothers against decapentaplegic homolog 6 (*smad6b*), fibroblastic growth factor 4 (*fgf4*), NGFI-A binding protein 1a (*nab1a*), BAI1-associated protein 2b (*baiap2b*), GRB2-related adaptor protein a (*grapa*), Phosphodiesterase 8A (*pde8a*), tRNA nucleotidyl transferase (*trnt1*), and heat shock protein beta 11 (*hspb11*).

Table 3.3. List of differentially expressed genes compared to control in primary *Carassius auratus* RGC culture after 24 h 1000 nM SNa treatment (FDR < 0.05).

Gene symbol	Gene Name	Uniport Accession	Fold Change	P-Value	FDR Adjusted P-Value
<i>smad6b</i>	Mothers against decapentaplegic homolog 6	tr Q1L8Y3 Q1L8Y3_DANRE	0.40	7.34E-11	2.80E-07
<i>fgf4</i>	Fibroblast growth factor 4	tr Q9DFC9 Q9DFC9_DANRE	0.29	5.03E-10	1.78E-06
<i>nab1a</i>	NGFI-A binding protein 1a	tr Q1LWI4 Q1LWI4_DANRE	0.28	9.87E-07	2.33E-03
<i>baiap2b</i>	BAI1-associated protein 2b	tr U3JAA2 U3JAA2_DANRE	0.46	1.65E-06	3.63E-03
<i>grapa</i>	GRB2-related adaptor protein a	tr Q503S8 Q503S8_DANRE	0.35	3.21E-06	6.43E-03
<i>pde8a</i>	Phosphodiesterase 8A	tr H9GZ87 H9GZ87_DANRE	0.31	1.25E-05	2.08E-02
<i>trnt1</i>	tRNA nucleotidyl transferase	tr A7MCH7 A7MCH7_DANRE	0.08	1.30E-05	2.14E-02
<i>hspb11</i>	Heat shock protein beta 11	sp A5JV83 HSPBB_DANRE	0.33	2.60E-05	3.88E-02

3.3.4. qRT-PCR validation of DGE analysis

In order to validate the expression of DEGs identified by RNA-seq, 5 down-regulated genes and primer pairs were designed based on the corresponding assembled unigene sequence. The fold-changes in RNA-seq and qPCR, respectively for DEGs were: 0.46 and 0.42 ($P < 0.05$) for *baiap2b*, 0.29 and 0.58 ($P < 0.05$) for *fgf4*, 0.35 and 0.52 ($P < 0.05$) for *grapa*, 0.28 and 0.48 ($P < 0.05$) for *nab1a*, and 0.40 and 0.41 ($P < 0.05$) for *smad6b* (Fig. 3.5). Overall, the expression profiles obtained by RNA-seq analysis and qPCR were comparable in the direction of change.

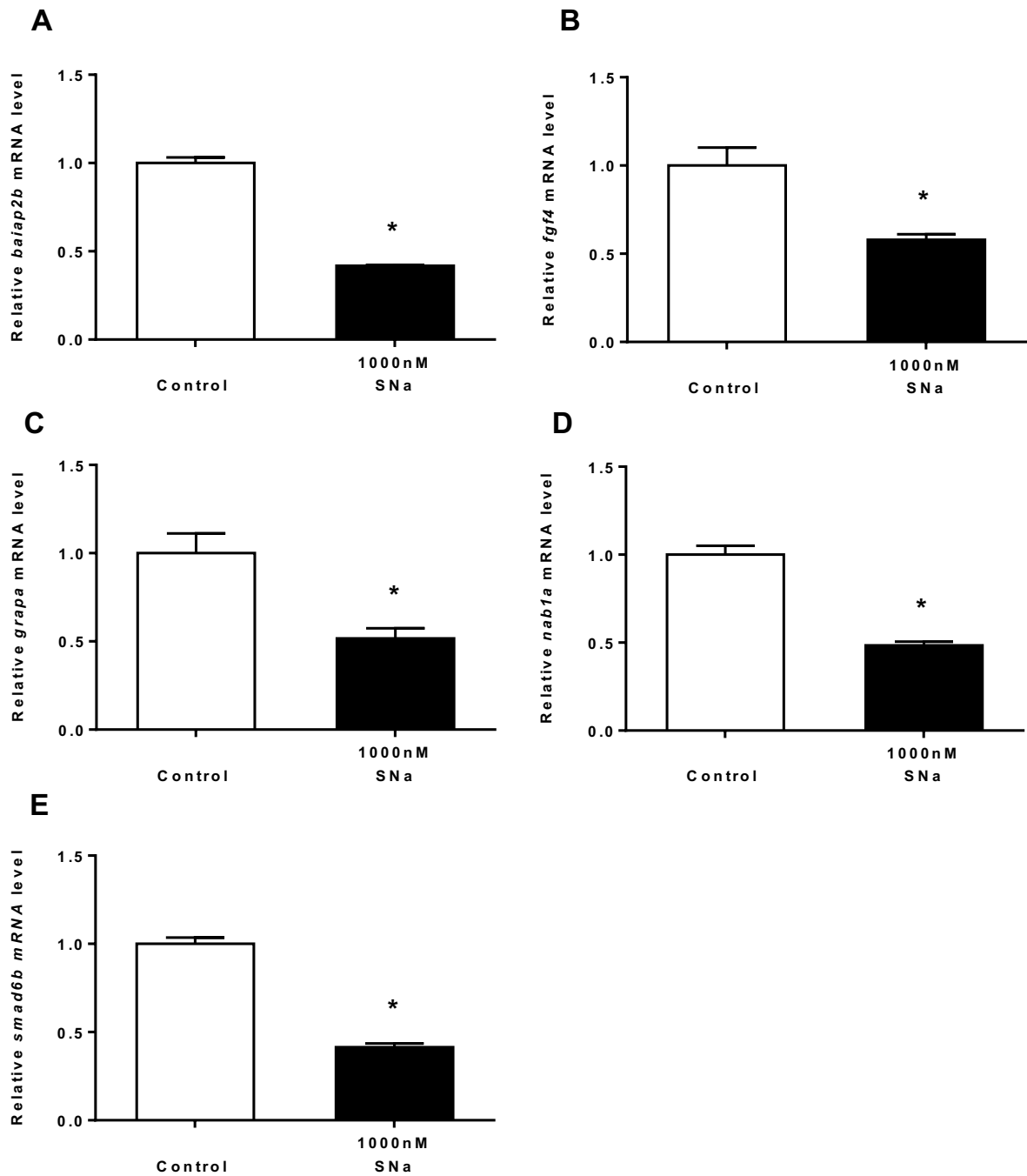


Figure 3.5. Quantitative real-time PCR analysis for (A) *baiap2b*, (B) *fgf4*, (C) *grapa*, (D) *nab1a* and (E) *smad6b* mRNA in primary *Carassius auratus* RGC culture exposed to 1000 nM SNa. Data were normalized and defined as fold change relative to control. Bars represent the mean + SEM (n = 4). Treatment groups marked by asterisks have significantly different mRNA levels compared to control (P < 0.05).

3.3.5. Gene set enrichment analysis

GSEA was conducted using Pathway Studio to identify pathways that were significantly enriched in RGCs following SNa exposure. A total of 17 pathways were statistically significant ($P < 0.05$) and had a median fold change $> 5\%$ (Table 3.4). Pathways were grouped by three categories: cell processes (4 pathways), cell signaling (2 pathways), and receptor signaling (11 pathways). Cell processes involved in adherens and tight junction assembly such as nectins, claudins, cadherins (Fig. 3.6), and junctional adhesion molecules (JAMs) were all significantly increased (10-17%) indicating that SNa up-regulates gene networks involved in cell-cell junctions. GSEA for cell signaling pathway enrichment revealed actin cytoskeleton regulation and T cell activation pathways (Fig. 3.7) were significantly increased in SNa treated RGCs. SNa treatment significantly increased genes involved in four different T-cell receptor signaling pathways. Besides the T-cell receptor, other receptors such as glucagon receptor, dopamine D1 receptor (Fig. 3.8), tumor necrosis factor receptor (TNFR), tumor necrosis factor receptor superfamily member 1A (TNFSF1A), and neural cell adhesion molecule I (NCAMI) shared similar CREB/ELK-SRF signaling. In addition, interleukin 6 receptor (ILR) and ephrin receptor (ephrinR) signaling pathways were also responsive to SNa treatment.

Table 3.4. GSEA of responses in primary *Carassius auratus* RGC culture mediated by 1000 nM SN (P < 0.05). Only pathways with a median fold change greater than 5 % are presented. The number of measured entities in the pathway is reported along with the number of measured entities and median fold change for the pathway.

Gene Set Category		Total # of entities	# of measured entities	Median change	P-value
Ariadne Cell Process Pathways	Adherens Junction Assembly (Nectin)	104	57	1.10	0.045
	Tight Junction Assembly (Claudins)	137	62	1.13	0.022
	Adherens Junction Assembly (Cadherins)	133	53	1.14	0.016
	Tight Junction Assembly (JAMs)	119	55	1.17	0.024
Ariadne Cell Signaling Pathways	Actin Cytoskeleton Regulation	551	357	1.10	0.009
	T Cell Activation	957	490	1.11	0.003
Ariadne Receptor Signaling Pathways	IL6R -> STAT signaling	8	8	1.08	0.047
	EphrinR -> actin signaling	216	143	1.12	0.020
	T-cell receptor -> NF-kB signaling	176	33	1.15	0.000
	T-cell receptor -> AP-1 signaling	180	33	1.17	0.025
	T-cell receptor -> CREBBP signaling	176	25	1.19	0.027
	GlucagonR -> CREB/ELK-SRF/SP1 signaling	42	27	1.20	0.040
	DopamineR1 -> CREB/ELK-SRF signaling	40	25	1.20	0.016
	T-cell receptor -> ATF/CREB signaling	195	45	1.21	0.021
	TNFR -> CREB/ELK-SRF signaling	45	30	1.23	0.050
	TNFRSF1A -> CREB/ELK-SRF signaling	41	32	1.23	0.014
	NCAM1 -> CREB/ELK-SRF/MYC signaling	27	21	1.26	0.046

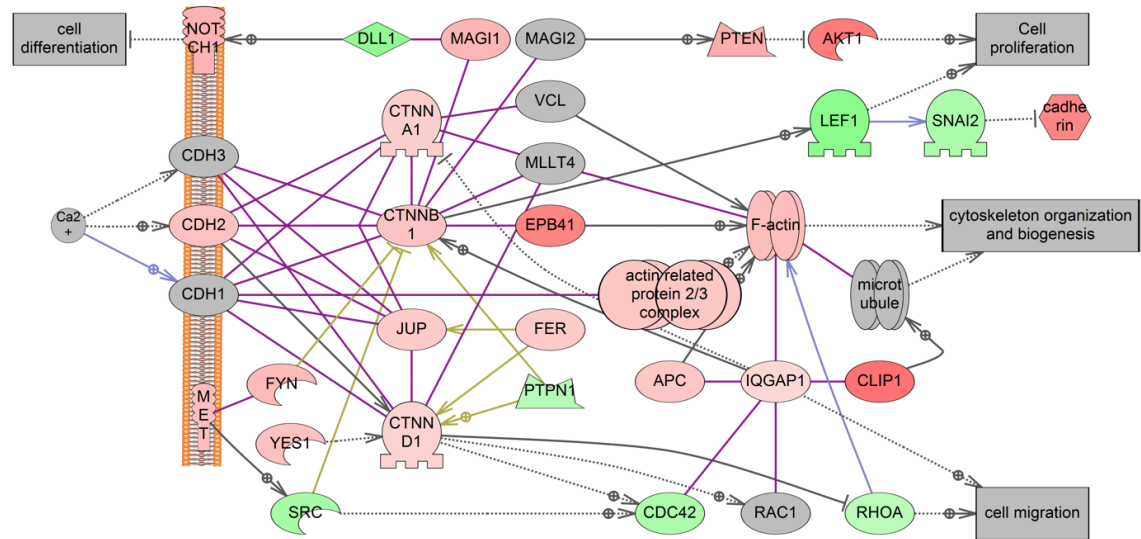
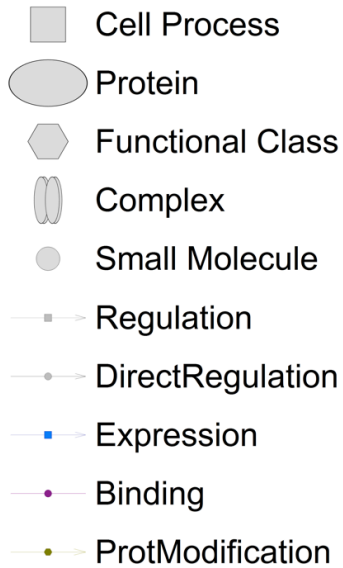


Figure 3.6. Cadherin adherens junction assembly was significantly enriched by GSEA in primary *Carassius auratus* RGC culture after 1000 nM SNa treatment ($P < 0.05$). Red indicates that the gene or process is increased while green indicates that the gene or process is decreased.

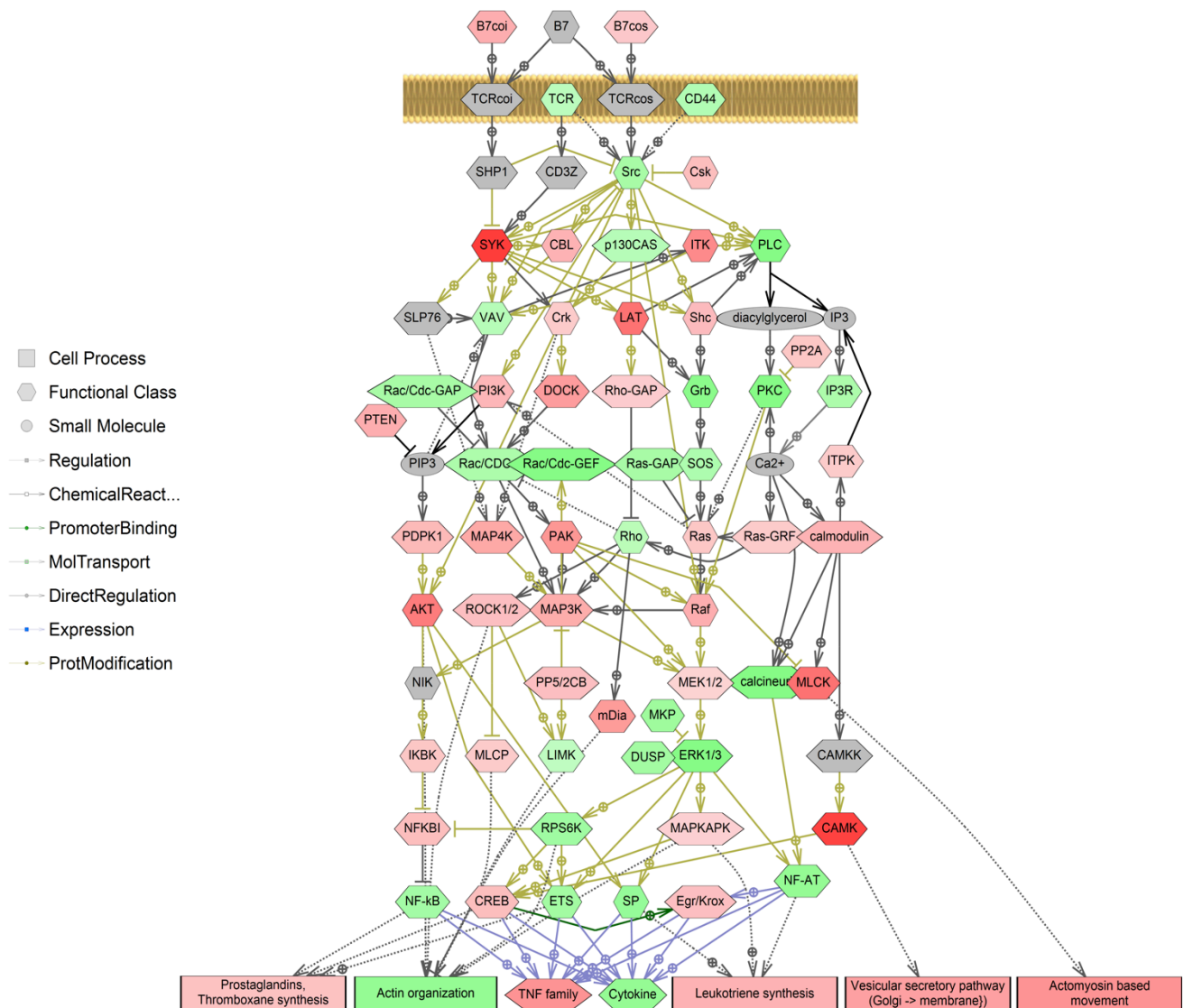


Figure 3.7. T cell activation signaling was significantly enriched by GSEA in primary *Carassius auratus* RGC culture after 1000 nM SNa treatment ($P < 0.05$). Red indicates that the gene is increased and green indicates that the gene is decreased.

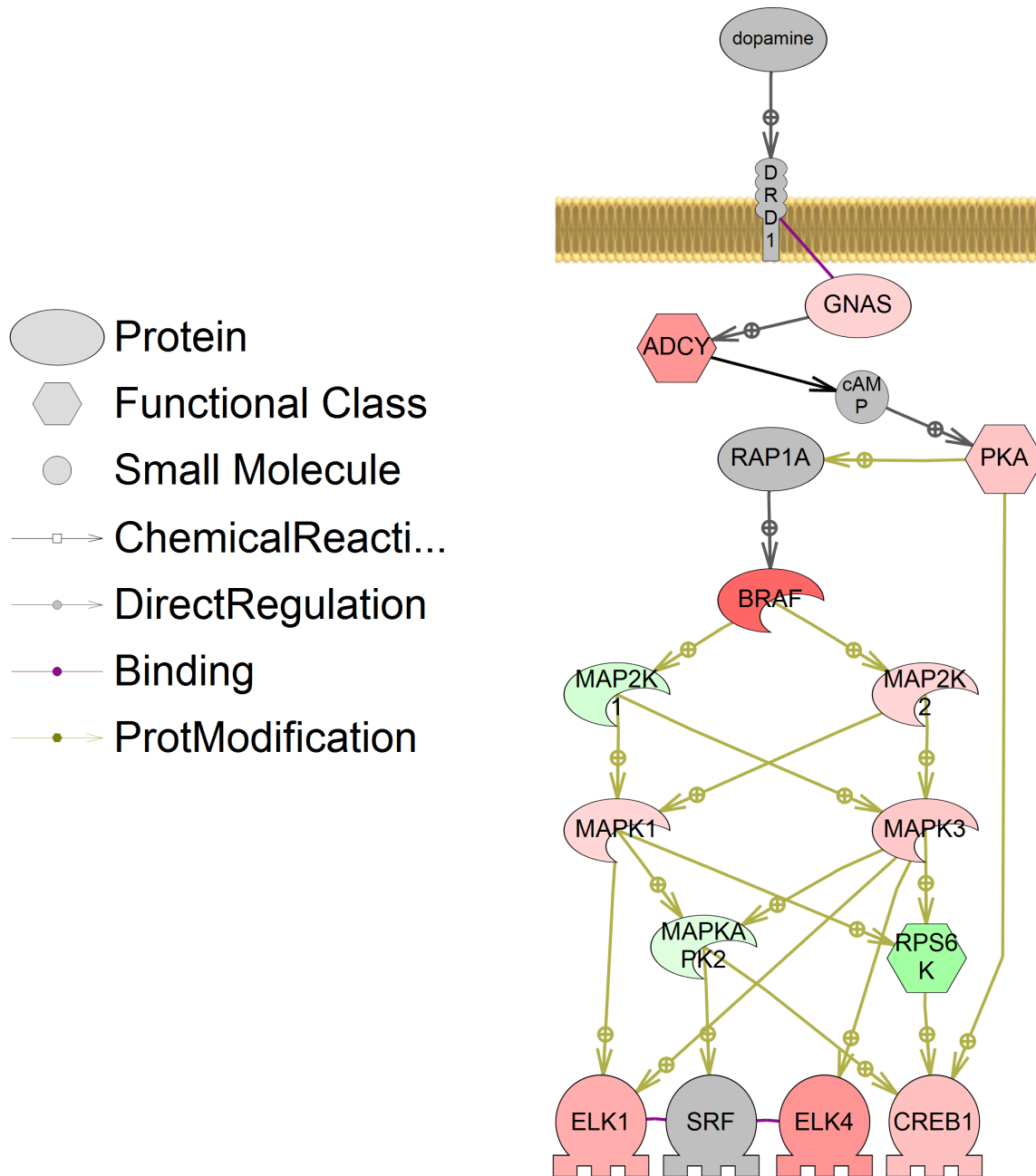


Figure 3.8. Dopamine D1 receptor signaling pathway was significantly enriched by GSEA in primary *Carassius auratus* RGC culture after 1000 nM SNa treatment ($P < 0.05$). Red indicates that the gene is increased and green indicates that the gene is decreased.

3.3.6. Sub-network enrichment analysis

Pathway Studio was queried to further identify gene sub-networks that were significantly regulated by SNa treatment. SNEA revealed a total of 192 cellular processes that were significantly responsive to SNa exposure. Sub-networks that included processes related to CNS and immune system were major biological themes regulated by SNa (Table 3.5). All 19 sub-networks involved in processes related to the CNS were consistently increased (7-70%). Some of these sub-networks included neurogenesis, glial cell development, neuronal activity, synaptic plasticity, axon guidance and extension. A total of 19 sub-networks were associated with the cellular processes of the immune system. There were 18 sub-networks that were increased (5-53%) and 1 sub-network that was decreased (-13%), indicating that SNa has a largely stimulatory effect on diverse processes in RGCs. These included for example immune system activation, immunoreactivity, lymphocyte activation, macrophage response leukocyte function and differentiation. As examples of sub-networks significantly regulated by SNa in each major biological theme, both neurogenesis (Fig. 3.9) and immune system activation (Fig.3.10) are presented.

Table 3.5. Cell processes identified by SNEA that were regulated by 1000 nM SNa in primary *Carassius auratus* RGC culture. Only sub-networks with a median fold change greater than 5 % in the cell process are presented ($P < 0.05$). Reported here are only some major cell processes affected by SN in RGCs.

	Gene Set Seed	Total # in pathway	# of Measured Neighbors	Median change	P-value
Processes related to CNS	Axon guidance	210	160	1.17	0
	Transmission of nerve impulse	598	321	1.1	0
	Cognition	212	126	1.11	0.004
	Innervation	172	113	1.08	0.005
	Brain function	150	89	1.14	0.006
	Cerebellum development	14	8	1.44	0.007
	Neuronal activity	263	133	1.06	0.008
	Neuroproliferation	6	5	1.7	0.01
	Hindbrain development	15	11	1.44	0.013
	Synaptic transmission	509	288	1.13	0.013
	Synaptic plasticity	454	284	1.1	0.013
	Schwann cell formation	15	12	1.26	0.016
	Memory	721	385	1.08	0.016
	Neuron development	103	69	1.1	0.029
	Dentate gyrus development	6	6	1.34	0.03
	Neurogenesis	561	383	1.11	0.031
	Central nervous system function	25	15	1.26	0.041
	Axon extension	74	59	1.16	0.042
Glial cell development	17	11	1.25	0.044	
Processes related to immunity	B-cell activation	233	105	1.1	0.001
	Leukocyte function	158	74	1.09	0.003
	Granulocyte adhesion	52	27	1.11	0.009
	Peritoneal macrophage function	10	5	1.34	0.014
	Immunoreactivity	463	260	1.13	0.014
	Eosinophil degranulation	43	15	1.31	0.015
	T-cell homeostases	100	50	1.05	0.016
	Respiratory burst	185	92	1.1	0.017
	NK cell mediated cytotoxicity	367	133	1.09	0.018
	Leukocyte accumulation	84	43	1.1	0.019
	Leukocyte differentiation	9	5	1.53	0.022
	B lymphocyte proliferation	277	148	1.07	0.022
	Lymphocyte activation	277	131	1.11	0.023
	Lymphocyte aggregation	10	6	1.32	0.027
	Macrophage response	48	19	1.1	0.028
	Immune system activation	163	76	1.07	0.033
	Leukocyte tethering / rolling	106	58	1.11	0.041
	Phagocyte activity	167	80	1.1	0.046
Granulosa cell differentiation	46	34	-1.13	0.047	

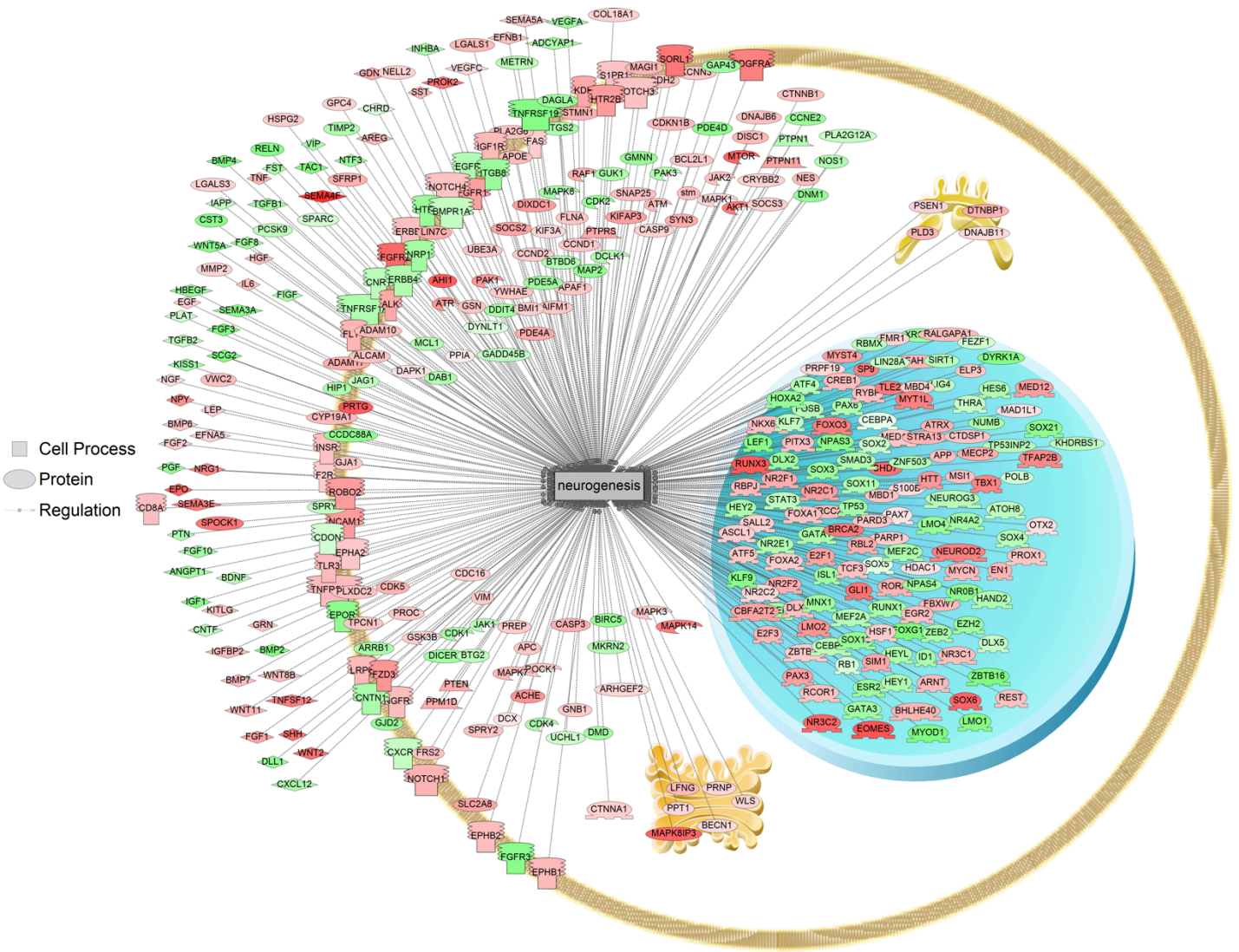


Figure 3.9. Genes involved in neurogenesis were significantly enriched by SNEA in primary *Carassius auratus* RGC culture after 1000 nM SNa treatment ($P < 0.05$). Red indicates that the gene is increased and green indicates that the gene is decreased.

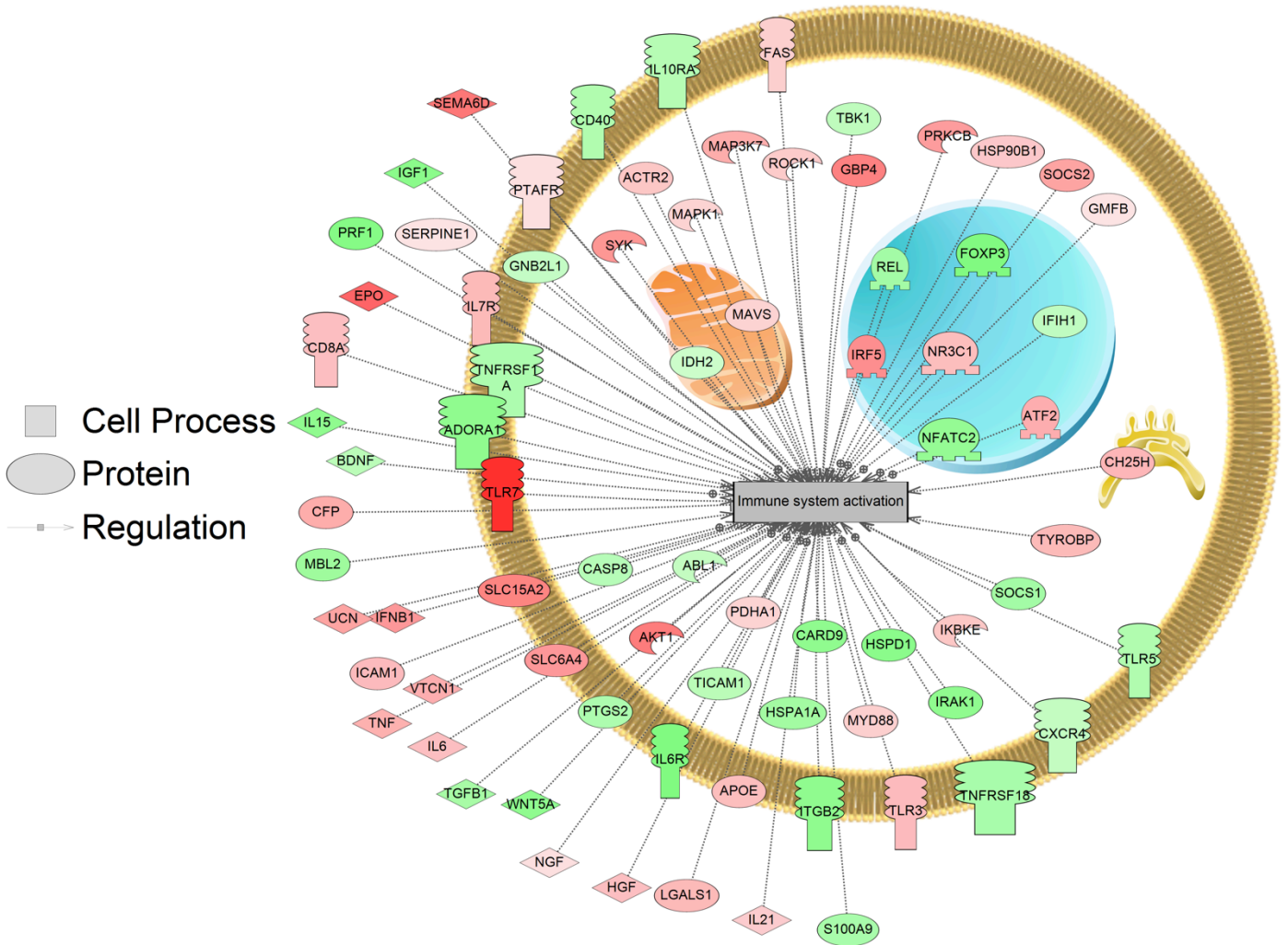


Figure 3.10. Genes involved in immune system activation were significantly enriched by SNEA in primary *Carassius auratus* RGC culture after 1000 nM SNa treatment ($P < 0.05$). Red indicates that the gene is increased and green indicates that the gene is decreased.

3.4. Discussion

RNA sequencing and *de novo* transcriptome assembly and analysis were used to elucidate the regulatory actions of SNa on gene networks in goldfish radial glia. We were able to characterize this cell type at the molecular level for which limited information exists in fish species. A total of 12,180 non-redundant unigenes were identified and GO ontology analysis revealed a diverse receptor and signaling molecule profile suggesting that RGCs can respond and synthesize an array of hormones, peptides, cytokines, and growth factors. RGCs express receptors for various neurotransmitters including 5-HT (1A, 2B, 2C, 6), DA (D2, D4), GABA (GABA_A, GABA_B), acetylcholine (M4, M5), adrenaline (α 2a, α 2c, β 1, β 2), adenosine (A1, A2B), and histamine (H1, H3). Previous studies in fish demonstrate that DA can regulate RGCs to increase aromatase B, while also regulating protein networks associated with progenitor cell functions (Xing et al., 2015b, 2016a). RGCs are also likely under the direct control of 5-HT, as 5-HT neurons share a close distribution with RGCs in the zebrafish paraventricular organ and *in vivo* inhibition of 5-HT synthesis decreases RGC proliferation (Pérez et al., 2013). In support of our data, goldfish RGCs have previously been documented to express adenosine A1 receptors (Beraudi et al., 2003) and activation of this receptor in rabbit RGCs causes ATP-evoked increases in calcium that regulate proliferation (Uckermann et al., 2002). In mice, RGC fate is under the control of GABA excitation where high levels of activation result in quiescence, while low levels of excitation cause either symmetrical or differentiating asymmetrical cell divisions (Song et al., 2012). Although nothing is known in RGCs, histamine H1, H2, and H3 receptors are expressed by mammalian astrocytes and regulate astrocytic functions such as calcium influx, energy metabolism,

neurotransmitter clearance, neurotrophic activity, and immune response (Jurič et al., 2016). Together, this panel of neurotransmitter receptors expressed by these cells suggests goldfish RGCs are in communication with numerous neuronal subtypes.

In culture, goldfish RGCs also express receptors for hormones, such as growth hormone (*ghra*), growth hormone-releasing hormone (*ghrh*), thyroid hormone (*thrab*, *thrb*), thyrotropin releasing-hormone (*trhr2*), prolactin-releasing peptide (*prlhr2a*), prolactin (*prlrb*), oxytocin (*oxtr*), and vasopressin (*avpr2l*). Isotocin and vasotocin in fish, or the mammalian homologs oxytocin and vasopressin, are released from magnocellular and parvocellular neurons. Given the close interactions in the preoptic nucleus between RGCs and SNa-immunoreactive magnocellular and parvocellular neuron cell bodies shown in Chapter 2, identifying receptors for oxytocin and vasopressin in RGCs support the proposal that these neuronal populations are communicating with surrounding RGCs. Previously RGCs have been shown to be under the control of hormones especially during development. For instance, maternal thyroid hormone deficiency in rat causes decreased number and length of RGCs resulting in impaired neuronal migration (Pathak et al., 2011).

The GO analysis identified many immune system pathways, cytokines, and cytokine receptors suggesting fish RGCs have important functions in brain immune reactivity. RGCs are the main macroglia in fish brain since they lack typical stellate astrocytes (Grupp et al., 2010) so RGCs likely share some functions with mammalian astrocytes in order to maintain normal brain homeostasis. Thought to only involve microglia, neuroinflammation is also regulated by mammalian astrocytes (Farina et al., 2007; Liu et al., 2011; Norden et al., 2016). The transcriptome of goldfish RGCs reveal

key proinflammatory molecules and receptors including interleukin/interleukin receptors, toll-like receptors, tumour necrosis factor/tumour necrosis factor receptors, and transforming-growth factor β (TGF β). Although their role in neuroinflammation is less established than that in astrocytes, RGCs in fish brain respond to inflammatory cues to initiate the regenerative response. Unlike mammals, where after brain injury neuroinflammation causes a glial scar that obstructs neurogenesis (Ekdahl et al., 2003; Fitch and Silver, 2011), neuroinflammation in fish directly activates RGC proliferation and subsequent neurogenesis through leukotriene C4 signaling (Kyritsis et al., 2012). In addition, the expression of chemokine/chemokine receptors implicates RGCs in the control of processes such as neural migration, axonal guidance, and neural regeneration that involve chemotaxis (Stumm et al., 2002; Stumm and Höllt, 2007; Diotel et al., 2010b). RGCs in the zebrafish brain express the chemokine Cxcl2 and its receptor Cxcr4 (Diotel et al., 2010b) and also the chemokine receptor Cxcr5, which regulates RGC proliferation and differentiation (Kizil et al., 2012).

Further validating this primary culture as RGCs, several fish RGC markers were identified in the transcriptomic data, including: aromatase B (*cyp191b*), brain fatty acid binding protein (*blbp*), calcium binding protein β (*s100b*), connexin 43 (*cx43*), glial fibrillary acidic protein (*gfap*), glial high affinity glutamate transporter (*slc1a3a*), glutamine synthase (*glula*), nestin (*nes*), sex determining region Y box 2 (*sox2*), and vimentin (*vim*). These are markers that have been identified and used in zebrafish and provide the cell with the ability of transmitter uptake (*slc1a3a*, *glula*), neuroestrogen production (*cyp19a1b*), and generation of calcium waves (*cx32*) (Than-Trong and Bally-Cuif, 2015). Furthermore, identification of several steroidogenic enzyme transcripts such

as steroidogenic acute regulatory protein (*star*), 17 α -hydroxylase (*cyp17a1*), 17 β -hydroxysteroid dehydrogenase (*hsd17b10*), aromatase B (*cyp19a1b*), and 5 α -reductase (*srdsal*), suggest these cells are capable of *de novo* estrogen production from cholesterol and are able to produce progesterone and pregnenolone intermediates, confirming previous observations that these are steroidogenic cells (Xing et al., 2014). Here we also show that cultured goldfish RGCs express progesterone receptor (*pgr*), androgen receptor (*ar*), G-protein coupled estrogen receptor (*gper1*), estrogen receptor α (*esr1*), estrogen receptor β 1 (*esr2b*), and estrogen receptor β 2 (*esr2a*). This data supports other reports in zebrafish that *in vivo* RGCs express Pgr protein (Diotel et al., 2011c) and the observed similar distribution of *ar*, *esr*, *esr2a*, and *esr2b* mRNAs with aromatase B expression in RGCs (Diotel et al., 2011a). The expression of nuclear estrogen receptor mRNA has been documented before in goldfish RGC cultures (Xing et al., 2015a), however this is the first time *gper1* has been shown to be expressed by RGCs. Previously, we failed to clone *gper1* from RGCs, suggesting it is lowly expressed in some cultures. The deep coverage obtained by RNA-Seq of 10 different cultures is the likely explanation for this difference. The combination of numerous steroidogenic enzymes and steroid receptors expressed by RGCs support the previous hypothesis that RGCs are both a source and target of neurosteroids (Diotel et al., 2011a).

Another aim of this study was to further understand the neuronal-RGC interactions between SNa-positive neurons and RGCs in the preoptic area (Chapter 2) by characterizing the transcriptomic responses to SNa exposure. Through differential gene analysis SNa decreased various genes such as *smad6b*, *nab1a*, and *fgf4*. In teleost fish, Smad6 is duplicated however very few studies have investigated either Smad6a or

Smad6b. Nonetheless, its mammalian homologue Smad6 is a negative regulator of bone morphogenic proteins (BMP) (Wrana, 2000; Sieber et al., 2009) and has been linked to the regulation of various stem/progenitor cell behaviours (Ding et al., 2014). For example, inhibiting BMP signaling in neuronal precursor cells by transfection with Smad6 prevents astrocyte differentiation and promotes neurogenesis (Setoguchi et al., 2004). Although further investigations are required to determine the role of Smad6b in RGCs, effects of SNa to decrease *smad6b* may implicate SNa in the regulation of BMP signaling.

Our study shows SNa can decrease *nab1a* mRNA levels, the orthologue to mammalian *nab1*. Nerve growth factor-induced gene A binding protein 1 (NAB1) is a active corepressor that negatively regulates the transcriptional activity of nerve growth factor-induced gene A (*NGFI-A*) (Swirnoff et al., 1998). NGFI-A is an immediate-early gene and is responsive to various extracellular stimuli such as growth factors, hormones, and neurotransmitters in order to regulate the growth, proliferation, and differentiation of a variety of cell types (O'Donovan et al., 1999). Furthermore, the NGFI-A gene is highly conserved between fish and mammals, in particular the repressor domain, where the NAB1 transcriptional cofactor binds and inhibits expression of NGFI-A target genes, is both 94% similar and identical between mouse and zebrafish (Burmeister and Fernald, 2005). NGFI-A is involved in the intracellular mechanisms that convert mitogenic signals to regulate both astrocyte growth and proliferation. Cultured astrocytes exposed to glial mitogens stimulate NGFI-A expression while site-directed mutagenesis of the DNA binding domain of NGFI-A causes inhibition of proliferation in stimulated astrocytes (Hu and Levin, 1994; Mayer et al., 2009). NAB1 completely blocks transcription facilitated by NGFI-A thereby making the concentration of NAB1 in a cell critical for NGFI-A

function (Thiel et al., 2000). Therefore, our data suggests SNa may decrease NAB1A concentrations within RGCs to effectively decrease the strength of extracellular stimuli needed to control NGFI-A synthesis and subsequent activation of downstream targets.

Here we also show, SNa may be involved in regulation fgf signaling in RGCs, through the inhibition of *fgf4* expression. Fgfs are a group polypeptide growth factor that regulate cell proliferation, differentiation, and migration in the developing and mature CNS (Dono, 2003; Reuss and Von Bohlen Und Halbach, 2003). Fgfs elicit diverse physiological effects due to the ability of different fgf ligands to bind to multiple fgf receptors with varying binding affinities. Human fgf4 is able to activate all four fgf receptors but has a higher affinity for fgfr1, 2, and 4 (Ornitz et al., 1996; Reuss and Von Bohlen Und Halbach, 2003). Fgf signaling is important in the regulation of RGC self-renewal and differentiation (Kang et al., 2009; Sahara and O’Leary, 2009). Mutant mice with three fgf receptor genes (*fgfr1-3*) simultaneously deleted resulted in decreases in RGC populations caused by increased rate of transition to more differentiated states. This suggests fgf signaling is required to maintain the self-renewal of RGCs as a progenitor cell while inhibiting their differentiation to a more committed fate (Kang et al., 2009).

GSEA identified many transcripts regulated by SNa in RGCs that were involved in immune receptor signaling, dopamine receptor signaling, cell-cell junctions and cell-cell communication. Transcripts involved in both tight (claudins, JAMs) and adherens (nectin, cadherins) junction assembly were significantly affected by SNa. In zebrafish, RGCs express the tight junction protein claudin-3 along their fibers and tight junction protein 1 (ZO-1) on processes lining the ventricle and their endfeet facing the meninges, suggesting RGCs form junctional complexes between subpial and ventricular borders

(Grupp et al., 2010). In the continuously growing optic nerve of fish, similar tight junction expression is found which potentially generates glia-neuronal interactions that form microenvironments favoring growth (Mack and Wolburg, 2006; Parrilla et al., 2009). Cell-cell adhesion molecules are important in neuronal cell migration, axon guidance, synapse formation, and forming glial networks (Togashi et al., 2009). For example, RGCs mediates neuronal migration and directs axon formation through N-cadherin adhesions (Xu et al., 2015). Also involved in cell-cell adhesion and communication, ephrin receptor and NCAM receptor signaling pathways were identified having transcripts regulated by SNa exposure. Ephrin signaling is involved in neurogenesis where in the developing mammalian neocortex ephrin signaling is required to maintain the self-renewal of RGCs (Laussu et al., 2014). Furthermore, both ephrins (Benson et al., 2005; Moss et al., 2005) and NCAM (Doherty and Walsh, 1991) regulate neurite outgrowth, a process which has been previously shown to be stimulated by SN in rat cerebellar granule cells (Gasser et al., 2003). Therefore, as SNa is shown here to regulate genes involved in the assembly of adherens and tight junctions, it may implicate this neuropeptide in regulating processes that involve glial-glial and/or glial-neuron interactions. In addition, GSEA showed SNa caused an increase in genes involved in DRD1 signaling which supports previous data in goldfish RGC cultures that have shown functional D1R signaling through the cAMP/PKA/p-CREB pathway (Xing et al., 2015b). Likewise, the putative SN receptor activates similar G-protein cAMP/PKA mechanisms (Trudeau et al., 2012). The expression of the SNa receptor remains to be confirmed in RGCs because it has not yet been identified, however future studies should identify signaling pathways that mediate the effects in RGCs elicited by SNa.

Both GSEA and SNEA indicate that the immune response is a major theme enriched in RGCs following SNa exposure. The results from GSEA show changes in the expression levels of genes involved in IL-6R signaling, TNFR signaling, T-cell activation, and several T-cell receptor signaling pathways. It has been established that neuropeptides such as vasoactive intestinal peptide (Maimone et al., 1993), substance P (Gitter et al., 1994), and somatostatin (Grimaldi et al., 1997) can regulate IL-6 expression in astrocytes. SNEA indicated that SNa exposed RGCs caused the stimulation of genes responsible for many immune system processes. Some of these included, immune system activation, phagocyte activity, leukocyte function, macrophage response, lymphocyte aggregation, and activation. Such regulation of immune system responses has been previously reported for SN. After experimental autoimmune encephalomyelitis is induced in the rat brain, there is a close correlation between SN-immunoreactivity and macrophage infiltration indicating SN may play a role in leukocyte recruitment of the CNS (Storch et al., 1996). SN has been documented to affect various cells involved in the inflammatory response. Both *in vivo* and *in vitro*, SN can stimulate the migration of human monocytes also acting synergistically with other sensory neuropeptides like substance P or somatostatin (Reinisch et al., 1993). SN is also an effective chemoattractant for human eosinophils comparable in its potency to interleukin-8 (Dunzendorfer et al., 1998b). Moreover, SN can stimulate natural killer cell migration and cytokine release (Feistritzer et al., 2005). Our enrichment analyses provide some molecular mechanisms that explain the documented effects of SN in the immune system and propose SN as a proinflammatory regulator of RGCs due to the upregulation of immune-related genes, although future studies are needed to address this hypothesis.

Gene networks related to processes of the CNS were significantly regulated by SNa in cultured RGCs. Some of the CNS processes that were SNa-responsive included neurogenesis, synaptic plasticity, neuron development, glial cell development, axon extension and guidance. All pathways in this biological theme showed significantly higher gene expression levels than control, suggesting SNa has a stimulatory effect over these processes. Regulation of transcripts involved in these CNS processes by SNa may have implications in controlling key RGC functions in the fish brain. RGCs are involved in neurogenesis generating new neurons in the adult fish CNS and are involved in the guidance of migrating young neurons (Zupanc and Clint, 2003). Previously, SN has been shown to act as a trophic substance stimulating neurite outgrowth (Gasser et al., 2003) and also activating the Jak2/Stat3 pathway to promote neuroprotection and enhance neurogenesis in murine models of stroke (Shyu et al., 2008). Therefore, the changes in gene networks observed here are consistent with documented neurogenic and neuroprotective effects of SN. Given the neuroplastic effects of SN and its ability to significantly increase the expression of transcripts related to processes such as neurogenesis and synaptic plasticity, future works should address if SNa can stimulate neurogenesis in the stem-like RGC.

In summary, this study used next generation sequencing and *de novo* assembly to generate the first reference transcriptome for RGCs in fish. These data revealed that these neuroendocrine cells express an array of hormone, neurotransmitter, and neuropeptide receptors suggesting a multiplicity of new functions critical to neuronal-glia communication. The identification of immune system pathways, proinflammatory signals and receptors indicate RGCs may also be involved in regulating neuroinflammation

processes in the fish brain. Exploring neuronal-RGC interactions, we show here RGCs elicit transcriptomic responses to SNa, suggesting RGCs can be under control of neuropeptides. Gene networks related to immune responses and CNS physiology were affected by SNa, suggesting this neuropeptide may play a role in regulating these processes in RGCs.

Chapter 4: Secretoneurin-A regulated proteomic profiles and networks in goldfish radial glial cells *in vitro*

4.1. Introduction

Radial glial cells (RGCs) are a macroglial subtype present during the CNS development of all vertebrates and are characterized by their bipolar morphology (Schmechel and Rakic, 1979) and stem-like progenitor properties (Florio and Huttner, 2014). RGCs line the ventricle with their cell body and have an elongated radial fiber terminating with endfeet on the walls of blood vessels or at the pial surface (Barry et al., 2014). Due to this unique morphology, their radial processes are used as scaffolds for migration of newborn neurons (Rakic, 1971; Silver et al., 1982). As stem cells, RGCs are capable of undergoing neurogenesis and/or gliogenesis to produce neurons or other glial cells (Radakovits et al., 2009). RGC populations are transient in mammals as they differentiate into astrocytes at the end of cortical development. In contrast, RGCs are abundant throughout the adult brain in teleost fish, supporting unsurpassed high levels of neurogenesis and regenerative abilities (Pellegrini et al., 2007; Strobl-Mazzulla et al., 2010). In addition, teleost RGCs express various steroidogenic enzymes (Diotel et al., 2011b; Xing et al., 2014) and exclusively express the estrogen-synthesizing enzyme, aromatase B (*cyp19a1b*) (Forlano et al., 2001; Pellegrini et al., 2005; Tong et al., 2009), making them neuroendocrine cells producing neuroestrogens and other steroids in the CNS. Although RGCs in fish have established roles in neurogenesis and neurosteroidogenesis, very little is known about other potential functions and the regulatory factors that control them. Because RGCs are the main macroglia in fish CNS

(Grupp et al., 2010) they share close interactions with a variety of neurons and since RGCs express various neurotransmitter, neuropeptide, and hormone receptors (Chapter 3) they may be under functional control of neuronal-glia interactions.

The investigations described in Chapter 2 revealed the close neuroanatomical relationship between the soma of secretoneurin A (SNa)-immunoreactive preoptic neurons and RGCs along the third ventricle in goldfish and zebrafish. The neuropeptide SN is generated from endoproteolytic processing of its precursor protein SgII and has well-established functions in endocrine, nervous, and immune systems (Fisher-Colbrie et al. 1995; Zhao, Zhang, et al. 2009). Due to the genome duplication in teleost fish there are two SgII paralogs, SgIIa and SgIIb, which produce their respective SNa and SNb peptides (Zhao et al., 2010). Both *in vivo* and *in vitro*, SNa inhibits *cyp19a1b* mRNA expression in goldfish RGCs, implicating SNa in the control of neuroestrogen production (Chapter 2). Furthermore, data from transcriptome sequencing of cultured goldfish RGCs showed gene networks related to immune responses and CNS physiology were responsive to 1000 nM SNa (Chapter 3). Altogether, this anatomical and transcriptomic data proposes SNa is a regulator of RGC function and supports previous findings that suggest neuronal-RGC interactions are integral in regulating this cell type to maintain proper brain homeostasis. Therefore, building on our previous transcriptomic data, the objectives of this study were to (1) characterize the RGC proteome, for which limited information exists in fish species, (2) determine the differentially regulated proteins over a range of SNa concentrations and (3) identify protein networks responsive to SNa regulation.

4.2. Material and methods

4.2.1. Experimental animals

All procedures used were approved by the University of Ottawa Protocol Review Committee and followed standard Canadian Council on Animal Care guidelines on the use of animals in research. Common adult female goldfish (*Carassius auratus*) were purchased from a commercial supplier (Mt. Parnell Fisheries Inc., Mercersburg, PA, USA) and handled as described in Chapter 2.

4.2.2. Cell culture and exposure

Cell culture methods used in the present study have been previously established and validated (Xing et al., 2015b) and all culture procedures and exposures were described previously in Chapter 2.

4.2.3. Protein extraction, isobaric tagging for relative and absolute quantitation (iTRAQ), and LC-MS/MS

Proteins were quantified as previously described (Koh et al., 2012), and dissolved in denaturant buffer (0.1 % SDS (w/v)) and dissolution buffer (0.5 M triethylammonium bicarbonate, pH 8.5) in the iTRAQ Reagents 8-plex kit (AB Sciex Inc., Foster City, CA, USA). For each sample, 100 µg of protein were reduced, alkylated, trypsin-digested, and labeled according to the manufacturer's instructions (AB Sciex Inc.). Two 8-plex iTRAQ labelling reactions were conducted, each with 2 biological replicates. Peptides from the control group were labeled with either iTRAQ tags 113 or 114. The three treatments of different doses were labelled as follows: 10 nM SNa (115, 116), 100 nM SNa (117, 118)

and 1000 nM SNa (119, 121). This labelling scheme was repeated in a second experiment, thus the data are derived from a sample size of 4 biological replicates per group.

Labeled peptides were combined for each iTRAQ experiment and desalted with C18-solid phase extraction and dissolved in strong cation exchange (SCX) solvent A (25 % (v/v) acetonitrile, 10 mM ammonium formate, and 0.1 % (v/v) formic acid, pH 2.8). The peptides were fractionated using an Agilent HPLC 1260 with a polysulfoethyl A column (2.1 × 100 mm, 5 μm, 300 Å; PolyLC, Columbia, MD, USA). Peptides were eluted with a linear gradient of 0–20 % solvent B (25 % (v/v) acetonitrile and 500 mM ammonium formate, pH 6.8) over 50 min., followed by ramping up to 100 % solvent B in 5 min. The absorbance at 280 nm was monitored and a total of 14 fractions were collected. The fractions were lyophilized and resuspended in LC solvent A (0.1 % formic acid in 97 % water (v/v), 3 % acetonitrile (v/v)). A hybrid quadrupole Orbitrap (Q Exactive) MS system (Thermo Fisher Scientific) was used with high energy collision dissociation (HCD) in each MS and MS/MS cycle. The MS system was interfaced with an automated Easy-nLC 1000 system (Thermo Fisher Scientific). Each sample fraction was loaded onto an Acclaim Pepmap 100 pre-column (20 mm × 75 μm; 3 μm-C18) and separated on a PepMap RSLC analytical column (250 mm × 75 μm; 2 μm-C18) at a flow rate at 350 nl/min during a linear gradient from solvent A (0.1% formic acid (v/v)) to 25 % solvent B (0.1% formic acid (v/v) and 99.9 % acetonitrile (v/v)) for 80 min, and to 100 % solvent B for additional 15 min.

The raw MS/MS data files were processed by a thorough database searching approach considering biological modification and amino acid substitution against the National Center for Biotechnology Information (NCBI) Cyprinidae database

(downloaded on March 23 2016) using the ProteinPilot v4.5 with the Fraglet and Taglet searches under ParagonTM algorithm (Shilov et al., 2007). The following parameters were considered for all the searching: fixed modification of methylmethane thiosulfonate-labeled cysteine, fixed iTRAQ modification of amine groups in the N-terminus, lysine, and variable iTRAQ modifications of tyrosine. For protein quantification, only MS/MS spectra that were unique to a particular protein and where the sum of the signal-to-noise ratios for all the peak pairs > 9 were used for quantification. To be identified as being significantly differentially expressed, a protein was quantified with at least three unique spectra in at least two of the biological replicates, along with a Fisher's combined probability of < 0.05 and a fold change < 0.5 or > 1.5 .

4.2.4. Gene ontology and pathway analysis

Gene ontology terms were assigned using protein annotation through evolutionary relationships (PANTHER) in order to classify all proteins identified in RGC cultures (Mi et al., 2015). Gene ontology categories for biological processes, molecular functions, cellular components, protein classes, and pathways were used to identify the distribution of proteins within each gene ontology category in RGC cultures. Pathway Studio 9.0 (Elsevier) and ResNet 10.0 were used to build a protein interaction network for SNa effects in RGCs. Official gene symbols were manually retrieved using gene card (<http://www.genecards.org>) in order to map proteins into Pathway Studio. The number of proteins that successfully mapped to Pathway Studios using Name + Alias were as follows for each of the 3 treatments: 10 nM SNa = 99, 100 nM SNa = 231, and 1000 nM SNa = 499. Interaction networks were based upon expression, binding, and regulatory

interactions in the database and were constructed using direct connections with one neighbour. Sub-network enrichment analysis (SNEA) for cell processes was performed in Pathway Studio to determine if differentially expressed proteins were related to specific biological functions. The P value for gene seeds was set at $P < 0.05$ and the criterion of > 5 members per cell process or group was required for inclusion as a significantly regulated gene network.

4.3. Results

4.3.1. Identification and gene ontology classification of radial glial cell proteins

A total of 1,363 unique RGC proteins were identified and assigned GO terms for functional classification. The GO annotated proteins were classified in three main categories: biological function, molecular function, and cellular component (Fig. 4.1). A variety of biological functions were identified with 1,546 unique biological processes classified into 12 functional groups. The most represented biological functions included cellular process (438 proteins), metabolic process (414), and cellular component organization or biogenesis (199). Other important biological function allocations included developmental process (86 proteins), response to stimulus (65), immune system process (30), and biological adhesion (11). A broad array of 893 molecular functions were categorized into 9 function groups. The molecular functions most represented in the RGC proteome were binding (334 proteins) and catalytic (299), structural molecule (177), and transporter (38) activities. When organized by cellular component, RGC proteins were enriched in the cell part (379 proteins), organelle (238), and macromolecular complex (165). Most proteins identified were further classified into protein class, with nucleic acid binding (187 proteins), cytoskeletal proteins (147), and enzyme molecular (90) being the most represented classes detected in RGCs (Fig. 4.2). Lastly, a total of 535 proteins were represented by 102 pathways. The top 25 represented pathway ontologies are presented in Table 4.1. Proteins were most enriched in Parkinson disease (31 proteins), integrin signaling pathway (28), ubiquitin proteasome pathway (26), cytoskeletal regulation by Rho GTPase (26), Huntington disease (25), and inflammation mediate by chemokine and cytokine signaling (24) (Table 4.1).

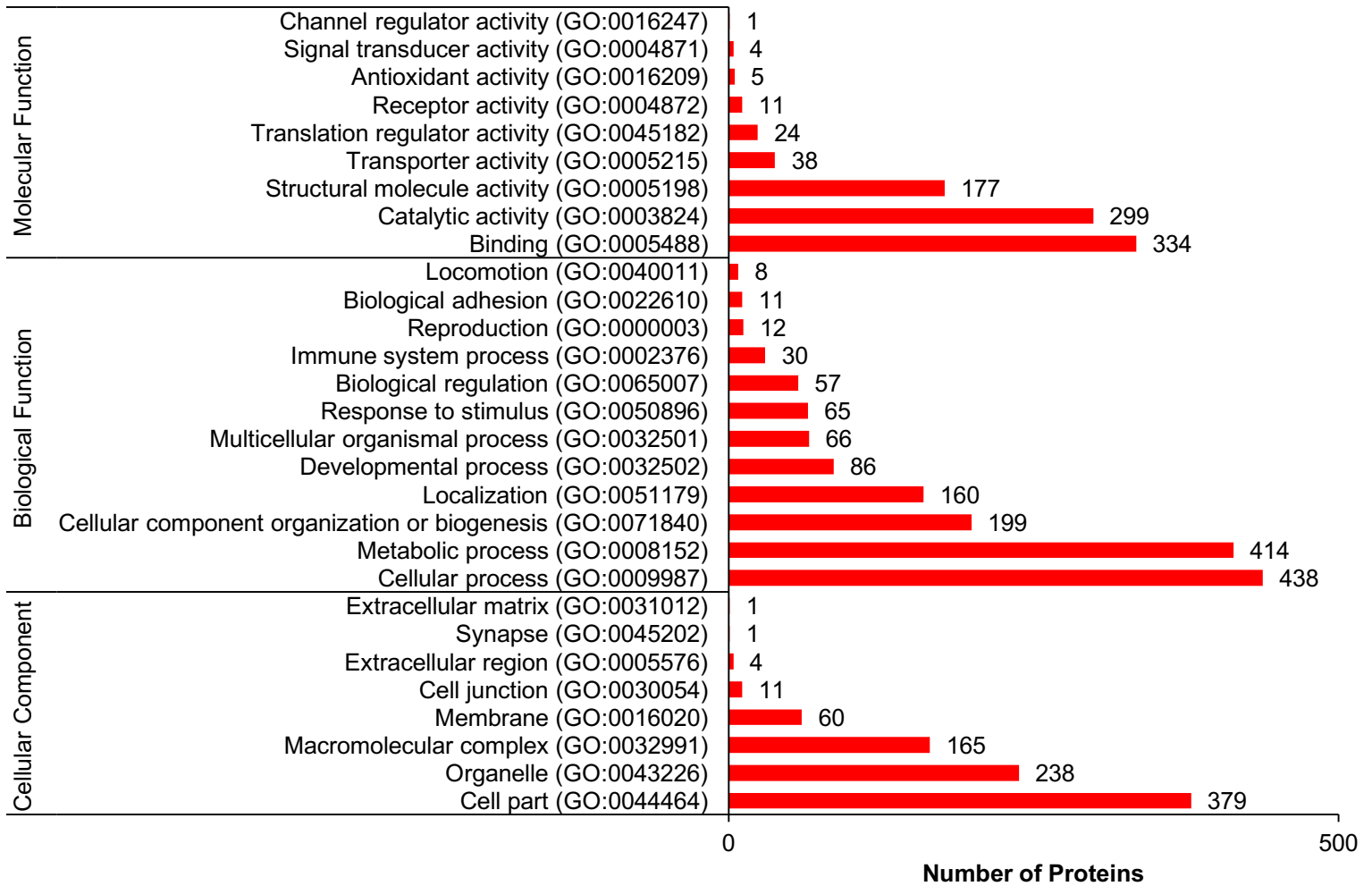


Figure 4.1. GO classification of identified *Carassius auratus* RGC proteins into molecular function, biological function, and cellular component categories. The number of proteins ascribed to each classification is provided along with accession number.

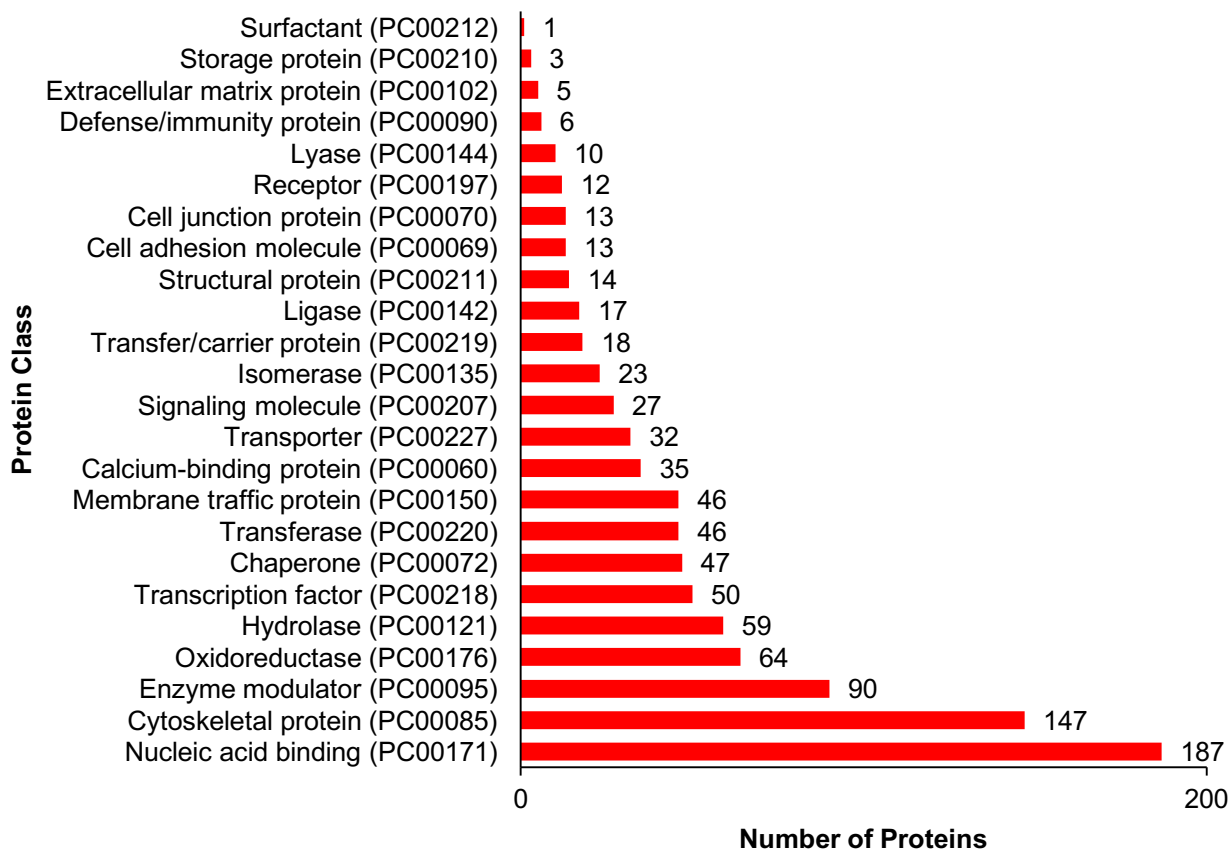


Figure 4.2. GO classification of identified *Carassius auratus* RGC proteins by protein class. The number of proteins ascribed to each classification is provided along with accession number.

Table 4.1. Top 25 assigned pathway ontologies of identified *Carassius auratus* RGC proteins based on number of protein identified in each pathway.

Pathway Name	Pathway Accession	# of proteins identified
Parkinson disease	P00049	31
Integrin signalling pathway	P00034	28
Ubiquitin proteasome pathway	P00060	26
Cytoskeletal regulation by Rho GTPase	P00016	26
Huntington disease	P00029	25
Inflammation mediated by chemokine and cytokine signaling pathway	P00031	24
FGF signaling pathway	P00021	15
EGF receptor signaling pathway	P00018	15
CCKR signaling map	P06959	14
Wnt signaling pathway	P00057	14
Angiogenesis	P00005	13
Gonadotropin-releasing hormone receptor pathway	P06664	12
Cadherin signaling pathway	P00012	12
Alzheimer disease-presenilin pathway	P00004	10
T cell activation	P00053	10
Nicotinic acetylcholine receptor signaling pathway	P00044	10
Ras Pathway	P04393	10
Glycolysis	P00024	10
Cell cycle	P00013	10
Apoptosis signaling pathway	P00006	8
TGF-beta signaling pathway	P00052	7
De novo purine biosynthesis	P02738	7
PDGF signaling pathway	P00047	7
Dopamine receptor mediated signaling pathway	P05912	7
Axon guidance mediated by Slit/Robo	P00008	6

4.3.2. Quantitative proteomic responses in primary cultures of radial glia to secretoneurin-A *in vitro*

For a protein to be significantly differentially expressed, a minimum of three unique spectra in at least two of the biological replicates, a fold change < 0.5 or > 1.5 , along with a Fisher's combined probability of < 0.05 were required. Using this level of stringency a total of 609 proteins showed differential expression (Fig. 4.3) with 17 different expression patterns being recognized (Table 4.2). At 10 nM, 100 nM, and 1000 nM SNa, there were 5, 195, and 489 down-regulated proteins, respectively, whereas the number of up-regulated proteins were 72, 44, and 51, respectively. Generally, there was a shift to more down-regulated proteins as the concentration of SNa increased. The overlap of the differentially regulated proteins between doses is shown in Figure 4.4. A total of 10 common proteins were regulated between the three doses, some examples of these include H1 histone, glutamyl-prolyl-tRNA synthetase, Rho GDP dissociation inhibitor γ , vimentin A2, and small nuclear ribonucleoprotein-associated protein. As an example of the differentially regulated proteins, Table 4.3 highlights the top 20 proteins most significantly regulated by each dose of SNa.

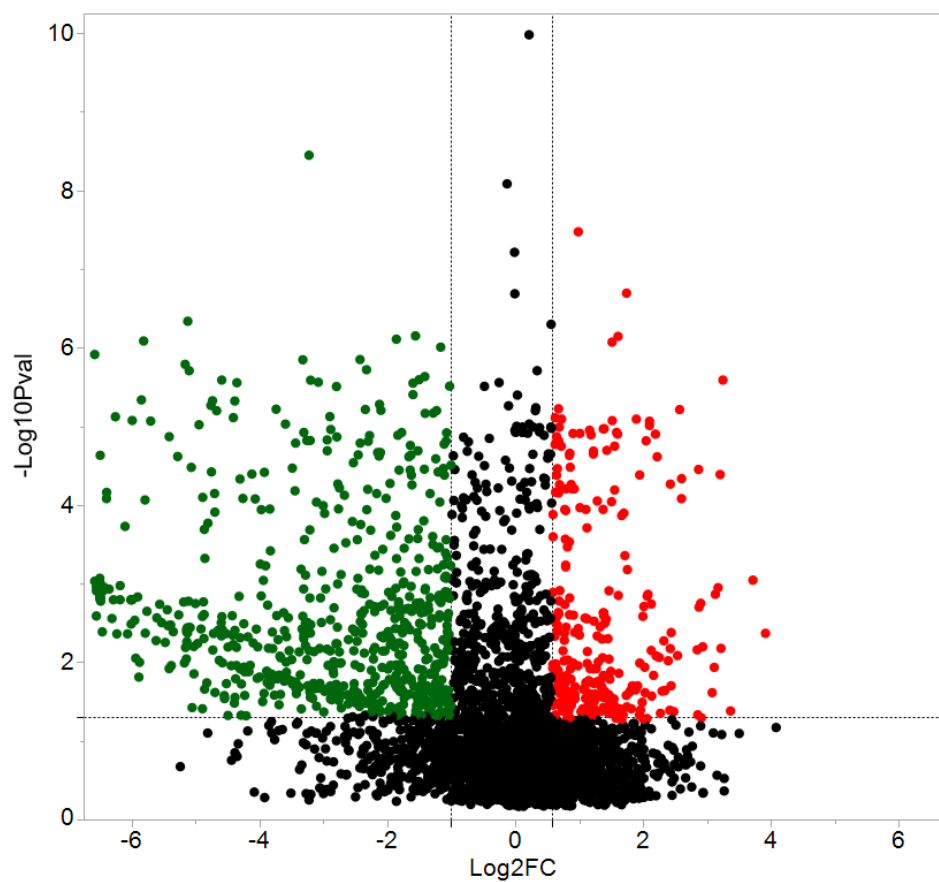


Figure 4.3. Volcano plots for protein expression in *Carassius auratus* RGCs treated with various concentrations of SNa. Protein expression using a cut off of > 1.5 or < 0.5 and $P < 0.05$. Red and green dots represent significantly up- or down- regulated proteins, respectively.

Table 4.2. Expression patterns of the differentially regulated proteins in *Carassius auratus* RGCs treated with various concentrations of SNa. CTL = control.

Expression pattern	10nM/CTL	100nM/CTL	1000nM/CTL	Number of protein IDs
I	↑	↑	↑	5
II	↑	↑	-	9
III	↑	-	↑	3
IV	↑	-	-	31
V	↑	-	↓	20
VI	↑	↓	↓	4
VII	-	↑	↑	11
VIII	-	↑	-	18
IX	-	↑	↓	1
X	-	-	↑	25
XI	-	-	-	757
XII	-	-	↓	288
XIII	-	↓	↑	6
XIV	-	↓	-	7
XV	-	↓	↓	176
XVI	↓	-	-	3
XVII	↓	↓	↑	1
XVIII	↓	↓	-	1

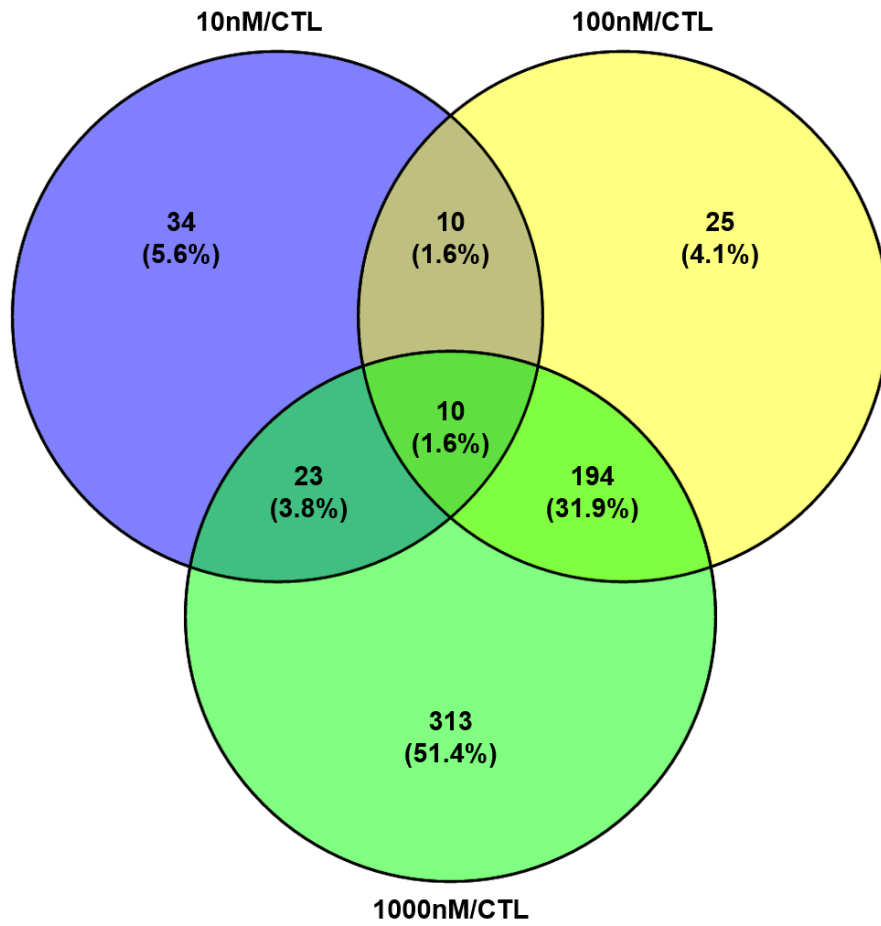


Figure 4.4. Venn diagram showing the number of commonly expressed and dose-dependent (10-100 nM) differentially regulated proteins following SNa exposure of *Carassius auratus* RGCs. CTRL = control.

Table 4.3. The 20 most significantly differentially expressed proteins identified by iTRAQ in *Carassius auratus* RGCs treated with various concentrations of SNa. All fold changes are relative to control.

Dose	Accession	Protein	% coverage protein ID	Fold Change	P - value
10nM	A7MCL7_DANRE	Cystatin 14a, tandem duplicate 2	47	3.34	2.02E-07
	Q6DN21_CARAU	Calmodulin long form	99.33	5.94	6.11E-06
	A0A0C5Q0E9_MEGAM	Fibroblast growth factor receptor 1b	11.62	1.54	7.76E-06
	E7F1X7_DANRE	Serine and arginine repetitive matrix 1	33.69	1.65	8.06E-06
	VIM2_CARAU	Vimentin A2	44.03	3.72	8.07E-06
	F1QNJ3_DANRE	Testin LIM domain protein	25.51	4.29	8.58E-06
	F1Q5X0_DANRE	Synaptosome associated protein 29 kDa	44.74	4.29	9.73E-06
	B0UXN7_DANRE	C-Abl oncogene 2, non-Receptor tyrosine kinase	20.18	3.00	1.19E-05
	C0LYZ3_9TELE	High-mobility group box 1	55.44	2.02	1.23E-05
	A0A0R4IMX7_DANRE	SH3 and PX domains 2B	25.68	1.87	1.23E-05
	X1WGZ7_DANRE	Glutamyl-prolyl-tRNA synthetase	25.03	4.57	1.25E-05
	E7F354_DANRE	Tyrosine 3-Monooxygenase/Tryptophan 5-Monooxygenase	57.89	3.03	1.25E-05
	Q802W6_DANRE	Arhgdia protein	39.41	2.70	2.01E-05
	Q6Y3R4_CARAU	H1 histone	34.03	4.66	2.43E-05
	B3DGP9_DANRE	Protein tyrosine kinase 2aa	11.29	1.58	3.44E-05
	Q6NYA1_DANRE	Heterogeneous nuclear ribonucleoprotein A/Bb	36.25	7.30	3.53E-05
	Q802Y1_DANRE	Serine/arginine-rich splicing factor 4	39.34	1.57	4.18E-05
	143BA_DANRE	Tyrosine 3-Monooxygenase/Tryptophan 5-Monooxygenase activation protein beta	77.46	0.15	6.06E-05
	RBM8A_DANRE	RNA-binding protein 8A	22.99	1.90	6.22E-05
	F1QG80_DANRE	Ribosomal protein L22	34.75	1.60	7.03E-05

100 nM	Q5U7N6_DANRE	Talin 1	18.95	0.45	9.82E-07
	Q4U0S2_DANRE	Myosin, heavy chain 11a, smooth muscle	24.77	0.49	3.08E-06
	E7FEK9_DANRE	Golgin A4	40.17	0.04	4.72E-06
	F1QIN6_DANRE	CAP-GLY domain containing linker protein 2	43.21	0.05	4.76E-06
	Q1LXT2_DANRE	Eukaryotic translation elongation factor 2a, tandem duplicate 1	26.11	1.60	5.96E-06
		Acidic leucine-rich nuclear phosphoprotein 32 family member			
	F1QTN7_DANRE	A	27.38	0.13	7.51E-06
	E7EYW2_DANRE	Epsin 2	16.27	0.02	8.56E-06
	Q7ZW39_DANRE	Phosphoribosyl pyrophosphate synthetase 1A	22.33	0.08	9.34E-06
	F1R1J9_DANRE	AHNAK nucleoprotein	53.03	2.60	1.08E-05
	Q502F6_DANRE	Zgc:112271 protein	75.58	0.29	1.20E-05
	EIF3L_DANRE	Eukaryotic translation initiation factor 3 subunit L	22.57	0.28	1.30E-05
	C0LYZ3_9TELE	High-mobility group box 1	55.44	1.57	1.35E-05
	Q7ZU46_DANRE	Heat shock protein 4a	28.45	0.14	1.36E-05
	Q0PWB8_DANRE	PDZ and LIM domain 3b	32.7	0.11	1.51E-05
	Q9DF20_DANRE	Fragile X mental retardation 1	40.77	0.10	1.51E-05
	A4FUN5_DANRE	ISY1 splicing factor homolog	57.54	0.32	1.75E-05
	Q1LYC9_DANRE	Calpain, small subunit 1 a	47.69	0.35	2.04E-05
	Q6DRC1_DANRE	Small nuclear ribonucleoprotein F	48.84	0.17	2.90E-05
	F1QYM4_DANRE	Eukaryotic translation initiation factor 4h	55.08	0.50	3.11E-05
F1Q7S0_DANRE	Vesicle transport through interaction with t-SNAREs 1A	41.94	0.03	3.32E-05	
1000 nM	Q5U7N6_DANRE	Talin 1	18.95	0.11	3.56E-09
	A0JMJ1_DANRE	Scinderin like a	33.06	0.03	4.60E-07
	Q0GC55_CARAU	Heat shock protein 47 kDa	24.81	0.34	7.06E-07
	Q6PBR5_DANRE	ATPase, H ⁺ transporting, V1 subunit G isoform 1	80.51	3.05	7.17E-07
	F1RDG4_DANRE	si:dkey-222f2.1	55.02	0.28	7.79E-07
	Q7ZTZ6_DANRE	STIP1 homology and U-Box containing protein 1	34.51	0.02	8.19E-07
	F1R1J9_DANRE	AHNAK nucleoprotein	53.03	2.86	8.48E-07
	Q804W1_DANRE	Parvalbumin isoform 4b	45.87	0.01	1.22E-06
	F1QFN1_DANRE	ELKS/RAB6-interacting/CAST family member 1b	31.20	0.19	1.41E-06

EIF3L_DANRE	Eukaryotic translation initiation factor 3 subunit L	22.57	0.10	1.42E-06
Q7SXA1_DANRE	Ribosomal protein L26	55.17	0.03	1.63E-06
E7F049_DANRE	Kinectin 1	26.47	0.20	1.90E-06
Q7ZW39_DANRE	Phosphoribosyl pyrophosphate synthetase 1A	22.33	0.03	1.96E-06
Q803A9_DANRE	DnaJ (Hsp40) homolog, subfamily B, member 11	11.94	0.38	2.32E-06
A0A0R4I9C6_DANRE	Ubiquitin-fold modifier 1	73.33	0.35	2.55E-06
B8JJS6_DANRE	Programmed cell death protein 10-B	32.86	9.51	2.58E-06
F1QTN7_DANRE	Acidic leucine-rich nuclear phosphoprotein 32 family member A	27.38	0.04	2.58E-06
A4FUN5_DANRE	ISY1 splicing factor homolog	57.54	0.11	2.59E-06
Q502F6_DANRE	zgc:112271	75.58	0.12	2.74E-06
Q9W792_DANRE	T-complex polypeptide 1	26.98	0.05	2.78E-06

4.3.3. Identifying cellular processes affected by secretoneurin-A using sub-network enrichment analysis

The major objective of this study was to identify cellular processes that were responsive to SNa in RGCs through the analysis of significantly regulated proteins. Processes that were regulated by all concentrations of SNa included actin organization, cytoskeleton organization and biogenesis, apoptosis, mRNA processing, RNA splicing, translation, cell growth and proliferation. At the low 10 nM SNa dose, proteins that were increased are related to processes such as blood vessel development, actin organization, cytoskeleton organization and biogenesis, cell proliferation, growth, and migration (Fig. 4.5). The proteins affected by 100 nM SNa control similar processes such as cell proliferation and growth, however, proteins involved in these processes were down-regulated compared to 10 nM SNa (Fig. 4.6.). Similarly, 1000 nM SNa caused down-regulation of proteins related to cell processes including actin organization, cytoskeleton organization and biogenesis, cell proliferation, growth, and migration. In addition, other protein responses at 1000nM SNa resulted in enrichment of processes related to neurite outgrowth and nerve fiber regeneration (Fig. 4.7A) and tight and gap junction assembly (Fig. 4.7B). Both 100 nM and 1000 nM SNa cause changes in proteins in similar cellular processes including cell cycle, mitochondrial function (mitochondrial membrane permeability, depolarization, damage), and RNA processes (RNA metabolism, processing, splicing). In addition, SNEA was used to map differentially expressed proteins that are implicated in human diseases. Major themes in disease networks that were altered by 1000 nM SNa included diseases of the CNS (brain injuries, Alzheimer disease, Parkinson disease, cerebral infraction, brain ischemia), diseases of the cardiovascular system (heart

failure, cardiomyopathies, heart injury, cardiac hypertrophy), and neoplasms (lung, ovarian, colorectal, pancreatic, prostatic, breast, endometrial) As an example of altered disease networks, those associated with the CNS are shown in Figure 4.8.

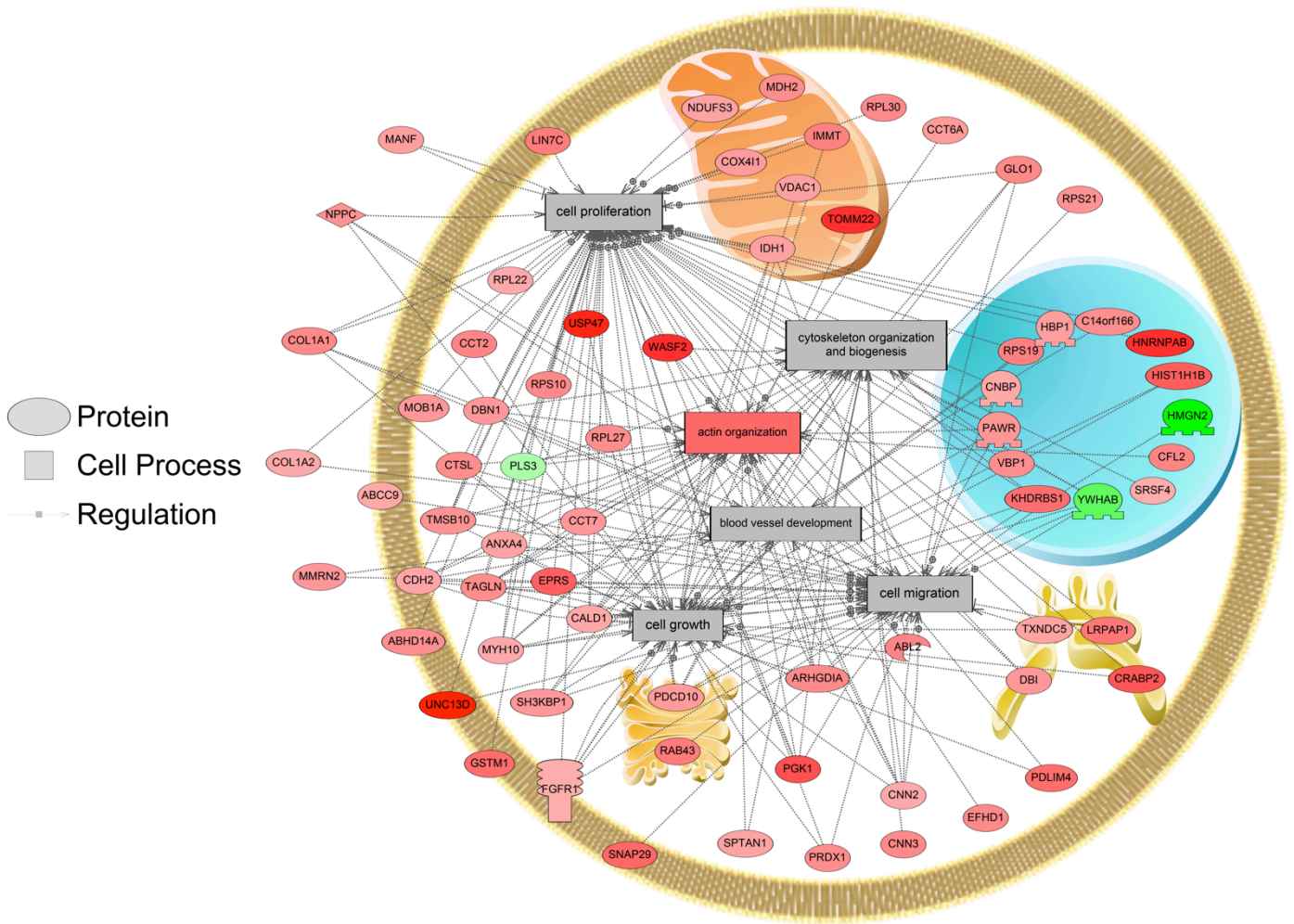


Figure 4.5. Proteins involved in cellular processes (blood vessel development, actin organization, cytoskeleton organization and biogenesis, cell proliferation, growth, and migration) that were significantly enriched by SNEA in primary *Carassius auratus* RGC culture after 10 nM SNa treatment ($P < 0.05$). Red indicates that the protein is increased and green indicates that the protein is decreased.

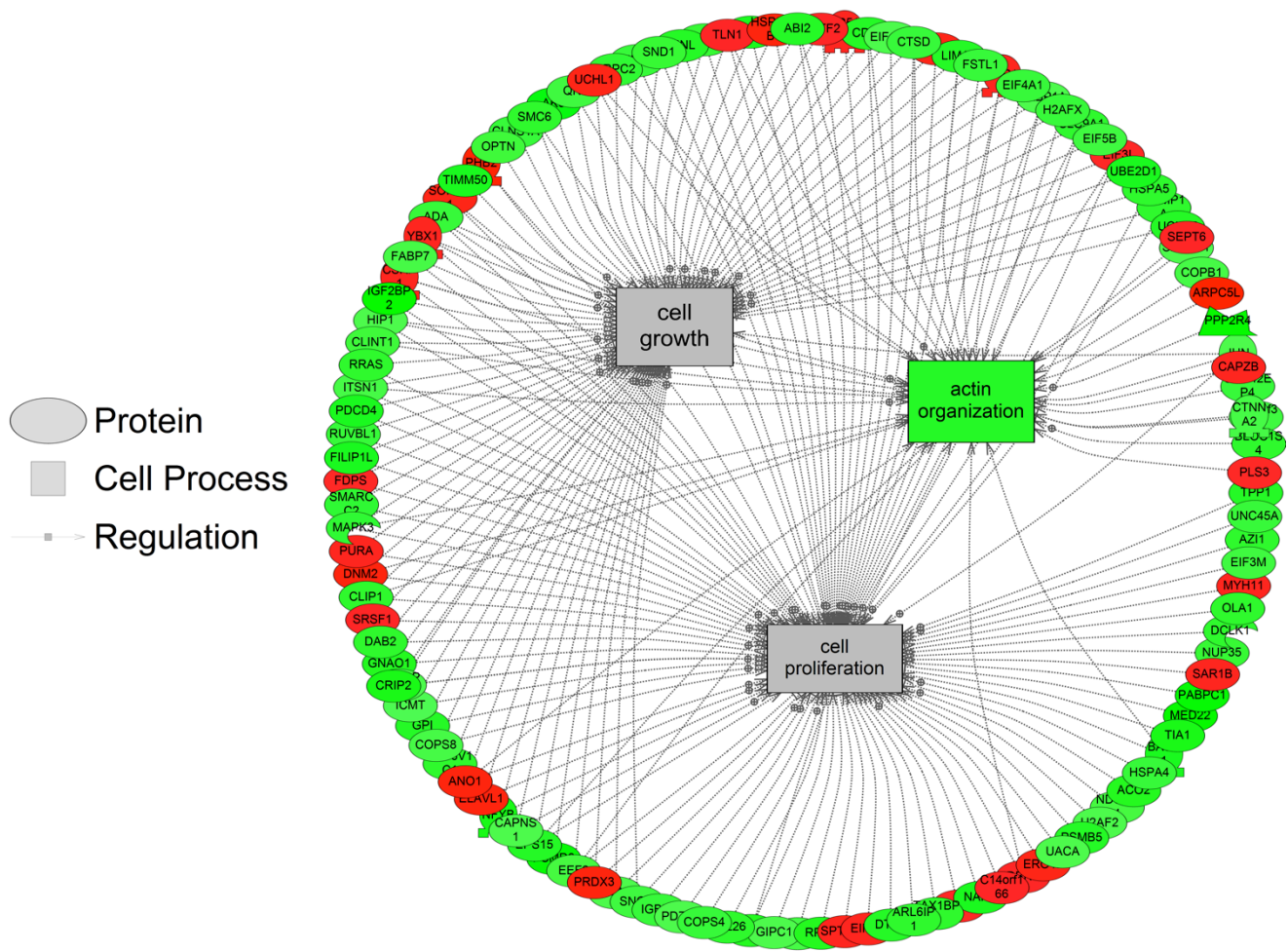


Figure 4.6. Proteins involved in cellular processes (actin organization, cell proliferation, and growth) that were significantly enriched by SNEA in primary *Carassius auratus* RGC culture after 100 nM SNa treatment ($P < 0.05$). Red indicates that the protein is increased and green indicates that the protein is decreased.

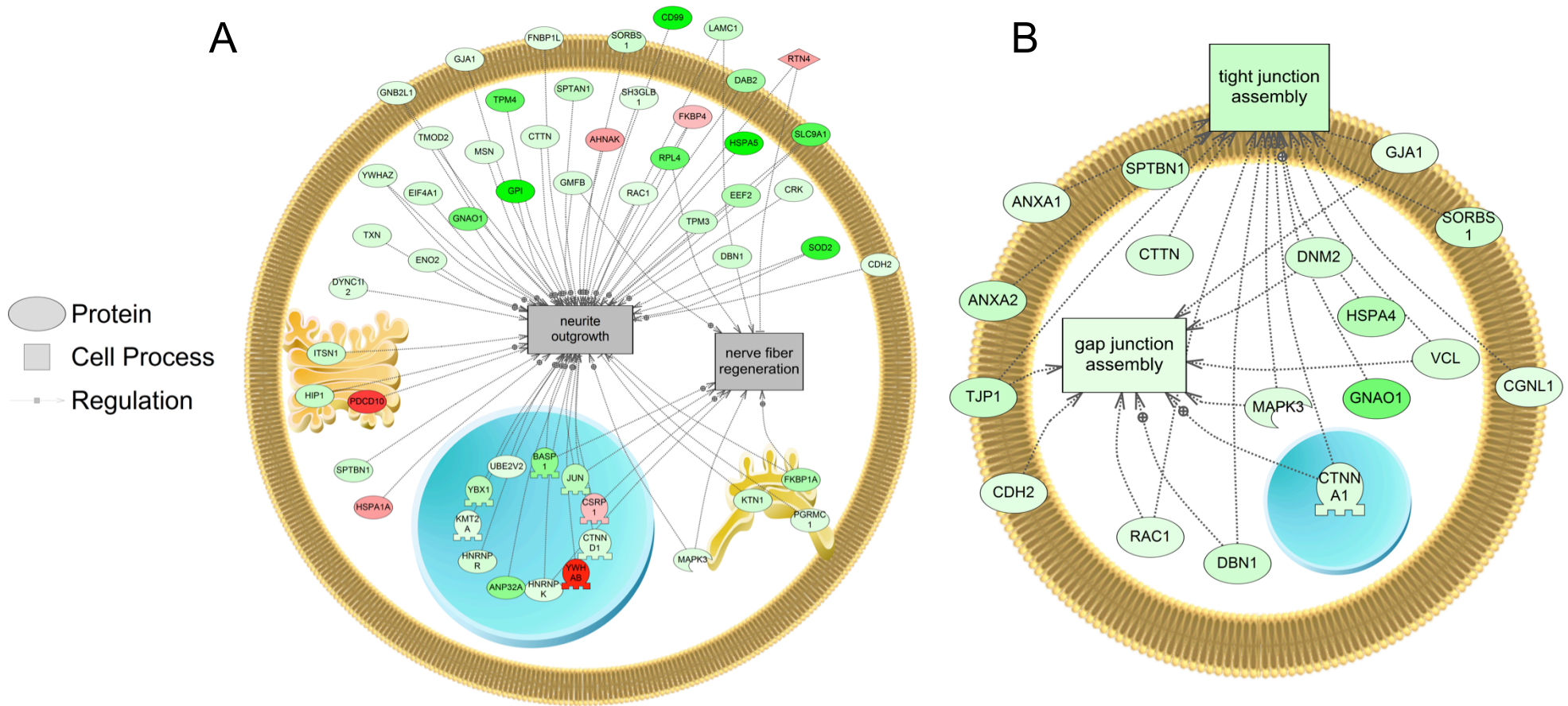


Figure 4.7. Proteins involved in cellular processes of (A) neurite outgrowth and nerve fiber regeneration and (B) tight and gap junction assembly that were significantly enriched by SNEA in primary *Carassius auratus* RGC culture after 1000 nM SNa treatment ($P < 0.05$). Red indicates that the protein is increased and green indicates that the protein is decreased.

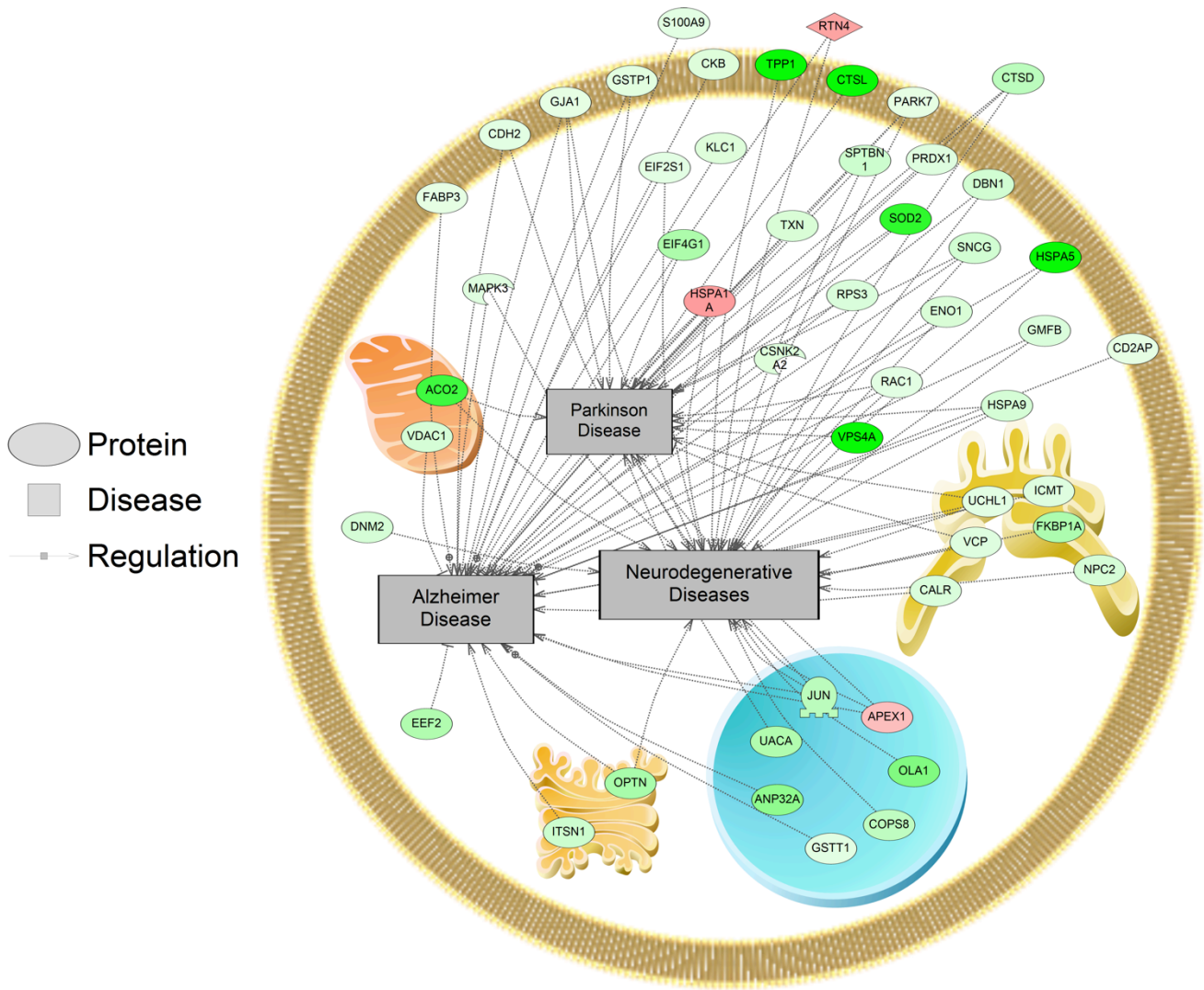


Figure 4.8. Proteins involved in Alzheimer, Parkinson, and neurodegenerative diseases that were significantly enriched by SNEA in primary *Carassius auratus* RGC culture after 1000nM SNa treatment ($P < 0.05$). Red indicates that the protein is increased and green indicates that the protein is decreased.

4.4. Discussion

This study used quantitative proteomics to determine the protein responses and cellular processes that may underlie SNa regulation of RGC function. This is our second study to characterize the goldfish RGC proteome, and we were able to identify 1,363 unique proteins, which is double than the previous study (Xing et al., 2016a). A total of 609 proteins showed differential expression across three doses of SNa, with higher doses eliciting more down-regulated protein responses. Across all doses, SNa regulated proteins involved in cell processes including actin organization, cell growth, cell proliferation and cell migration. All previous research on the effects of SN in the CNS focused on neurons, so this is the first study to characterize the effects of SN in any glial cell type.

Assigning pathway ontologies to the identified proteins showed many immune system pathways including, chemokine and cytokine signaling, T cell activation, TGF β signaling, toll receptor signaling pathway, B cell activation, and interleukin signaling pathway. In addition, many neurotransmitter (5-HT, DA, ACh, glutamate, GABA, histamine) and hormone (thyrotrophin-release hormone, oxytocin, corticotropin releasing factor) receptor-mediated pathways were identified further providing support that neuronal-glial interactions are important in the control of this cell type. Our proteomic data shows the presence of several well-characterized RGC markers including BLBP, GFAP, tight junction protein ZO-1, Sox2, and vimentin (Mack and Tiedemann, 2013; Than-Trong and Bally-Cuif, 2015) confirming that these cultured cells are indeed RGCs. Furthermore, analysis of the differentially regulated proteins shows that SNa can regulate key RGC markers. At all doses, SNa increased the expression of the intermediate filament, vimentin. However, the 1000 nM SNa treatment decreased RGC markers BLBP

and ZO-1. These markers are lost when RGCs differentiate into neurons therefore this data suggests SNa down-regulates at least some of the progenitor-like characteristics of this cell type.

A low dose of 10 nM SNa up-regulated proteins known to be involved in processes of blood vessel development, actin organization, cytoskeleton organization and biogenesis, cell growth, migration, and proliferation. It has been previously established that SN can induce angiogenesis and vasculogenesis in the mouse (Kirchmair et al., 2004a; b) supporting our data that 10 nM SNa induces the expression of proteins involved in blood vessel development. RGCs in mouse have been shown to regulate brain angiogenesis through their interactions with blood vessels (Ma et al., 2013). Since SNa can regulate proteins involved in blood vessel formation this may influence the ability of RGCs to regulate this process. As a chemoattractant, SN has the ability to stimulate the migration of various cell types. SN can stimulate the migration of human monocytes both *in vivo* and *in vitro* at nanomolar concentrations (Reinisch et al., 1993). Similarly, SN induces eosinophil (Dunzendorfer et al., 1998a), dendritic cell (Dunzendorfer et al., 2001), and fibroblast (Kahler et al., 1996) chemotaxis. These studies indicate the chemotactic activity of SN is dose-dependent with maximal effects between 0.1 – 100 nM and higher doses elicit an inhibitory effect. Interestingly, here we report proteins involved in cell migration are decreased by a high dose of 1000 nM SNa, indicating SNa may dose-dependently regulate proteins involved in cell migration. In addition, both 100 nM and 1000 nM doses also regulated actin organization, cell growth and cell proliferation protein networks, however, these higher doses decreased expression of proteins involved in these cell processes.

Following treatments with 1000 nM SNa, protein changes in sub-networks related to tight and gap junction assembly were observed. These cell processes were also identified by GSEA of transcriptomic responses under identical conditions and were found to be increased by SNa (Chapter 3). Unlike the transcriptomic response, proteins involved in tight and gap junction assembly were down-regulated indicating there may be complex regulation at the level of the transcriptome and proteome of molecular pathways that control these processes. Among the adherens junctions that were regulated by SNa, N-cadherin (cadherin 2) is a calcium-dependent adhesion molecule (Takeichi, 1995) and is expressed to uphold RGC apical-basal polarity while anchoring adjacent RGCs to each other to create stem-cell niches (Hatta et al., 1987; Kadowaki et al., 2007; Shikanai et al., 2011; Rago et al., 2014). N-cadherin controls mouse RGC function in neuronal migration and directing axon formation (Shikanai et al., 2011; Xu et al., 2015). Furthermore, N-cadherin through its interactions with its effector β -catenin regulates RGC proliferation and differentiation (Machon et al., 2003; Woodhead et al., 2006; Zhang et al., 2010). Reduction in mouse N-cadherin levels cause RGCs to migrate from the stem-cell niche and stimulate neuronal differentiation (Zhang et al., 2010). In our study, N-cadherin levels were increased at 10 nM and decreased at 1000 nM SNa. Therefore, these data on N-cadherin expression indicate a role for SNa in the regulation of RGC-mediated neuronal migration, RGC proliferation, and differentiation.

Proteins involved in cellular processes such as neurite outgrowth and nerve fiber regeneration were also affected in RGCs following treatment with 1000 nM SNa. A high dose of SNa significantly decreased proteins known to be involved in neurite outgrowth. Although SNEA did not show that this cellular process was enriched at lower doses, the

data indicates that SNa has inhibitory effects on proteins that regulate neurite outgrowth. In contrast, SN stimulated neurite outgrowth in mouse cerebellar granule cells with a maximal effect concentration of 100 nM (Gasser et al., 2003). Proteins related to nerve fiber regeneration were also decreased in goldfish RGCs exposed to 1000 nM SNa. Previous findings show SN treatment induces neural regeneration and neurogenesis in murine models of stroke (Shyu et al., 2008). The data obtained from goldfish reveal protein networks that may underlie the role of SN in tissue repair, and specifically in stem cell-like RGCs. SNa increased the expression of reticulon 4 (RTN4) which was found in both nerve fiber regeneration and neurite outgrowth protein networks. RTN4 is a negative regulator of neurite plasticity in mammals by inhibiting neurite outgrowth and axonal regeneration (Chen et al., 2000; GrandPré et al., 2000; Oertle et al., 2003). However, the major neurite growth inhibitor protein region of the RTN4 is absent in zebrafish RTN4 (Diekmann et al., 2005) and is required for successful zebrafish axon regeneration (Welte et al., 2015). Therefore, given the opposite effects of RTN4 observed in zebrafish, future work should be directed towards elucidating the effects of SNa on neurite outgrowth and axon regeneration in fish through mechanisms involving RTN4.

Many protein sub-networks were identified that correspond to diseases of the CNS and cardiovascular system, along with several neoplasms. Protein networks in RGCs related to Alzheimer disease, Parkinson disease, brain ischemia and brain injury were all affected by 1000 nM SNa. Changes in these networks are consistent with previous studies that have associated SN with neuropathological conditions. SN is differentially regulated in brain ischemia (Martí et al., 2001; Shyu et al., 2008; Hasslacher et al., 2014), Alzheimer disease (Kaufmann et al., 1998; Marksteiner et al., 2002; Lechner et al., 2004),

and epilepsy (Pirker et al., 2001; Marti et al., 2002). Besides functioning as a marker for impaired neurotransmission and excitation, SN has been demonstrated to be increased in the circulation after heart failure and has protective effects to reduce myocardial ischemia injury, cardiomyocyte apoptosis and induce angiogenesis (Albrecht-Schgoer et al., 2012; Røsjø et al., 2012). Here we show SNa can regulate sub-networks related to cardiovascular diseases such as cardiomyopathies, heart injury, cardiomegaly and heart failure. In addition, many neoplasm sub-networks were enriched after SNa treatment including lung, ovarian, colorectal, pancreatic, prostatic, breast, and endometrial. Importantly, SN has been shown to be expressed in several types of neuroendocrine tumors including prostate, lung, rectal, pancreatic, thyroid, duodenum, appendix (Weiler et al., 1988; Ischia et al., 1998; Portela-Gomes et al., 2010). Altogether, it is suggested that these networks underlie the molecular responses and mechanisms that may explain the involvement of SN in these diseased states.

The teleost brain has become a popular model for neurogenesis and neuroendocrinology because of the persistent abundance of progenitor RGCs in the adult brain and the high aromatase activity present in RGCs (Zupanc, 2006; Diotel et al., 2010a; Than-Trong and Bally-Cuif, 2015). Our research has implications in these fields as characterizing the RGC proteome can elucidate the molecular mechanisms that underlie these unique functions of fish RGCs. Given RGCs play critical roles in brain homeostasis we aimed to investigate the interactions of a novel neuropeptide, SNa with RGCs to better understand if neuropeptides can exert regulatory effects over this cell type. For the first time, we show the RGC proteome is responsive to nanomolar concentrations of SNa. Proteins regulated by SNa may be involved in many cell processes including

blood vessel development, actin organization, cytoskeleton organization and biogenesis, neurite outgrowth, nerve fiber regeneration, cell growth, migration, and proliferation. At lower doses SNa increased proteins involved in cell growth, migration, and proliferation whereas high doses down-regulated proteins involved in these processes indicating SNa has dose-dependent regulatory effects. These data further expands our knowledge of the biological actions of SNa in the CNS specifically its effects on glia. The results presented provide a strong foundation for future research that can determine the morphological and physiological outcomes in RGCs exposed to SNa. Lastly, we acknowledge that some differentially regulated proteins should be further validated by western blot experiments, however because of time restrictions this will have to proceed in the near future.

Chapter 5: General discussion and future directions

5.1. Implications of secretoneurin-A regulation of aromatase B in the preoptic nucleus

The results presented in this thesis has shown the co-regionalization of SNa-immunoreactive cell bodies of magnocellular and parvocellular neurons with RGCs in both the goldfish and zebrafish preoptic nucleus (Chapter 2). These SNa-positive neurons have previously been documented to co-localize with isotocin, the fish homolog to mammalian oxytocin, and it may be possible for these two neuropeptides to be co-released (Canosa et al., 2011). The magnocellular and parvocellular cells in the preoptic nucleus of teleost fish are equivalent to the oxytocin- and vasopressin-producing cells of the mammalian paraventricular and supraoptic nuclei (Batten, 1986). Besides neuroanatomical evidence, transcriptome sequencing indicates RGCs express oxytocin and vasopressin receptors (Chapter 3) further supporting our proposal that these neuronal populations are communicating with surrounding RGCs. We demonstrated that SNa both *in vivo* and *in vitro* can reduce *cyp19a1b* mRNA expression, therefore suggesting SNa can regulate neuroestrogen production in RGCs (Chapter 2). By regulating local estrogen levels, SNa may control paracrine estrogen signaling to surrounding magnocellular and parvocellular neurons. The magnocellular and parvocellular neurons of the goldfish preoptic nucleus have the highest mRNA and protein abundances of the membrane bound estrogen receptor, GPR30, and also co-localizes with isotocin (Mangiamele et al., 2016). The fish preoptic nucleus contains the main nuclear estrogen receptors ER- α , ER- β 1, and ER- β 2 (Kah et al., 1997; Menuet et al., 2002; Diotel et al., 2011a). While it is not known

in goldfish or zebrafish, Atlantic croaker magnocellular neurons contain ER- β 1 but not ER- β 2 (Hawkins et al., 2005). This expression of estrogen receptors in magnocellular and parvocellular neurons suggests estrogens can regulate isotocin and vasotocin systems. The mammalian oxytocin and vasopressin systems are well established for being under the control of estrogens (Amico and Seif, 1981; Ivell and Walther, 1999; Caligioni and Franci, 2002; Auger et al., 2011; Mecawi and Elias, 2011; Mecawi et al., 2011; Santollo and Daniels, 2015). Although less investigated in fish, estrogens regulate vasotocin secretion in the catfish (Chaube et al., 2012). Therefore by regulating local estrogen paracrine signaling through *cyp19a1b* expression SNa may be implicated in regulating hormone systems imperative in reproductive behaviours and osmoregulation.

The expression of *cyp19a1b* in RGCs is regulated by estradiol itself through the binding of ERs to functional estrogen response elements in the *cyp19a1b* promoter (Callard et al., 2001; Menuet et al., 2005; Diotel et al., 2010a). Importantly, Xing et al. (2016) demonstrated direct ER- α -dependent effects of E2 on *cyp19a1b* in our RGC culture system. By altering estrogen levels, SNa may impact this auto-regulatory feedback loop affecting the neuroendocrine function of these cells. There are many potential downstream physiological effects of altered estrogen levels as the brain expresses a wide distribution of estrogen receptors and therefore is a target of estrogen signaling to control processes such as sexual behaviour, synaptic plasticity, and neurogenesis (Garcia-Segura, 2008; Okada et al., 2008; Ubuka et al., 2014; Elisabeth et al., 2015).

5.2. Transcriptomic and proteomic responses suggest SNa exert trophic and immunogenic effects

Previous reports have identified that SN in the rodent CNS exerts trophic-like functions to stimulate neurite outgrowth in cerebellar granule cells (Gasser et al., 2003) and promote neuroprotection and neuronal plasticity (Shyu et al., 2008). In conjunction, SN has chemoattractive functions to regulate inflammatory responses (Fischer-Colbrie et al., 2005). We aimed to investigate related effects and other potential functions of SN in a critical cell type of the regenerative capable teleost brain. Besides their neuroendocrine functions, RGCs are neuronal precursors and respond to inflammatory signals to increase proliferation and subsequent neurogenesis following brain injury (Kyritsis et al., 2012). Although we did not test directly the involvement of SNa in regulating RGCs in neurogenesis, transcriptomic responses show SNa has a largely stimulatory effect on transcripts involved in CNS functions. Most notable are neurogenesis, glial cell development, axon guidance, neuronal activity, and synaptic plasticity (Chapter 3). Again at the molecular level, this trophic-like effect was also observed in the RGC proteome where a low dose of SNa increased expression of proteins involved in cell growth, proliferation and migration (Chapter 4). However, at higher doses, proteins involved in these cellular processes were decreased, indicating that these potential trophic effects are dose-dependent in goldfish RGCs. Together, these altered gene and protein networks involved in CNS processes, cell growth, proliferation, and migration suggest SNa may function to regulate these stem-like RGCs in neurogenesis, however future work is needed to fully address this hypothesis. Furthermore, there was a major enrichment of gene networks related to immune processes caused by SNa suggesting this neuropeptide

may elicit immunogenic effects in RGCs (Chapter 3). As we have shown, RGCs through their expression of immune system pathways, proinflammatory signals and receptors are suspected to be active participants in regulating neuroinflammatory processes (Chapter 3 and 4). SNa may therefore be a proinflammatory factor released from neurons that trigger appropriate responses in surrounding glia. Similar mechanisms have been observed for other granins, such as chromogranin A. In the rat brain, chromogranin A triggers a phenotypic transformation of microglia activating them to produce nitric oxide and TNF α (Taupenot et al., 1996; Ciesielski-treska et al., 1998; Ulrich et al., 2002). In addition, SN is differentially regulated in many neurodegenerative conditions such as Alzheimer disease (Kaufmann et al., 1998; Marksteiner et al., 2002; Lechner et al., 2004) which involve reactive microglia and astrocytes (Liu et al., 2011). Our data shows that SNa can regulate proteins known to be involved in neurodegenerative diseases (Chapter 4) and provide potential immune-related mechanisms (Chapter 3) that may explain the involvement of SNa in activating glia in these conditions. These transcriptomic and proteomic responses provide a framework for future studies to target these physiological, behaviour, and morphological effects of SNa in RGCs (see below).

5.3. Concluding remarks

The results presented in this thesis (Fig 5.1.) provide the first evidence that RGCs are under neuronal control through the release of the granin-derived neuropeptide – SNa. Given the lack of information on the influences of SNa on glia, we provide the beginning investigations of how RGCs are controlled by neuropeptides. In the goldfish preoptic area, SNa from neurons affect surrounding RGCs by reducing *cyp19a1b* expression. Through transcriptomic and proteomic responses we propose SNa exert neurogenic and

immunogenic effects in RGCs. These molecular responses provide insight for future research that addresses the effects of SNa in glia or other cell types. We have also generated the first reference RGC transcriptome for any fish species, revealing diverse receptor and molecular signaling profiles, indicating that RGCs can respond to and synthesize an array of hormones, peptides, cytokines, and growth factors. In combination with our proteomic characterization, these datasets provide understanding of the molecular functions of these cells and will have impacts in the fields of neurogenesis and neuroendocrinology for which this cell type has become a favourable model.

5.4. Future Directions

The extensive new data presented provide numerous possible directions for future research on new functions and regulation of RGCs. Here, we identify four main lines of investigation that should be considered.

1. Comparison of the differentially expressed transcriptome to the differentially expressed proteome in response to SNa is an important next step. This will help to analyze if there are some directional correlation between mRNAs and proteins while determining which mRNAs and proteins that share a common directional change or discordant directional change, as these are most likely SNa-regulated.

Transcriptome/proteome relationships following dopamine receptor activation have been reported for the whole hypothalamus of goldfish (Popesku et al., 2010). Utilizing an amenable *in vitro* cell system, such as our RGC culture, should allow refined time-course analysis to better establish the transcript-protein relationship.

2. It will be essential to identify the signal transduction pathways that mediate effects of SNa in RGCs. The putative SN receptor has yet to be identified, however, data suggest

SN acts through both G-protein coupled receptors and non-G-protein coupled receptor growth factor-like signaling cascade (Zhao et al., 2010; Trudeau et al., 2012). Possible mechanisms include activating PKC, PKA, MAPK signaling cascades, increases in Ca²⁺ signaling, or through Jak/Stat3 signaling pathway. Notably, GSEA in Chapter 3 identified increases in several receptor-signaling pathways involving cAMP response element-binding protein (CREB) / ETS domain-contain protein (ELK)-serum response factor (SRF) signaling. Therefore taking advantage of our RGC culture, future *in vitro* pharmacological assays should be conducted to determine SNa-induced signaling pathways in RGCs.

3. The cellular processes that are associated with the altered gene and protein networks should be identified. Although our study provided the molecular mechanisms in which SNa may regulate these cellular processes further research is needed to determine the physiological outcomes of SNa exposure. These could include a combination of *in vitro* and/or *in vivo* models utilizing our new *scg2a/b* knockout zebrafish lines (Hu et al., unpublished data) to study the responses and behaviour of RGCs in the absence of SN signaling.

4. The evolutionary relationships between teleost and mammalian RGCs should be established. Comparison of the goldfish RGC transcriptome and proteome with corresponding mammalian glial datasets would help to determine the cellular nature teleost RGCs. Current data suggest they are astrocyte-like, but it is clear from our transcriptomic and proteomic data that teleost RGCs are complex and multifunctional. By identifying the molecular similarities and differences this may elucidate the permissive

molecular systems that allow for successful regeneration in the teleost brain compared to mammals, while discovering further functions unique to fish RGCs.

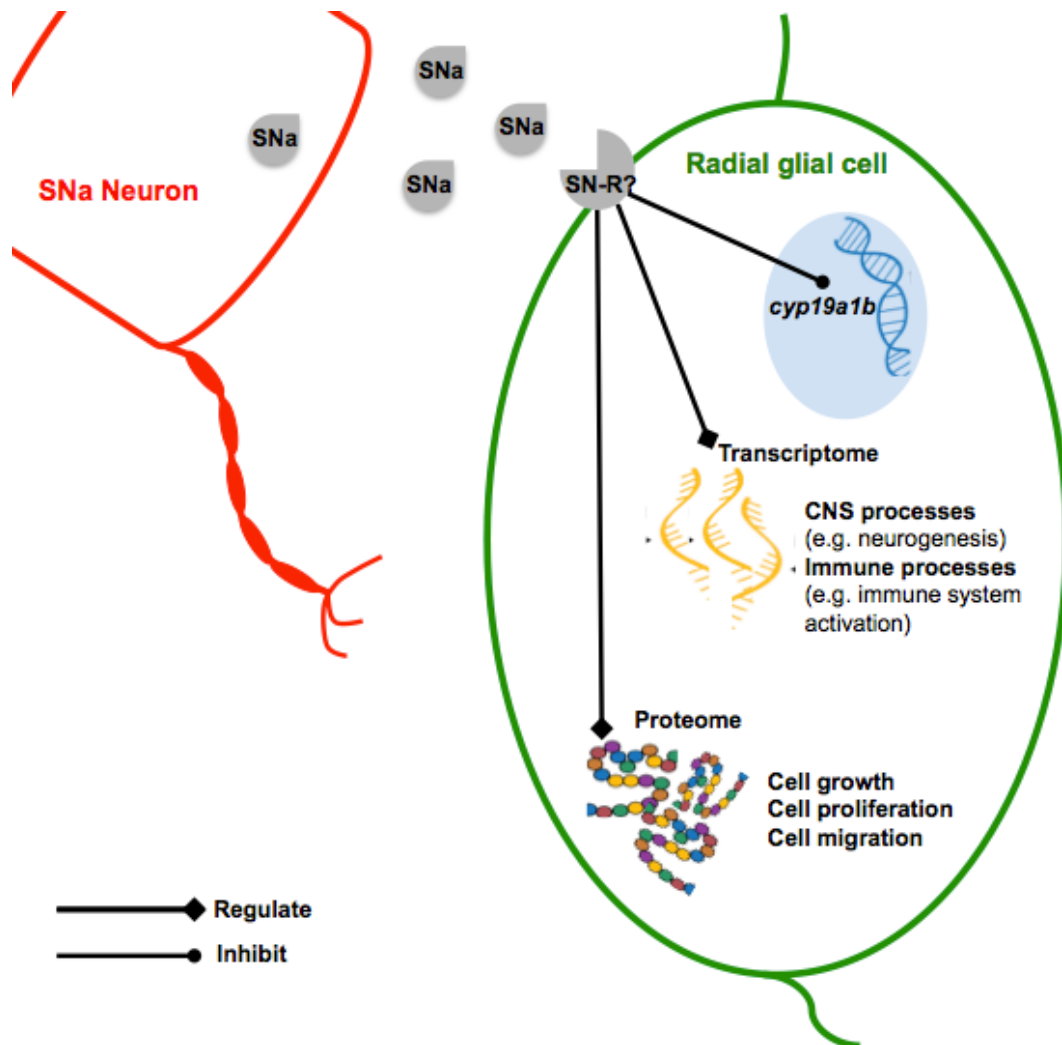


Figure 5.1. Summary of the *in vitro* effects of SNa on goldfish radial glial cells as determined by transcriptomics and proteomics.

Appendix 1: Zebrafish telencephalic stab lesion assay implicates aromatase B and secretogranin II systems in injury and repair

A1.1. Introduction

Teleost models offer an excellent opportunity to investigate the mechanisms involved in successful regeneration in the brain because of their unique ability of adult regeneration (Grandel and Brand, 2013). These proliferative and regenerative capacities in fish brain are partly due to the persistent abundance of RGCs (Pellegrini et al., 2007; Strobl-Mazzulla et al., 2010). RGCs are a bipolar shaped progenitor cell type present in the developing central nervous system (CNS) of all vertebrates (Rakic, 1972; Götz and Huttner, 2005). As a stem-like cell, RGCs can differentiate into neurons or other glia cell types (Radakovits et al., 2009). However, in mammals RGCs are mainly a transient cell type differentiating into astrocytes at the end of cortical development and only two populations remaining in adulthood – the anterior part of the subventricular zone of the lateral ventricle and subgranular zone of the dentate gyrus. These two areas are the only constitutive neurogenic regions of the adult mammalian brain, which explains the limited capacity for neurogenesis in mammals (Brunner et al., 2010; Ming and Song, 2011). Another unique feature of fish RGCs is their capacity for neuroestrogen producing through the expression of the estrogen-synthesizing enzyme, aromatase B (*cyp19a1b*) (Forlano et al., 2001). Neuroestrogens have an established role in the mammalian brain as being neuroprotective and having antiapoptotic effects in neurogenesis and brain repair (Garcia-Segura, 2008; Saldanha et al., 2009; Scott et al., 2012). However, in the teleost brain, which exhibits both high aromatase activity and extensive neurogenesis, the

neurogenic effects of neuroestrogens remain inconclusive. Two studies in zebrafish found anti-proliferative effects of 17- β estradiol in several regions of the male brain (Diotel et al., 2013; Makantasi and Dermon, 2014). However, one study in goldfish found that genes related to RGC function and dopamine neuron recovery were aromatase-dependent after a neurotoxin treatment that affects catecholaminergic neurons including those producing dopamine (Xing et al., 2016b).

Although the fish brain has remarkable regenerative abilities after brain injury, little is known on both the regulatory factors that control this response and the involvement of aromatase B. Due to the emerging data in rodents suggesting the neuroprotective and neurogenic properties of SN (Shyu et al., 2008) we wanted to investigate if this neuropeptide was involved in the regenerative response in fish. SN is found in dense-core secretory vesicles in cells of the nervous and endocrine tissues and is generated from the endoproteolytic processing of its precursor protein secretogranin (SgII) (Kirchmair et al., 1993; Fisher-Colbrie et al., 1995). In teleost fish there are two SgII isoforms, SgIIa (*scg2a*) and SgIIb (*scg2b*), which produce their respective SNa and SNb peptides caused by the whole genome duplication process that occurred around the teleost emergence (Zhao et al., 2010). The precursor protein SgII is poorly conserved in fish with exception of the SN domain which is conserved from fish to mammals (Zhao et al. 2009). Besides its immune and neuroendocrine functions, SN has an established role in brain tissue repair aiding in functional neural regeneration and neurogenesis (Shyu et al., 2008). In addition, SN is differentially regulated in brain ischemia (Martí et al., 2001; Shyu et al., 2008; Hasslacher et al., 2014), Alzheimer disease (Kaufmann et al., 1998; Marksteiner et al., 2002; Lechner et al., 2004), and epilepsy (Pirker et al., 2001; Marti et

al., 2002). Therefore, the objective of this study was to study the transcriptomic responses of *cyp19a1b*, *scg2a*, and *scg2b* after telencephalic injury in order to implicate these systems in neuronal repair mechanisms.

A1.2. Methods

A1.2.1. Animal care

All procedures used were approved by the University of Ottawa Protocol Review Committee and followed standard Canadian Council on Animal Care guidelines on the use of animals in research. Zebrafish (*Danio rerio*) were held in a closed re-circulated facility at 28.5 °C and on a 14-10 h light-dark cycle. For sacrifice, fish were anesthetized on ice before severing the spinal cord.

A1.2.2. Telencephalic injury

Methods used for this assay were followed as previously described (Diotel et al., 2013). Briefly, adult female zebrafish were anesthetized with 3-aminobenzoic acid ethylester (MS222) and a sterile 30 G ½” needle was inserted in one of the telencephalic hemispheres guided by landmarks on the head. Then using pressure the needle was inserted to penetrate a depth of 1.5 mm. In addition, an external control group of fish were handled and anesthetized in the same way however with no telencephalic injury. Fish were then allowed to recover and then sacrificed two and four days post injury (dpi).

A1.2.3. RNA extraction, cDNA synthesis, and qRT-PCR

A total of 9 injured or non-injured (contralateral control) telencephali were pooled and 5 external control telencephalons were pooled before RNA extraction. For information on RNA extraction, cDNA synthesis, and qRT-PCR refer to Chapter 2.

Table A1.1. Primers (5' → 3') used for qRT-PCR

Gene	Primer Sequence (Forward)	Primer Sequence (Reverse)
<i>cyp19a1b</i>	GCAAAGGGGACAAACCTAATC	TGACGAGGACAAACTGTAAACC
<i>scg2a</i>	CGCTTCATCTAAAACCAACACC	AGGCGTCCAATCATCAGTTC
<i>scg2b</i>	TGATGACGATGCGGTAGATG	GGTGTCTCTTTTGGCGAGTG
<i>eef1a</i>	GAGCTTCTCCACCTACCCTC	TGCAGACTTTGTGACCTTGC

A1.2.4. Statistics

Before analysis, data was tested for normality (Shapiro-Wilk's test) and homogeneity of variance (Levene's test). Data that were not normally distributed were transformed to meet parametric assumptions. Comparison of more than two groups was performed using two-way analysis of variance (ANOVA) followed by a Tukey post-hoc in Graphpad Prism (version 6.0). $P < 0.05$ were considered to be statistically significant.

A1.3. Results

A1.3.1. Stab lesions in the zebrafish telencephalon affects the mRNA levels of *scg2a*, *scg2b*, and *cyp19a1b*

To understand the involvement of SgIIa, SgIIb, and aromatase B in the regenerative response a zebrafish telencephalic stab lesion assay was performed. A two-way ANOVA analysis was used to investigate the effects of injury and time post injury on the expression of *scg2a*, *scg2b*, and *cyp19a1b*. At two dpi there were no significant changes ($P < 0.05$) in *scg2a* (Fig. A.1.1A), *scg2b* (Fig. A.1.1B), and *cyp19a1b* (Fig. A.1.1C) mRNA levels in the injured hemisphere compared to both external and contralateral controls. After four dpi, *scg2a* mRNA levels significantly decreased in the injured hemisphere ($P < 0.05$) compared to the external control (Fig. A.1.1A), while *scg2b* mRNA levels significantly decreased ($P < 0.05$) compared to both external and contralateral controls (Fig. A.1.1B). Similarly, injury caused a significant decrease in *cyp19a1b* mRNA levels compared to external control ($P < 0.05$) (Fig. A.1.1C).

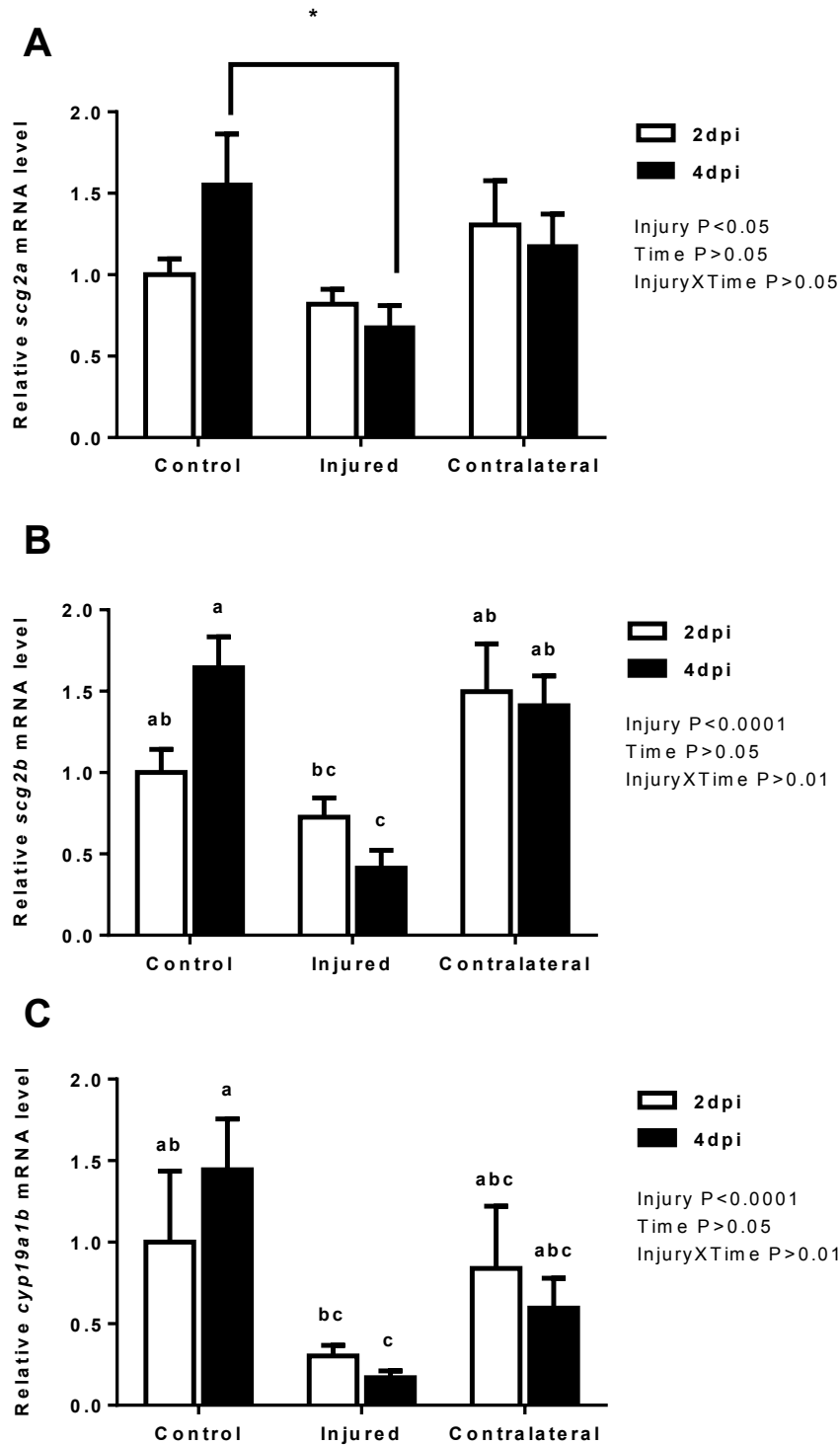


Figure A1.1. Quantitative real-time PCR analysis showing the effects of telencephalic injury on the relative amounts of *scg2a* (A), *scg2b* (B), and *cyp19a1b* (C) mRNA in female zebrafish 2 and 4 days post injury (dpi). Data were normalized and defined as fold change relative to control. Bars represent the mean + SEM (n = 6). Two-way ANOVA followed by Tukey's test was performed to test the effects of injury and time post injury. Groups marked by an asterisk or different letters are significantly different (P < 0.05).

A1.4. Discussion

Using a zebrafish telencephalic stab lesion assay we showed the responses of aromatase B and both SgIIa and SgIIb in order to study their involvement in the regeneration paradigm. It should be noted that in comparison to other studies here we included an external control to control for potential responses that were not related specifically to injury. After injury *cyp19a1b* mRNA levels slightly decreased 4 dpi compared to external control but not to contralateral controls with no response observed at 2 dpi. A similar study, but in males, found that compared to a contralateral control, *cyp19a1b* mRNA levels drop rapidly after 30 min, then re-stabilizes around 24 h, before dropping again from 48 h onwards (Diotel et al., 2013). Although only two time points were used in the present study, we show *cyp19a1b* mRNA levels are not altered at 2 dpi and only slightly decreased at 4 dpi during a time where there is significant increases in proliferation at the ventricular surface (Diotel et al., 2013). Therefore this supports previous findings that aromatase B expression and ventricular/periventricular cell proliferation have an inverse relationship suggesting aromatase B may not be involved in compensatory neurogenesis.

This is the first study to investigate the SgII systems following brain injury in fish. To our surprise, both *scg2a* and *scg2b* mRNA expression decreased at 4 dpi in the injured telencephali, with a more robust response in *scg2b*. We predicted increases in these transcripts given SN, the SgII-derived peptide, has previously been shown to increase following brain injury and in pathophysiological conditions of the CNS (Martí et al., 2001; Marti et al., 2002; Shyu et al., 2008). The time points chosen for this study were based on responses of another member of the granin family, SgIII, in reactive mouse

astrocytes (Paco et al., 2010). Since SN functions to regulate immune system responses through promoting chemotaxis of several types of immune system cells (Fischer-Colbrie et al., 2005) and levels of key cytokines involved in active inflammatory responses have been shown to peak by 24 h post injury in the zebrafish brain (Kyritsis et al., 2012), the time points used in our study may have been too long post injury to see potential increases in the the expression of SN precursors SgIIa and SgIIb. Furthermore, after experimental autoimmune encephalomyelitis is induced in the rat brain, there is a close correlation between SN-immunoreactivity and macrophage infiltration indicating SN may play a role in leukocyte recruitment in the CNS (Storch et al., 1996). Consequently, future studies should investigate the rapid responses of SgIIa and SgIIb after injury to better correlate with the timing of the immune response and also use immunohistochemistry to localize the expression of SNa and SNb relative to the site of injury. Nonetheless, we show that telencephalic injury can affect *scg2a* and *scg2b* mRNA levels, which implicates SgII and potentially the bioactive peptides it generates in injury and repair in the adult fish brain.

Appendix 2: Other research contributions

Xing, L., McDonald, H., **Da Fonte, D. F.**, Gutierrez-Villagomez, J. M., Trudeau, V. L. 2015. Dopamine D1 receptor activation regulates the expression of the estrogen synthesis gene aromatase B in radial glial cells. *Frontiers in Neuroscience* 9: 310.

Xing, L., Martyniuk, C. J., Esau, C., **Da Fonte, D. F.**, Trudeau, V. L. 2016. Proteomic profiling reveals dopaminergic regulation of progenitor cell functions of goldfish radial glial cells in vitro. *Journal of proteomics* 144: 123-132.

Xing, L., Gutierrez-Villagomez, J. M., **Da Fonte, D. F.**, Venables, M. J., Trudeau, V. L. 2016. Dehydroabietic acid cytotoxicity in goldfish radial glial cells in vitro. *Aquatic Toxicology* 180: 78-83.

References

- Adamski J, Husen B, Marks F, Jungblut PW. 1992. Purification and properties of oestradiol 17 beta-dehydrogenase extracted from cytoplasmic vesicles of porcine endometrial cells. *Biochem J* 288 (Pt 2:375–81.
- Agneter E, Sitte HH, Stöckl-Hiesleitner S, Fischer-Colbrie R, Winkler H, Singer E a. 1995. Sustained dopamine release induced by secretoneurin in the striatum of the rat: a microdialysis study. *J Neurochem* 65:622–625.
- Albrecht-Schgoer K, Schgoer W, Holfeld J, Theurl M, Wiedemann D, Steger C, Gupta R, Semsroth S, Fischer-Colbrie R, Beer AGE, Stanzl U, Huber E, Misener S, Dejaco D, Kishore R, Pachinger O, Grimm M, Bonaros N, Kirchmair R. 2012. The angiogenic factor secretoneurin induces coronary angiogenesis in a model of myocardial infarction by stimulation of vascular endothelial growth factor signaling in endothelial cells. *Circulation* 126:2491–2501.
- Altschul SF, Gish W, Miller W, Myers EW, Lipman DJ. 1990. Basic local alignment search tool. *J Mol Biol* 215:403–10.
- Alunni A, Bally-Cuif L. 2016. A comparative view of regenerative neurogenesis in vertebrates. *Development* 143:741–753.
- Amico JA, Seif SM. 1981. Oxytocin in Human Plasma : Correlation with Neurophysin and Stimulation with Estrogen *. *J Clin Endocrinol Metab* 52:988–993.
- Anders S, Huber W, Nagalakshmi U, Wang Z, Waern K, Shou C, Raha D, Gerstein M, Snyder M, Mortazavi A, Williams B, McCue K, Schaeffer L, Wold B, Robertson G, Hirst M, Bainbridge M, Bilenky M, Zhao Y, Zeng T, Euskirchen G, Bernier B, Varhol R, Delaney A, Thiessen N, Griffith O, He A, Marra M, Snyder M, Jones S, Licatalosi D, Mele A, Fak J, Ule J, Kayikci M, Chi S, Clark T, Schweitzer A, Blume J, Wang X, Darnell J, Darnell R, Smith A, Heisler L, Mellor J, Kaper F, Thompson M, Chee M, Roth F, Giaever G, Nislow C, Marioni J, Mason C, Mane S, Stephens M, Gilad Y, Wang L, Feng Z, Wang X, Wang X, Zhang X, Robinson M, Smyth G, Whitaker L, Robinson M, McCarthy D, Smyth G, Robinson M, Smyth G, Cameron A, Trivedi P, Robinson M, Oshlack A, Loader C, McCullagh P, Nelder J, Agresti A, Engström P, Tommei D, Stricker S, Smith A, Pollard S, Bertone P, Morrissy A, Morin R, Delaney A, Zeng T, McDonald H, Jones S, Zhao Y, Hirst M, Marra M, Kasowski M, Grubert F, Heffelfinger C, Hariharan M, Asabere A, Waszak S, et al. 2010. Differential expression analysis for sequence count data. *Genome Biol* 11:R106.
- Ang CW, Dotman CH, Winkler H, Fischer-Colbrie R, Sonnemans MAF, Van Leeuwen FW. 1997. Specific expression of secretogranin II in magnocellular vasopressin neurons of the rat supraoptic and paraventricular nucleus in response to osmotic stimulation. *Brain Res* 765:13–20.
- Anouar Y, Benie T, Monti MDE, Counis R. 1991. Chromogranin A Messenger Ribonucleic Acid Levels in the Female Rat Pituitary but Not in the Adrenal. 129.
- Anouar Y, Desmoucelles C, Yon L, Leprince J, Breault L, Gallo-Payet N, Vaudry H. 1998. Identification of a novel secretogranin II-derived peptide (SgII(187-252)) in adult and fetal human adrenal glands using antibodies raised against the human recombinant peptide. *J Clin Endocrinol Metab* 83:2944–2951.
- Anouar Y, Duval J. 1992. Direct estradiol down-regulation of secretogranin II and

- chromogranin mRNA levels in rat pituitary cells. 88:97–104.
- Anuka E, Gal M, Stocco DM, Orly J. 2013. Expression and roles of steroidogenic acute regulatory (StAR) protein in “non-classical”, extra-adrenal and extra-gonadal cells and tissues. *Mol Cell Endocrinol* 371:47–61.
- Auger CJ, Coss D, Auger AP, Forbes-lorman RM. 2011. Epigenetic control of vasopressin expression is maintained by steroid hormones in the adult male rat brain. *PNAS* 108:4242–4247.
- Back S a, Gorenstein C. 1989. Histochemical visualization of neutral endopeptidase-24.11 (enkephalinase) activity in rat brain: cellular localization and codistribution with enkephalins in the globus pallidus. *J Neurosci* 9:4439–55.
- Balthazart J, Ball GF. 1998. New insights into the regulation and function of brain estrogen synthase (aromatase). *Trends Neurosci*:243–249.
- Barry DS, Pakan JMP, McDermott KW. 2014. Radial glial cells: key organisers in CNS development. *Int J Biochem Cell Biol* 46:76–9.
- Bartolomucci A, Possenti R, Mahata SK, Fischer-Colbrie R, Loh YP, Salton SRJ. 2011. The extended granin family: Structure, function, and biomedical implications. *Endocr Rev* 32:755–797.
- Bassetti M, Huttner WB, Zanini A, Rosa P. 1990. Co-localization of secretogranins/chromogranins with thyrotropin and luteinizing hormone in secretory granules of cow anterior pituitary. *J Histochem Cytochem* 38:1353–1363.
- Batten TFC. 1986. Ultrastructural characterization of neurosecretory fibres immunoreactive for vasotocin , isotocin , somatostatin , LHRH and CRF in the pituitary of a teleost fish, *Poecilia latipinna*. *Cell Tissue Res* 244:661–672.
- Bauer JW, Kirchmair R, Egger C, Fischer-Colbrie R. 1993. Histamine induces a gene-specific synthesis regulation of secretogranin II but not of chromogranin A and B in chromaffin cells in a calcium-dependent manner. *J Biol Chem* 268:1586–1589.
- Benson MD, Romero MI, Lush ME, Lu QR, Henkemeyer M, Parada LF. 2005. Ephrin-B3 is a myelin-based inhibitor of neurite outgrowth. *Proc Natl Acad Sci U S A* 102:10694–9.
- Beraudi A, Traversa U, Villani L, Sekino Y, Nagy JI, Poli A. 2003. Distribution and expression of A1 adenosine receptors, adenosine deaminase and adenosine deaminase-binding protein (CD26) in goldfish brain. *Neurochem Int* 42:455–464.
- Blázquez M, Bosma PT, Chang JP, Docherty K, Trudeau VL. 1998. ??-aminobutyric acid up-regulates the expression of a novel secretogranin-II messenger ribonucleic acid in the goldfish pituitary. *Endocrinology* 139:4870–4880.
- Blázquez M, Shennan KI. 2000. Basic mechanisms of secretion: sorting into the regulated secretory pathway. *Biochem Cell Biol* 78:181–91.
- Boutahricht M, Guillemot J, Montero-Hadjadje M, Bellafqih S, El Ouezzani S, Alaoui A, Yon L, Vaudry H, Anouart Y, Magoul R. 2005. Biochemical characterisation and immunohistochemical localisation of the secretogranin II-derived peptide EM66 in the hypothalamus of the Jerboa (*Jaculus orientalis*): Modulation by food deprivation. *J Neuroendocrinol* 17:372–378.
- Brunne B, Zhao S, Derouiche A, Herz J, Petra M, Frotscher M, Bock HH. 2010. Origin, maturation, and astroglial transformation of secondary radial glial cells in the developing dentate gyrus. *Glia* 58:1553–1569.
- Burmeister SS, Fernald RD. 2005. Evolutionary conservation of the Egr-1 immediate-

- early gene response in a teleost. *J Comp Neurol* 481:220–232.
- Calegari F, Coco S, Taverna E, Bassetti M, Verderio C, Corradi N, Matteoli M, Rosa P. 1999. A regulated secretory pathway in cultured hippocampal astrocytes. *J Biol Chem* 274:22539–22547.
- Caligioni CS, Franci CR. 2002. Oxytocin secretion induced by osmotic stimulation in rats during the estrous cycle and after ovariectomy and hormone replacement therapy. *Life Sci* 71:2821–2831.
- Callard G V., Tchoudakova A V., Kishida M, Wood E. 2001. Differential tissue distribution, developmental programming, estrogen regulation and promoter characteristics of cyp19 genes in teleost fish. *J Steroid Biochem Mol Biol* 79:305–314.
- Callard G V, Petro Z, Ryan KJ. 1981. Estrogen synthesis in vitro and in vivo in the brain of a marine teleost (*Myoxocephalus*). *Gen Comp Endocrinol* 43:243–255.
- Canosa LF, Lopez GC, Scharrig E, Lesaux-Farmer K, Somoza GM, Kah O, Trudeau VL. 2011. Forebrain mapping of secretoneurin-like immunoreactivity and its colocalization with isotocin in the preoptic nucleus and pituitary gland of goldfish. *J Comp Neurol* 519:3748–65.
- Chaube R, Singh RK, Joy KP. 2012. Estrogen regulation of brain vasotocin secretion in the catfish *Heteropneustes fossilis*: An interaction with catecholaminergic system. *Gen Comp Endocrinol* 175:206–213.
- Chen MS, Huber a B, van der Haar ME, Frank M, Schnell L, Spillmann a a, Christ F, Schwab ME. 2000. Nogo-A is a myelin-associated neurite outgrowth inhibitor and an antigen for monoclonal antibody IN-1. *Nature* 403:434–439.
- Chetverukhin VK, Polenov a L. 1993. Ultrastructural radioautographic analysis of neurogenesis in the hypothalamus of the adult frog, *Rana temporaria*, with special reference to physiological regeneration of the preoptic nucleus. II. Types of neuronal cells produced. *Cell Tissue Res* 271:351–362.
- Ciesielski-treska J, Ulrich G, Taupenot L, Chasserot-golaz S, Corti A, Aunis D, Bader M. 1998. Chromogranin A Induces a Neurotoxic Phenotype in Brain Microglial Cells *. *J Biol Chem* 273:14339–14346.
- Clint SC, Zupanc GKH. 2001. Neuronal regeneration in the cerebellum of adult teleost fish, *Apteronotus leptorhynchus*: Guidance of migrating young cells by radial glia. *Dev Brain Res* 130:15–23.
- Conn MP, Janovick JA, Braden TD, Maurer RA, Jenness L. 1992. SIIp : A Unique Secretogranin / Chromogranin.
- Courel M, Soler-Jover A, Rodriguez-Flores JL, Mahata SK, Elias S, Montero-Hadjadje M, Anouar Y, Giuly RJ, O'Connor DT, Taupenot L. 2010. Pro-hormone secretogranin II regulates dense core secretory granule biogenesis in catecholaminergic cells. *J Biol Chem* 285:10030–10043.
- Cozzi MG, Rosa P, Greco A, Hille A, Huttner WB, Zanini A, De Camilli P. 1989. Immunohistochemical localization of secretogranin II in the rat cerebellum. *Neuroscience* 28:423–441.
- Crawford JL, McNeilly AS. 2002. Co-localisation of gonadotrophins and granins in gonadotrophs at different stages of the oestrous cycle in sheep. *J Endocrinol* 174:179–194.
- Diekmann H, Klinger M, Oertle T, Heinz D, Pogoda HM, Schwab ME, Stuermer CAO.

2005. Analysis of the reticulon gene family demonstrates the absence of the neurite growth inhibitor Nogo-A in fish. *Mol Biol Evol* 22:1635–1648.
- Ding ZY, Liang HF, Jin GN, Chen WX, Wang W, Datta PK, Zhang MZ, Zhang B, Chen XP. 2014. Smad6 suppresses the growth and self-renewal of hepatic progenitor cells. *J Cell Physiol* 229:651–660.
- Diotel N, Page Y Le, Mouriec K, Tong S-K, Pellegrini E, Vaillant C, Anglade I, Brion F, Pakdel F, Chung B, Kah O. 2010a. Aromatase in the brain of teleost fish: Expression, regulation and putative functions. *Front Neuroendocrinol* 31:172–192.
- Diotel N, Do Rego J-L, Anglade I, Vaillant C, Pellegrini E, Vaudry H, Kah O. 2011a. The Brain of Teleost Fish, a Source, and a Target of Sexual Steroids. *Front Neurosci* 5:1–15.
- Diotel N, Do Rego JL, Anglade I, Vaillant C, Pellegrini E, Gueguen MM, Mironov S, Vaudry H, Kah O. 2011b. Activity and expression of steroidogenic enzymes in the brain of adult zebrafish. *Eur J Neurosci* 34:45–56.
- Diotel N, Servili A, Gueguen M-M, Mironov S, Pellegrini E, Vaillant C, Zhu Y, Kah O, Anglade I. 2011c. Nuclear Progesterone Receptors Are Up-Regulated by Estrogens in Neurons and Radial Glial Progenitors in the Brain of Zebrafish. *PLoS One* 6:e28375.
- Diotel N, Vaillant C, Gabbero C, Mironov S, Fostier A, Gueguen MM, Anglade I, Kah O, Pellegrini E. 2013. Effects of estradiol in adult neurogenesis and brain repair in zebrafish. *Horm Behav* 63:193–207.
- Diotel N, Vaillant C, Gueguen MM, Mironov S, Anglade I, Servili A, Pellegrini E, Kah O. 2010b. Cxcr4 and Cxcl12 expression in radial glial cells of the brain of adult zebrafish. *J Comp Neurol* 518:4855–4876.
- Doherty P, Walsh FS. 1991. The contrasting roles of N-CAM and N-cadherin as neurite outgrowth-promoting molecules. *J Cell Sci Suppl* 15:13–21.
- Dono R. 2003. Fibroblast growth factors as regulators of central nervous system development and function. *Am J Physiol Regul* 284:R867–R881.
- Dunzendorfer S, Kaser A, Meierhofer C, Tilg H, Wiedermann CJ. 2001. Cutting Edge: Peripheral Neuropeptides Attract Immature and Arrest Mature Blood-Derived Dendritic Cells. *J Immunol* 166:2167–2172.
- Dunzendorfer S, Meierhofer C, Wiedermann CJ. 1998a. Signaling in neuropeptide-induced migration of human eosinophils. *J Leukoc Biol* 64:828–34.
- Dunzendorfer S, Schratzberger P, Reinisch N, Kähler CM, Wiedermann CJ. 1998b. Secretoneurin, a novel neuropeptide, is a potent chemoattractant for human eosinophils. *Blood* 91:1527–32.
- Egger C, Kirchmair R, Kapelari S, Fischer-Colbrie R, Hogue-Angeletti RA, Winkler H. 1994. Bovine Posterior Pituitary: Presence of p65 (Synaptotagmin), PC1 PC2 and Secretoneurin in Large Dense Core Vesicles. *Neuroendocrinology* 59:169–175.
- Ekdahl CT, Claassen JH, Bonde S, Kokaia Z, Lindvall O. 2003. Inflammation is detrimental for neurogenesis in adult brain. *Proc Natl Acad Sci U S A* 100:13632–13637.
- Elisabeth P, Nicolas D, Colette V-C, Rita PM, Marie-Madeleine G, Ahmed N, Joel CN, Olivier K. 2015. Steroid modulation of neurogenesis: Focus on radial glial cells in zebrafish. *J Steroid Biochem Mol Biol*.
- Farina C, Aloisi F, Meinel E. 2007. Astrocytes are active players in cerebral innate

- immunity. *Trends Immunol* 28:138–145.
- Feistritzer C, Mosheimer BA, Colleselli D, Wiedermann CJ, Kähler CM. 2005. Effects of the neuropeptide secretoneurin on natural killer cell migration and cytokine release. *Regul Pept* 126:195–201.
- Fischer-Colbrie R, Kirchmair R, Kähler CM, Wiedermann CJ, Saria A. 2005. Secretoneurin: a new player in angiogenesis and chemotaxis linking nerves, blood vessels and the immune system. *Curr Protein Pept Sci* 6:373–85.
- Fischer-Colbrie R, Kirchmair R, Schobert A, Olenik C, Meyer DK, Winkler H. 1993. Secretogranin II is synthesized and secreted in astrocyte cultures. *J Neurochem* 60:2312–2314.
- Fisher-Colbrie R, Laslop A, Kirchmair R. 1995. Secretogranin II: Molecular properties, regulation of biosynthesis and processing to the neuropeptide secretoneurin.
- Fitch M., Silver J. 2011. CNS Injury, Glial Scars, and Inflammation: Inhibitory extracellular matrices and regeneration failure. *Exp Neurol* 2:294–301.
- Florio M, Huttner WB. 2014. Neural progenitors, neurogenesis and the evolution of the neocortex. *Development* 141:2182–94.
- Forlano PM, Deitcher DL, Myers DA, Bass AH. 2001. Anatomical distribution and cellular basis for high levels of aromatase activity in the brain of teleost fish: aromatase enzyme and mRNA expression identify glia as source. *J Neurosci* 21:8943–8955.
- Garcia-Segura LM. 2008. Aromatase in the brain: Not just for reproduction anymore. *J Neuroendocrinol* 20:705–712.
- Garcia-Segura LM, Wozniak a., Azcoitia I, Rodriguez JR, Hutchison RE, Hutchison JB. 1999. Aromatase expression by astrocytes after brain injury: Implications for local estrogen formation in brain repair. *Neuroscience* 89:567–578.
- Garlov PE. 2005. Plasticity of nonapeptidergic neurosecretory cells in fish hypothalamus and neurohypophysis. *Int Rev Cytol* 245:123–170.
- Gasser MC, Berti I, Hauser KF, Fischer-Colbrie R, Saria a. 2003. Secretoneurin promotes pertussis toxin-sensitive neurite outgrowth in cerebellar granule cells. *J Neurochem* 85:662–669.
- Gitter BD, Regoli D, Howbert JJ, Glasebrook AL, Waters DC. 1994. Interleukin-6 secretion from human astrocytoma cells induced by substance P. *J Neuroimmunol* 51:101–8.
- Goto-Kazeto R, Kight KE, Zohar Y, Place AR, Trant JM. 2004. Localization and expression of aromatase mRNA in adult zebrafish. *Gen Comp Endocrinol* 139:72–84.
- Götz M, Huttner WB. 2005. The cell biology of neurogenesis. *Nat Rev Mol Cell Biol* 6:777–788.
- Grabherr M, Haas B, Yassour M, Levin J, Thompson D, Amit I, Adiconis X, Fan L, Raychowdhury R, Zeng Q, Chen Z, Mauceli E, Hacohen N, Gnirke A, Rhind N, Palma F, Birren B, Nusbaum C, Lindblad-Toh K, Friedman N, Regev A. 2013. Trinity: reconstructing a full-length transcriptome without a genome from RNA-Seq data. *Nat Biotechnol* 29:644–652.
- Grandel H, Brand M. 2013. Comparative aspects of adult neural stem cell activity in vertebrates. *Dev Genes Evol* 223:131–147.
- GrandPré T, Nakamura F, Vartanian T, Strittmatter SM. 2000. Identification of the Nogo

- inhibitor of axon regeneration as a Reticulon protein. *Nature* 403:439–444.
- Grimaldi M, Florio T, Schettini G. 1997. Somatostatin inhibits interleukin 6 release from rat cortical type I astrocytes via the inhibition of adenylyl cyclase. *Biochem Biophys Res Commun* 235:242–8.
- Grupp L, Wolburg H, Mack AF. 2010. Astroglial structures in the zebrafish brain. *J Comp Neurol* 518:4277–4287.
- Hasslacher J, Lehner GF, Harler U, Beer R, Ulmer H, Kirchmair R, Fischer-Colbrie R, Bellmann R, Dunzendorfer S, Joannidis M. 2014. Secretoneurin as a marker for hypoxic brain injury after cardiopulmonary resuscitation. *Intensive Care Med* 40:1518–1527.
- Hatta K, Takagi S, Fujisawa H, Takeichi M. 1987. Spatial and temporal expression pattern of N-cadherin cell adhesion molecules correlated with morphogenetic processes of chicken embryos. *Dev Biol* 120:215–227.
- Hawkins MB, Godwin J, Crews D, Thomas P. 2005. The distributions of the duplicate oestrogen receptors ER- b a and ER- b b in the forebrain of the Atlantic croaker (*Micropogonias undulatus*): evidence for subfunctionalization after gene duplication. *Proceeding R Soc B*:633–641.
- Hayward JN. 1974. Physiological and morphological identification of hypothalamic magnocellular neuroendocrine cells in goldfish preoptic nucleus. *J Physiol* 239:103–124.
- Heckmann L-H, Sørensen PB, Krogh PH, Sørensen JG. 2011. NORMA-Gene: a simple and robust method for qPCR normalization based on target gene data. *BMC Bioinformatics* 12:250.
- Helle KB. 2004. The granin family of uniquely acidic proteins of the diffuse neuroendocrine system: comparative and functional aspects. *Biol Rev Camb Philos Soc* 79:769–794.
- Helle KB. 2010. Regulatory peptides from chromogranin A and secretogranin II: Putative modulators of cells and tissues involved in inflammatory conditions. *Regul Pept* 165:45–51.
- Hinsch K, Zupanc GKH. 2007. Generation and long-term persistence of new neurons in the adult zebrafish brain: A quantitative analysis. *Neuroscience* 146:679–696.
- Hoflehner J, Eder U, Laslop A, Seidah NG, Fischer-Colbrie R, Winkler H. 1995. Processing of secretogranin II by prohormone convertases: Importance of PC1 in generation of secretoneurin. *FEBS Lett* 360:294–298.
- Hu RM, Levin ER. 1994. Astrocyte Growth Is Regulated By Neuropeptides Through TGF- β and Basic Fibroblast Growth-Factor. *J Clin Invest* 93:1820–1827.
- Huttner WB, Programme B, Molecular E. 1991. The granin (secretogranin-chromogranin) family. *Trends Biochem Sci*:27–30.
- Ischia R, Culig Z, Eder U, Bartsch G, Winkler H, Fischer-Colbrie R, Klocker H. 1998. Presence of chromogranins and regulation of their synthesis and processing in a neuroendocrine prostate tumor cell line. *Prostate Suppl* 8:80–87.
- Ivell R, Walther N. 1999. The role of sex steroids in the oxytocin hormone system. *Mol Cell Endocrinol* 151:95–101.
- Jeng SR, Yueh WS, Pen YT, Gueguen MM, Pasquier J, Dufour S, Chang CF, Kah O. 2012. Expression of Aromatase in Radial Glial Cells in the Brain of the Japanese Eel Provides Insight into the Evolution of the cyp19a Gene in Actinopterygians. *PLoS*

One 7:1–13.

- Jögi A, Vallon-Christersson J, Holmquist L, Axelson H, Borg Å, Pählman S. 2004. Human neuroblastoma cells exposed to hypoxia: Induction of genes associated with growth, survival, and aggressive behavior. *Exp Cell Res* 295:469–487.
- Johnson MB, Wang PP, Atabay KD, Murphy E a, Doan RN, Hecht JL, Walsh C a. 2015. Single-cell analysis reveals transcriptional heterogeneity of neural progenitors in human cortex. *Nat Neurosci* 18:6–8.
- Jurič DM, Kržan M, Lipnik-Stangelj M. 2016. Histamine and astrocyte function. *Pharmacol Res* 111:774–783.
- Kadowaki M, Nakamura S, Machon O, Krauss S, Radice GL, Takeichi M. 2007. N-cadherin mediates cortical organization in the mouse brain. *Dev Biol* 304:22–33.
- Kah O, Anglade I, Linard B, Pakdel F, Salbert G, Bailhache T, Ducouret B, Saligaut C, Goff P Le, Valotaire Y, Jégo P. 1997. Estrogen receptors in the brain-pituitary complex and the neuroendocrine regulation of gonadotropin release in rainbow trout. *Fish Physiol Biochem*:53–62.
- Kahler C., Bellmann R, Reinisch N, Schratzberger P, Gruber B, Wiedermann CJ. 1996. Stimulation of human skin fibroblast migration by the neuropeptide secretoneurin.
- Kähler CM, Fischer-Colbrie R. 2002. Chromogranins: Functional and Clinical Aspects. In: Helle KB, Aunis D, editors. Boston, MA: Springer US. p 279–290.
- Kahler CM, Kaufmann G, Hogue-Angeletti R, Fischer-Colbrie R, Dunzendorfer S, Reinisch N, Wiedermann CJ. 1999. A soluble gradient of the neuropeptide secretoneurin promotes the transendothelial migration of monocytes in vitro. *Eur J Pharmacol* 365:65–75.
- Kähler CM, Kirchmair R, Kaufmann G, Kähler ST, Reinisch N, Fischer-Colbrie R, Hogue-Angeletti R, Winkler H, Wiedermann CJ. 1997. Inhibition of Proliferation and Stimulation of Migration of Endothelial Cells by Secretoneurin In Vitro. *Arterioscler Thromb Vasc Biol* 17:2029–2035.
- Kálmán M. 1998. Astroglial architecture of the carp (*Cyprinus carpio*) brain as revealed by immunohistochemical staining against glial fibrillary acidic protein (GFAP). *Anat Embryol (Berl)* 198:409–433.
- Kang W, Wong LC, Shi S-H, Hébert JM. 2009. The transition from radial glial to intermediate progenitor cell is inhibited by FGF signaling during corticogenesis. *J Neurosci* 29:14571–80.
- Kaslin J, Ganz J, Brand M. 2008. Proliferation, neurogenesis and regeneration in the non-mammalian vertebrate brain. *Philos Trans R Soc B Biol Sci* 363:101–122.
- Kaufmann WA, Barnas U, Humpel C, Nowakowski K, DeCol C, Gurka P, Ransmayr G, Hinterhuber H, Winkler H, Marksteiner J. 1998. Synaptic loss reflected by secretoneurin-like immunoreactivity in the human hippocampus in Alzheimer's disease. *Eur J Neurosci* 10:1084–1094.
- Kim HJ, Denli AM, Wright R, Baul TD, Clemenson GD, Morcos AS, Zhao C, Schafer ST, Gage FH, Kagalwala MN. 2015. REST Regulates Non-Cell-Autonomous Neuronal Differentiation and Maturation of Neural Progenitor Cells via Secretogranin II. *J Neurosci* 35:14872–14884.
- Kirchmair R, Benzer A, Troger J, Miller C, Marksteiner J, Saria A, Gasser RW, Hogue-Angeletti R, Fischer-Colbrie R, Winkler H. 1994a. Molecular characterization of immunoreactivities of peptides derived from chromogranin a (GE-25) and from

- secretogranin II (secretoneurin) in human and bovine cerebrospinal fluid. *Neuroscience* 63:1179–1187.
- Kirchmair R, Egger M, Walter DH, Eisterer W, Niederwanger A, Woell E, Nagl M, Pedrini M, Murayama T, Frauscher S, Hanley A, Silver M, Brodmann M, Sturm W, Fischer-Colbrie R, Losordo DW, Patsch JR, Schratzberger P. 2004a. Secretoneurin, an angiogenic neuropeptide, induces postnatal vasculogenesis. *Circulation* 110:1121–1127.
- Kirchmair R, Gander R, Egger M, Hanley A, Silver M, Ritsch A, Murayama T, Kaneider N, Sturm W, Kearny M, Fischer-Colbrie R, Kircher B, Gaenger H, Wiedermann CJ, Ropper AH, Losordo DW, Patsch JR, Schratzberger P. 2004b. The Neuropeptide Secretoneurin Acts as a Direct Angiogenic Cytokine In Vitro and In Vivo. *Circulation* 109:777–783.
- Kirchmair R, Hogue-Angeletti R, Gutierrez J, Fischer-Colbrie R, Winkler H. 1993. Secretoneurin—a neuropeptide generated in brain, adrenal medulla and other endocrine tissues by proteolytic processing of secretogranin II (chromogranin C). *Neuroscience* 53:359–365.
- Kirchmair R, Marksteiner J, Troger J, Mahata SK, Mahata M, Donnerer J, Amann R, Fischer-Colbrie R, Winkler H, Saria a. 1994b. Human and rat primary C-fibre afferents store and release secretoneurin, a novel neuropeptide. *Eur J Neurosci* 6:861–8.
- Kizil C, Dudczig S, Kyritsis N, Machate A, Blaesche J, Kroehne V, Brand M. 2012. The chemokine receptor *cxcr5* regulates the regenerative neurogenesis response in the adult zebrafish brain. *Neural Dev* 7:27.
- de Kock CPJ, Wierda KDB, Bosman LWJ, Min R, Kokksma J-J, Mansvelter HD, Verhage M, Brussaard AB. 2003. Somatodendritic secretion in oxytocin neurons is upregulated during the female reproductive cycle. *J Neurosci* 23:2726–2734.
- Koh J, Chen S, Zhu N, Yu F, Soltis PS, Soltis DE. 2012. Comparative proteomics of the recently and recurrently formed natural allopolyploid *Tragopogon mirus* (Asteraceae) and its parents. *New Phytol* 196:292–305.
- Kong C, Gill BM, Rahimpour R, Xu L, Feldman RD, Xiao Q, McDonald TJ, Taupenot L, Mahata SK, Singh B, O'Connor DT, Kelvin DJ. 1998. Secretoneurin and chemoattractant receptor interactions. *J Neuroimmunol* 88:91–98.
- Kroehne V, Freudenreich D, Hans S, Kaslin J, Brand M. 2011. Regeneration of the adult zebrafish brain from neurogenic radial glia-type progenitors. *Development* 138:4831–4841.
- Kyritsis N, Kizil C, Zocher S, Kroehne V, Kaslin J, Freudenreich D, Iltzsche A, Brand M. 2012. Acute inflammation initiates the regenerative response in the adult zebrafish brain. *Science* (80-) 338:1353–6.
- Landgraf R, Ludwig M. 1991. Vasopressin release within the supraoptic and paraventricular nuclei of the rat brain: osmotic stimulation via microdialysis. *Brain Res* 558:191–196.
- Langle SL, Poulain DA, Theodosis DT. 2002. Neuronal-glia remodeling: A structural basis for neuronal-glia interactions in the adult hypothalamus. *J Physiol Paris* 96:169–175.
- Laslop A, Becker A. 2002. Proteolytic processing of chromogranins is modified in brains of transgenic mice. *Ann New ...* 5:7–10.

- Laslop A, Tschernitz C. 1992. Effects of nerve growth factor on the biosynthesis of chromogranin A and B, secretogranin II and carboxypeptidase H in rat PC12 cells. *Neuroscience* 49:443–450.
- Laslop A, Weiss C, Savaria D, Eiter C, Tooze SA, Seidah NG, Winkler H. 1998. Proteolytic processing of chromogranin B and secretogranin II by prohormone convertases. *J Neurochem* 70:374–383.
- Laussu J, Khuong A, Gautrais J, Davy A. 2014. Beyond boundaries - Eph: Ephrin signaling in neurogenesis. *Cell Adhes Migr* 8:349–359.
- Lechner T, Adlassnig C, Humpel C, Kaufmann WA, Maier H, Reinstadler-Kramer K, Hinterhölzl J, Mahata SK, Jellinger KA, Marksteiner J. 2004. Chromogranin peptides in Alzheimer's disease. *Exp Gerontol* 39:101–113.
- Leenders F, Tesdorpf JG, Markus M, Engel T, Seedorf U, Adamski J. 1996. Porcine 80-kDa protein reveals intrinsic 17 β -hydroxysteroid dehydrogenase, fatty acyl-CoA-hydrolase/dehydrogenase, and sterol transfer activities. *J Biol Chem* 271:5438–5442.
- Liu W, Tang Y, Feng J. 2011. Cross talk between activation of microglia and astrocytes in pathological conditions in the central nervous system. *Life Sci* 89:141–146.
- Lu P, Jones LL, Snyder EY, Tuszynski MH. 2003. Neural stem cells constitutively secrete neurotrophic factors and promote extensive host axonal growth after spinal cord injury. *Exp Neurol* 181:115–129.
- Ludwig M. 1998. Dendritic release of vasopressin and oxytocin. *J Neuroendocrinol*:881–895.
- Ludwig M, Stern J, Ludwig M. 2015. Multiple signalling modalities mediated by dendritic exocytosis of oxytocin and vasopressin. *Philos Trans B* 370.
- Lyons DA, Talbot WS, Sofroniew M V, Lyons DA, Talbot WS. 2014. Glial Cell Development and Function in Zebrafish. *Cold Spring Harb Perspect Biol*:1–22.
- Ma S, Kwon HJ, Johng H, Zang K, Huang Z. 2013. Radial Glial Neural Progenitors Regulate Nascent Brain Vascular Network Stabilization Via Inhibition of Wnt Signaling. *PLoS Biol* 11.
- Machon O, Van Den Bout CJ, Backman M, Kemler R, Krauss S. 2003. Role of β -catenin in the developing cortical and hippocampal neuroepithelium. *Neuroscience* 122:129–143.
- Mack AF, Tiedemann K. 2013. Cultures of astroglial cells derived from brain of adult cichlid fish. *J Neurosci Methods* 212:269–275.
- Mack AF, Wolburg H. 2006. Growing axons in fish optic nerve are accompanied by astrocytes interconnected by tight junctions. *Brain Res* 1103:25–31.
- Mahata SK, Mahata M, Hortnag H, Fischer-Colbrie R, Steiner HJ, Dietze O, Winkler H. 1993. Concomitant changes of messenger ribonucleic acid levels of secretogranin II, VGF, vasopressin and oxytocin in the paraventricular nucleus of rats after adrenalectomy and during lactation. *J Neuroendocr* 5:323–330.
- Mahata SK, Mahata M, Steiner HJ, Fischer-Colbrie R, Winkler H. 1992. In situ hybridization: mRNA levels of secretogranin II, neuropeptides and carboxypeptidase h in brains of salt-loaded and brattleboro rats. *Neuroscience* 48:669–680.
- Maimone D, Cioni C, Rosa S, Macchia G, Aloisi F, Annunziata P. 1993. Norepinephrine and vasoactive intestinal peptide induce IL-6 secretion by astrocytes: Synergism with IL-1 β and TNF α *J Neuroimmunol* 47:73–81.

- Makantasi P, Dermon CR. 2014. Estradiol treatment decreases cell proliferation in the neurogenic zones of adult female zebrafish (*Danio Rerio*) brain. *Neuroscience* 277:306–320.
- Mangiamele LA, Gomez JR, Curtis NJ, Thompson RR. 2016. GPER / GPR30 , a Membrane Estrogen Receptor , Is Expressed in the Brain and Retina of a Social Fish (*Carassius auratus*) and Colocalizes With Isotocin. *J Comp Neurol*:1–19.
- Marksteiner J, Kaufmann W a, Gurka P, Humpel C. 2002. Synaptic proteins in Alzheimer’s disease. *J Mol Neurosci* 18:53–63.
- Marksteiner J, Kirchmair R, Mahata SK, Mahata M, Fischercolbrie R, Hogueangeletti R, Saria A, Winkler H. 1993. Distribution of Secretoneurin, a Peptide Derived From Secretogranin-Ii, in Rat-Brain - an Immunocytochemical and Radioimmunological Study. *Neuroscience* 54:923–944.
- Marti E, Blasi J, Ferrer I. 2002. Early induction of secretoneurin expression following kainic acid administration at convulsant doses in the rat and gerbil hippocampus. *Hippocampus* 12:174–185.
- Martí E, Ferrer I, Blasi J. 2001. Differential regulation of chromogranin A, chromogranin B and secretoneurin protein expression after transient forebrain ischemia in the gerbil. *Acta Neuropathol* 101:159–166.
- Martinez-Galan JR, Escobar del Ray F, Morreale de Escobar G, Santacana M, Ruiz-Marcos A. 2004. Hypothyroidism alters the development of radial glial cells in the term fetal and postnatal neocortex of the rat. *Dev Brain Res* 153:109–114.
- Martyniuk CJ, Alvarez S, Lo BP, Elphick J, Marlatt VL. 2012. Hepatic protein expression networks associated with masculinisation in the female fathead minnow (*Pimephales promelas*). *J Proteome Res*.
- Martyniuk CJ, Denslow ND. 2012. Exploring androgen-regulated pathways in teleost fish using transcriptomics and proteomics. *Integr Comp Biol* 52:695–704.
- Mayer SI, Rössler OG, Endo T, Charnay P, Thiel G. 2009. Epidermal-growth-factor-induced proliferation of astrocytes requires Egr transcription factors. *J Cell Sci* 122:3340–3350.
- McKeown KA, Moreno R, Hall VL, Ribera AB, Downes GB. 2012. Disruption of *Eaat2b*, a glutamate transporter, results in abnormal motor behaviors in developing zebrafish. *Dev Biol* 362:162–171.
- Mecawi AS, Elias LLK. 2011. Oestradiol Potentiates Hormone Secretion and Neuronal Activation in Response to Hypertonic Extracellular Volume Expansion in Ovariectomised Rats *Neuroendocrinology*. *J Neuroendocrinol* 23:481–489.
- Mecawi AS, Vilhena-franco T, Araujo IG, Reis LC, Elias LLK, Antunes-rodrigues J, As M, Ig A, Lc R. 2011. Estradiol potentiates hypothalamic vasopressin and oxytocin neuron activation and hormonal secretion induced by hypovolemic shock. *Am J Physiol - Regul Integr Comp Physiol* 301:905–915.
- Mellon SH, Griffin LD, Compagnone N a. 2001. Biosynthesis and action of neurosteroids. *Brain Res Brain Res Rev* 37:3–12.
- Menuet A, Pellegrini E, Anglade I, Blaise O, Laudet V, Kah O, Pakdel F. 2002. Molecular Characterization of Three Estrogen Receptor Forms in Zebrafish : Binding Characteristics , Transactivation Properties , and Tissue Distributions 1. *Biol Reprod*:1881–1892.
- Menuet A, Pellegrini E, Brion F, Gueguen MM, Anglade I, Pakdel F, Kah O. 2005.

- Expression and estrogen-dependent regulation of the zebrafish brain aromatase gene. *J Comp Neurol* 485:304–320.
- Mi H, Poudel S, Muruganujan A, Casagrande JT, Thomas PD. 2015. PANTHER version 10: expanded protein families and functions, and analysis tools. *Nucleic Acids Res* 44:D336-42.
- Mikwar M, Navarro-Martin L, Xing L, Volkoff H, Hu W, Trudeau VL. 2016. Stimulatory effect of the secretogranin-II derived peptide secretoneurin on food intake and locomotion in female goldfish (*Carassius auratus*). *Peptides* 78:42–50.
- Ming G li, Song H. 2011. Adult Neurogenesis in the Mammalian Brain: Significant Answers and Significant Questions. *Neuron* 70:687–702.
- Miyazaki T, Yamasaki M, Uchigashima M, Matsushima A, Watanabe M. 2011. Cellular expression and subcellular localization of secretogranin II in the mouse hippocampus and cerebellum. *Eur J Neurosci* 33:82–94.
- Möller G, Van Grunsven EG, Wanders RJA, Adamski J. 2001. Molecular basis of D-bifunctional protein deficiency. *Mol Cell Endocrinol* 171:61–70.
- Montero-Hadjadje M, Vaingankar S, Elias S, Tostivint H, Mahata SK, Anouar Y. 2008. Chromogranins A and B and secretogranin II: Evolutionary and functional aspects. *Acta Physiol* 192:309–324.
- Moss A, Alvares D, Meredith-Middleton J, Robinson M, Slater R, Hunt SP, Fitzgerald M. 2005. Ephrin-A4 inhibits sensory neurite outgrowth and is regulated by neonatal skin wounding. *Eur J Neurosci* 22:2413–2421.
- Niu B, Fu L, Sun S, Li W. 2010. Artificial and natural duplicates in pyrosequencing reads of metagenomic data. *BMC Bioinformatics* 11:187.
- Norden DM, Trojanowski PJ, Villanueva E, Navarro E, Godbout JP. 2016. Sequential activation of microglia and astrocyte cytokine expression precedes increased iba-1 or GFAP immunoreactivity following systemic immune challenge. *Glia* 64:300–316.
- O'Donovan KJ, Tourtellotte WG, Milbrandt J, Baraban JM. 1999. The EGR family of transcription-regulatory factors: Progress at the interface of molecular and systems neuroscience. *Trends Neurosci* 22:167–173.
- Oertle T, van der Haar ME, Bandtlow CE, Robeva A, Burfeind P, Buss A, Huber AB, Simonen M, Schnell L, Brösamle C, Kaupmann K, Vallon R, Schwab ME. 2003. Nogo-A inhibits neurite outgrowth and cell spreading with three discrete regions. *J Neurosci* 23:5393–5406.
- Okada M, Murase K, Makino A, Nakajima M, Kaku T, Furukawa S, Furukawa Y. 2008. Effects of estrogens on proliferation and differentiation of neural stem / progenitor cells. *Biomed Res* 29:163–170.
- Ornitz DM, Xu J, Colvin JS, McEwen DG, MacArthur CA, Coulier F, Gao G, Goldfarb M. 1996. Receptor specificity of the fibroblast growth factor family. *J Biol Chem* 271:15292–15297.
- Ozawa H, Picart R, Barret A, Tougard C. 1994. Heterogeneity in the Pattern of Distribution of the Specific Hormonal Product and Secretogranins within the Secretory Granules of Rat Prolactin Cells. *J Neuroendocrinol* 16:1097–1107.
- Ozawa H, Takata K. 1995. The granin family--its role in sorting and secretory granule formation. *Cell Struct Funct* 20:415–420.
- Paco S, Pozas E, Aguado F. 2010. Secretogranin III Is an Astrocyte Granin That Is Overexpressed in Reactive Glia. *Cereb Cortex* 20:1386–1397.

- Papadopoulos MC, Verkman AS. 2013. Aquaporin water channels in the nervous system. *Nat Rev Neurosci* 14:265–77.
- Parrilla M, Lillo C, Herrero-Turrión MJ, Arévalo R, Lara JM, Aijón J, Velasco A. 2009. Pax2 in the optic nerve of the goldfish, a model of continuous growth. *Brain Res* 1255:75–88.
- Pasmanik M, Callard G V. 1988. Changes in Brain Aromatase and 5 α -Reductase Reproductive Cycles in Goldfish (*Carassius auratus*)*. Society 122.
- Pathak A, Sinha RA, Mohan V, Mitra K, Godbole MM. 2011. Maternal thyroid hormone before the onset of fetal thyroid function regulates reelin and downstream signaling cascade affecting neocortical neuronal migration. *Cereb Cortex* 21:11–21.
- Pellegrini E, Menuet A, Lethimonier C, Adrio F, Gueguen MM, Tascon C, Anglade I, Pakdel F, Kah O. 2005. Relationships between aromatase and estrogen receptors in the brain of teleost fish. *Gen Comp Endocrinol* 142:60–66.
- Pellegrini E, Mouriec K, Anglade I, Manuet A, Le Page Y, Gueguen MM, Harmignon M-H, Brion F, Pakdel F, Kah O. 2007. Identification of aromatase-positive radial glial cells as progenitor cells in the ventricular layer of the forebrain in zebrafish. *J Comp Neurol* 504:287–297.
- Pérez MR, Pellegrini E, Cano-Nicolau J, Gueguen MM, Menouer-Le Guillou D, Merot Y, Vaillant C, Somoza GM, Kah O. 2013. Relationships between radial glial progenitors and 5-HT neurons in the paraventricular organ of adult zebrafish - potential effects of serotonin on adult neurogenesis. *Eur J Neurosci* 38:3292–3301.
- Peter RE. 1977. The preoptic nucleus in fishes: A comparative discussion of function-activity relationships. *Integr Comp Biol* 17:775–785.
- Peter RE, Gill VE. 1975. A stereotaxic atlas and technique for forebrain nuclei of the goldfish, *Carassius auratus*. *J Comp Neurol* 159:69–101.
- Peterson RS, Yarram L, Schlinger B a, Saldanha CJ. 2005. Aromatase is pre-synaptic and sexually dimorphic in the adult zebra finch brain. *Proc Biol Sci* 272:2089–2096.
- Pirker S, Czech T, Baumgartner C, Novak HM, Fürtinger S, Fischer-Colbrie R, Sperk G. 2001. Chromogranins as markers of altered hippocampal circuitry in temporal lobe epilepsy. *Ann Neurol* 50:216–226.
- Polenov a L, Chetverukhin VK. 1993. Ultrastructural radioautographic analysis of neurogenesis in the hypothalamus of the adult frog, *Rana temporaria*, with special reference to physiological regeneration of the preoptic nucleus. II. Types of neuronal cells produced. *Cell Tissue Res* 271:351–362.
- Polenov AL, Belenky MA, Garlov PE. 1979. Cell and Tissue The Hypothalamo-Hypophysial System in Acipenseridae. *Cell Tissue Res* 320:311–320.
- Popesku JT, Martyniuk CJ, Denslow ND, Trudeau VL. 2010. Rapid dopaminergic modulation of the fish hypothalamic transcriptome and proteome. *PLoS One* 5.
- Portela-Gomes GM, Grimelius L, Stridsberg M. 2010. Secretogranin III in human neuroendocrine tumours. A comparative immunohistochemical study with chromogranins A and B and secretogranin II. *Regul Pept* 165:30–35.
- Pouso P, Quintana L, López GC, Somoza GM, Silva AC, Trudeau VL. 2015. The secretogranin-II derived peptide secretoneurin modulates electric behavior in the weakly pulse type electric fish, *Brachyhyopomus gauderio*. *Gen Comp Endocrinol* 222:158–166.
- Pow D V., Morris JF. 1989. Dendrites of hypothalamic magnocellular neurons release

- neurohypophysial peptides by exocytosis. *Neuroscience* 32:435–439.
- Radakovits R, Barros CS, Belvindrah R, Patton B, Müller U. 2009. Regulation of radial glial survival by signals from the meninges. *J Neurosci* 29:7694–705.
- Rago L, Beattie R, Taylor V, Winter J. 2014. MiR379-410 cluster miRNAs regulate neurogenesis and neuronal migration by fine-tuning N-cadherin. *EMBO J* 33:906–920.
- Rakic P. 1971. Guidance of neurons migrating to the fetal monkey neocortex. *Brain Res* 33:471–476.
- Rakic P. 1972. Mode of cell migration to the superficial layers of fetal monkey neocortex. *J Comp Neurol* 145:61–83.
- Reaves Jr. TA, Hayward JN. 1980. Functional and morphological studies of peptide-containing neuroendocrine cells in goldfish hypothalamus. *J Comp Neurol* 193:777–788.
- Do Rego JL, Seong JY, Burel D, Leprince J, Luu-The V, Tsutsui K, Tonon M-C, Pelletier G, Vaudry H. 2009. Neurosteroid biosynthesis: Enzymatic pathways and neuroendocrine regulation by neurotransmitters and neuropeptides. *Front Neuroendocrinol* 30:259–301.
- Reinisch N, Kirchmair R, K?hler CM, Hogue-Angeletti R, Fischer-Colbrie R, Winkler H, Wiedermann CJ. 1993. Attraction of human monocytes by the neuropeptide secretoneurin. *FEBS Lett* 334:41–44.
- Reuss B, Von Bohlen Und Halbach O. 2003. Fibroblast growth factors and their receptors in the central nervous system. *Cell Tissue Res* 313:139–157.
- Rosa P, Zanini A. 1983. Purification of a sulfated secretory protein from the adenohypophysis. Immunochemical evidence that similar macromolecules are present in other glands. *Eur J Cell Biol* 31:94–98.
- Røsjø H, Stridsberg M, Florholmen G, Stensl?kken KO, Ottesen AH, Sjaastad I, Husberg C, Dahl MB, Øie E, Louch WE, Omland T, Christensen G. 2012. Secretogranin II; A protein increased in the myocardium and circulation in heart failure with cardioprotective properties. *PLoS One* 7.
- Rossoni E, Feng J, Tirozzi B, Brown D, Leng G, Moos F. 2008. Emergent synchronous bursting of oxytocin neuronal network. *PLoS Comput Biol* 4.
- Rothenaigier I, Krecsmarik M, Hayes J a, Bahn B, Lepier A, Fortin G, Götz M, Jagasia R, Bally-Cuif L. 2011. Clonal analysis by distinct viral vectors identifies bona fide neural stem cells in the adult zebrafish telencephalon and characterizes their division properties and fate. *Development* 138:1459–1469.
- Sahara S, O’Leary DDM. 2009. Fgf10 regulates transition period of cortical stem cell differentiation to radial glia controlling generation of neurons and basal progenitors. *Neuron* 63:48–62.
- Salas C, Broglio F, Rodríguez C. 2003. Evolution of Forebrain and Spatial Cognition in Vertebrates: Conservation across Diversity. *Brain Behav Evol* 62:72–82.
- Saldanha CJ, Burstein SR, Duncan KA. 2013. Induced synthesis of oestrogens by glia in the songbird brain. *J Neuroendocrinol* 25:1032–1038.
- Saldanha CJ, Duncan KA, Walters BJ. 2009. Neuroprotective actions of brain aromatase. *Front Neuroendocrinol* 30:106–118.
- Samia M, Larivière KE, Rochon MH, Hibbert BM, Basak a, Trudeau VL. 2004. Seasonal cyclicity of secretogranin-II expression and its modulation by sex steroids

- and GnRH in the female goldfish pituitary. *Gen Comp Endocrinol* 139:198–205.
- Sanghera MK, Simpson ER, Mcphaul MJ, Kozlowski G, Conley AJ, Lephart ED. 1991. Immunocytochemical Distribution of Aromatase Cytochrome P450 in the Rat Brain Using Peptide-Generated Polyclonal Antibodies. *Endocrinology* 129.
- Santollo J, Daniels D. 2015. Control of fluid intake by estrogens in the female rat : role of the hypothalamus. *Front Syst Neurosci* 9:1–11.
- Saria A, Troger J, Kirchmair R, Fischer-Colbrie R, Hogue-Angeletti R, Winkler H. 1993. Secretoneurin releases dopamine from rat striatal slices: a biological effect of a peptide derived from secretogranin II (chromogranin C). *Neuroscience* 54.
- Sato F, Hasegawa T, Katayama Y, Iwanaga T, Yanaihara N, Kanno T, Ishida N. 2000. Molecular cloning of equine chromogranin A and its expression in endocrine and exocrine tissues. *J Vet Med Sci* 62:953–9.
- Scammell JG, Sumners C, Reutter MA, Valentine DL, Jones LC. 1995. Regulation of secretogranin II mRNA in rat neuronal cultures. *Mol Brain Res*.
- Schmechel DE, Rakic P. 1979. Anatomy and Embryology A Golgi Study of Radial Glial Cells in Developing Monkey Telencephalon : Morphogenesis and Transformation into Astrocytes. *Anat Embryol (Berl)* 152:115–152.
- Schmid KW, Kunk B, Kirchmair R, Tötsch M, Böcker W, Fischer-Colbrie R. 1995. Immunohistochemical detection of secretoneurin, a novel neuropeptide endoproteolytically processed from secretogranin II, in normal human endocrine and neuronal tissues. *Histochem J* 27:473–481.
- Schneitler C, Kähler C, Wiedermann CJ, Hogue-Angeletti R, Fischer-Colbrie R. 1998. Specific binding of a 125I-secretoneurin analogue to a human monocytic cell line. *J Neuroimmunol* 86:87–91.
- Schratzberger P, Reinisch N, Kähler CM, Wiedermann CJ. 1996a. Deactivation of chemotaxis of human neutrophils by priming with secretogranin II-derived secretoneurin. *Regul Pept* 63:65–71.
- Schratzberger P, Woll E, Reinisch N, Kahler CM, Wiedermann CJ. 1996b. Secretoneurin-induced in vitro chemotaxis of human monocytes is inhibited by pertussis toxin and an inhibitor of protein kinase C.
- Schwarzer C, Marksteiner J, Kroesen S, Kohl C, Sperk G, Winkler H. 1997. Secretoneurin: A marker in rat hippocampal pathways. *J Comp Neurol* 377:29–40.
- Scott E, Zhang QG, Wang R, Vadlamudi R, Brann D. 2012. Estrogen neuroprotection and the critical period hypothesis. *Front Neuroendocrinol* 33:85–104.
- Setoguchi T, Nakashima K, Takizawa T, Yanagisawa M, Ochiai W, Okabe M, Yone K, Komiya S, Taga T. 2004. Treatment of spinal cord injury by transplantation of fetal neural precursor cells engineered to express BMP inhibitor. *Exp Neurol* 189:33–44.
- Shikanai M, Nakajima K, Kawauchi T. 2011. N-cadherin regulates radial glial fiber-dependent migration of cortical locomoting neurons. *Commun Integr Biol* 4:326–30.
- Shilov I V, Seymour SL, Patel AA, Loboda A, Tang WH, Keating SP, Hunter CL, Nuwaysir LM, Schaeffer D a. 2007. The Paragon Algorithm, a next generation search engine that uses sequence temperature values and feature probabilities to identify peptides from tandem mass spectra. *Mol Cell Proteomics* 6:1638–1655.
- Shyu W-C, Lin S-Z, Chiang M-F, Chen D-C, Su C-Y, Wang H-J, Liu R-S, Tsai C-H, Li H. 2008. Secretoneurin promotes neuroprotection and neuronal plasticity via the Jak2/Stat3 pathway in murine models of stroke. *J Clin Invest* 118.

- Sieber C, Kopf J, Hiepen C, Knaus P. 2009. Recent advances in BMP receptor signaling. *Cytokine Growth Factor Rev* 20:343–355.
- Silver J, Lorenz SE, Wahlsten D, Coughlin J. 1982. Axonal guidance during development of the great cerebral commissures: descriptive and experimental studies, in vivo, on the role of preformed glial pathways. *J Comp Neurol* 210:10–29.
- Simard M, Nedergaard M. 2004. The neurobiology of glia in the context of water and ion homeostasis. *Neuroscience* 129:877–896.
- Song J, Zhong C, Bonaguidi MA, Sun GJ, Hsu D, Gu Y, Meletis K, Huang ZJ, Ge S, Enikolopov G, Deisseroth K, Luscher B, Christian KM, Ming GL, Song H. 2012. Neuronal circuitry mechanism regulating adult quiescent neural stem-cell fate decision. *Nature* 489:150–154.
- Srinivasan S, Anitha M, Mwangi S, Heuckeroth RO. 2005. Enteric neuroblasts require the phosphatidylinositol 3-kinase/Akt/Forkhead pathway for GDNF-stimulated survival. *Mol Cell Neurosci* 29:107–119.
- Storch MK, Fischer-Colbrie R, Smith T, Rinner WA, Hickey WF, Cuzner ML, Winkler H, Lassmann H. 1996. Co-localization of secretoneurin immunoreactivity and macrophage infiltration in the lesions of experimental autoimmune encephalomyelitis. *Neuroscience* 71:885–893.
- Strobl-Mazzulla PH, Nuñez A, Pellegrini E, Gueguen MM, Kah O, Somoza GM. 2010. Progenitor radial cells and neurogenesis in pejerrey fish forebrain. *Brain Behav Evol* 76:20–31.
- Stumm R, Höllt V. 2007. CXC chemokine receptor 4 regulates neuronal migration and axonal pathfinding in the developing nervous system: Implications for neuronal regeneration in the adult brain. *J Mol Endocrinol* 38:377–382.
- Stumm RK, Rummel J, Junker V, Culmsee C, Pfeiffer M, Kriegelstein J, Höllt V, Schulz S. 2002. A Dual Role for the SDF-1/CXCR4 Chemokine Receptor System in Adult Brain: Isoform-Selective Regulation of SDF-1 Expression Modulates CXCR4-Dependent Neuronal Plasticity and Cerebral Leukocyte Recruitment after Focal Ischemia. *J Neurosci* 22:5865–5878.
- Swirnoff AH, Apel ED, Svaren J, Severson BR, Zimonjic DB, Popescu NC, Milbrandt J. 1998. Nab1, a corepressor of NGFI-A (Egr-1), contains an active transcriptional repression domain. *Mol Cell Biol* 18:512–24.
- Tait MJ, Saadoun S, Bell BA, Papadopoulos MC. 2008. Water movements in the brain: role of aquaporins. *Trends Neurosci* 31:37–43.
- Takeichi M. 1995. Morphogenetic roles of classic cadherins. *Curr Opin Cell Biol* 7:619–627.
- Taupenot L, Ciesielski-Treska J, Ulrich G, Chasserot-Golaz S, Aunis D, Bader M. 1996. Chromogranin A triggers a phenotypic transformation and the generation of nitric oxide in brain microglial cells. *Neuroscience* 72:377–389.
- Taupenot L, Harper K, O'Connor D. 2003. The chromogranin-secretogranin family. *N Engl J Med* 349:1134–1149.
- Tchoudakova a, Callard G V. 1998. Identification of multiple CYP19 genes encoding different cytochrome P450 aromatase isoenzymes in brain and ovary. *Endocrinology* 139:2179–2189.
- Than-Trong E, Bally-Cuif L. 2015. Radial glia and neural progenitors in the adult zebrafish central nervous system. *Glia* 63:1406–1428.

- Theodosios DT, Piet R, Poulain DA, Oliet SHR. 2004. Neuronal, glial and synaptic remodeling in the adult hypothalamus: Functional consequences and role of cell surface and extracellular matrix adhesion molecules. *Neurochem Int* 45:491–501.
- Thiel G, Kaufmann K, Magin A, Lietz M, Bach K, Cramer M. 2000. The human transcriptional repressor protein NAB1: Expression and biological activity. *Biochim Biophys Acta - Gene Struct Expr* 1493:289–301.
- Thomsen ER, Mich JK, Yao Z, Hodge RD, Doyle AM, Jang S, Shehata SI, Nelson AM, Shapovalova N V, Levi BP, Ramanathan S. 2015. Fixed single-cell transcriptomic characterization of human radial glial diversity. *Nat Methods* 13:87–93.
- Togashi H, Sakisaka T, Takai Y. 2009. Cell adhesion molecules in the central nervous system. *Cell Adh Migr* 3:29–35.
- Tong S-K, Mouriec K, Kuo M-W, Pellegrini E, Gueguen M-M, Brion F, Kah O, Chung B. 2009. A *cyp19a1b*-gfp (aromatase B) transgenic zebrafish line that expresses GFP in radial glial cells. *Genesis* 47:67–73.
- Trudeau VL, Martyniuk CJ, Zhao E, Hu H, Volkoff H, Decatur W a, Basak A. 2012. Is secretoneurin a new hormone? *Gen Comp Endocrinol* 175:10–8.
- Turquier V, Yon L, Grumolato L, Alexandre D, Fournier A, Vaudry H, Anouar Y. 2001. Pituitary adenylate cyclase-activating polypeptide stimulates secretoneurin release and secretogranin II gene transcription in bovine adrenochromaffin cells through multiple signaling pathways and increased binding of pre-existing activator protein-1-like. *Mol Pharmacol* 60:42–52.
- Ubuka T, Haraguchi S, Tobari Y, Narihiro M, Ishikawa K, Hayashi T, Harada N, Tsutsui K. 2014. Hypothalamic inhibition of socio-sexual behaviour by increasing neuroestrogen synthesis. *Nat Commun* 5:3061.
- Uckermann O, Grosche J, Reichenbach A, Bringmann A. 2002. ATP-evoked calcium responses of radial glial (Müller) cells in the postnatal rabbit retina. *J Neurosci Res* 70:209–218.
- Ulrich G, Ciesielski-Treska J, Taupenot L, Bader M. 2002. Chromogranin A-activated microglial cells induce neuronal apoptosis. *Ann N Y Acad Sci*:9-560–562.
- Untergasser A, Cutcutache I, Koressaar T, Ye J, Faircloth BC, Remm M, Rozen SG. 2012. Primer3 — new capabilities and interfaces. 40:1–12.
- Vallet VS, Li JY, Duval J. 1997. Secretogranin II (SgII) distribution and processing studies in human normal and adenomatous anterior pituitaries using new polyclonal antibodies. *Regul Pept* 68:155–163.
- Weiler R, Fisher-Colbrie R, Schmid KW, Feichtinger H, Bussolati G, Grimelius L, Krisch K, Kerl H, O'Connor D, Winkler H. 1988. Immunological studies on the occurrence and properties of chromogranin A and B and secretogranin II in endocrine tumors. *Am J Surg Pathol* 12:877–884.
- Weiler R, Meyerson G, Fischer-Colbrie R, Laslop A, Pohlman S, Floor E, Winkler H. 1990. Divergent changes of chromogranin A/secretogranin II levels in differentiating human neuroblastoma cells. *FEBS Lett* 265:27–29.
- Weiss C, Winkler H, Laslop A. 2001. Regulation of chromogranin biosynthesis by neurotrophic growth factors in neuroblastoma cells. *Neurochem Int* 38:43–52.
- Welte C, Engel S, Stuermer CAO. 2015. Upregulation of the zebrafish Nogo-A homologue, *Rtn4b*, in retinal ganglion cells is functionally involved in axon regeneration. *Neural Dev* 10:6.

- Wiedermann CJ. 2000. Secretoneurin: A functional neuropeptide in health and disease. *Peptides* 21:1289–1298.
- Woodhead GJ, Mutch CA, Olson EC, Chenn A. 2006. Cell-Autonomous beta-Catenin Signaling Regulates Cortical Precursor Proliferation. *J Neurosci* 26:12620–12630.
- Wrana JL. 2000. Regulation of Smad Activity. *Cell* 100:189–192.
- Xing L, Esau C, Trudeau VL. 2015a. Direct Regulation of Aromatase B Expression by 17beta-Estradiol and Dopamine D1 Receptor Agonist in Adult Radial Glial Cells. *Front Neurosci* 9:504.
- Xing L, Goswami M, Trudeau VL. 2014. Radial glial cell: critical functions and new perspective as a steroid synthetic cell. *Gen Comp Endocrinol* 203:181–5.
- Xing L, Martyniuk CJ, Esau C, Da Fonte DF, Trudeau VL. 2016a. Proteomic profiling reveals dopaminergic regulation of progenitor cell functions of goldfish radial glial cells in vitro. *J Proteomics* 144:123–132.
- Xing L, McDonald H, Da Fonte DF, Gutierrez-Villagomez JM, Trudeau VL. 2015b. Dopamine D1 receptor activation regulates the expression of the estrogen synthesis gene aromatase B in radial glial cells. *Front Neurosci* 9:1–12.
- Xing L, Venables MJ, Trudeau VL. 2016b. Role of aromatase and radial glial cells in neurotoxin-induced dopamine neuron degeneration and regeneration. *Gen Comp Endocrinol*:1–11.
- Xu C, Funahashi Y, Watanabe T, Takano T, Nakamuta S, Namba T, Kaibuchi K. 2015. Radial Glial Cell-Neuron Interaction Directs Axon Formation at the Opposite Side of the Neuron from the Contact Site. *J Neurosci* 35:14517–32.
- Yajima A, Ikeda M, Miyazaki K, Maeshima T, Narita N, Narita M. 2004. Manserin, a novel peptide from secretogranin II in the neuroendocrine system. *Neuroreport* 15:1755–1759.
- You ZB, Saria a, Fischer-Colbrie R, Terenius L, Gojny M, Herrera-Marschitz M. 1996. Effects of secretogranin II-derived peptides on the release of neurotransmitters monitored in the basal ganglia of the rat with in vivo microdialysis. *Naunyn Schmiedebergs Arch Pharmacol* 354:717–24.
- Zhang D, Popesku JT, Martyniuk CJ, Xiong H, Yao L, Xia X, Trudeau VL, Mcmillan SC, Xu ZT, Zhang J, Teh C, Korzh V, Vance L, Zhang D, Popesku JT, Martyniuk CJ, Xiong H, Duarte-guterman P, Yao L, Xia X, Trudeau VL. 2014. Profiling neuroendocrine gene expression changes following fadrozole-induced estrogen decline in the female goldfish Profiling neuroendocrine gene expression changes following fadrozole-induced estrogen decline in the female goldfish. :351–361.
- Zhang J, Woodhead GJ, Swaminathan SK, Noles SR, McQuinn ER, Pisarek AJ, Stocker AM, Mutch CA, Funatsu N, Chenn A. 2010. Cortical neural precursors inhibit their own differentiation via N-cadherin maintenance of beta-catenin signaling. *Dev Cell* 18:472–9.
- Zhao E, Basak A, Crump K, Trudeau VL. 2006a. Proteolytic processing and differential distribution of secretogranin-II in goldfish. *Gen Comp Endocrinol* 146:100–107.
- Zhao E, Basak A, Trudeau VL. 2006b. Secretoneurin stimulates goldfish pituitary luteinizing hormone production. *Neuropeptides* 40:275–282.
- Zhao E, Basak A, Wong AOL, Ko W, Chen A, Lopez GC, Grey CL, Canosa LF, Somoza GM, Chang JP, Trudeau VL. 2009a. The secretogranin II-derived peptide secretoneurin stimulates luteinizing hormone secretion from gonadotrophs.

- Endocrinology 150:2273–2282.
- Zhao E, Hu H, Trudeau VL. 2010. Secretoneurin as a hormone regulator in the pituitary. *Regul Pept* 165:117–122.
- Zhao E, McNeilly JR, McNeilly AS, Fischer-Colbrie R, Basak A, Seong JY, Trudeau VL. 2011. Secretoneurin stimulates the production and release of luteinizing hormone in mouse L β T2 gonadotropin cells. *Am J Physiol Endocrinol Metab* 301:E288-97.
- Zhao E, Zhang D, Basak A, Trudeau VL. 2009b. New insights into granin-derived peptides: evolution and endocrine roles. *Gen Comp Endocrinol* 164:161–174.
- Zupanc GK, Hinsch K, Gage FH. 2005. Proliferation, migration, neuronal differentiation, and long-term survival of new cells in the adult zebrafish brain. *J Comp Neurol* 488:290–319.
- Zupanc GK, Kompass KS, Horschke I, Ott R, Schwarz H. 1998. Apoptosis after injuries in the cerebellum of adult teleost fish. *Exp Neurol* 152:221–30.
- Zupanc GKH. 2006. Neurogenesis and neuronal regeneration in the adult fish brain. *J Comp Physiol A Neuroethol Sensory, Neural, Behav Physiol* 192:649–670.
- Zupanc GKH, Clint SC. 2003. Potential role of radial glia in adult neurogenesis of teleost fish. *Glia* 43:77–86.